**University of Alberta**

# Characterization of the motif requirements for the function of Aha1p and its homologue Hch1p

by

Natalie Katarina Horvat

A thesis submitted to the Faculty of Graduate Studies and Research
in partial fulfillment of the requirements for the degree of

Master of Science

Cell Biology


Fall 2013
Edmonton, Alberta

# ABSTRACT

The Hsp90 chaperone facilitates the maturation of client proteins, which are key players in cancer. Hsp90 inhibitor drugs, such as NVP-AUY922, are promising anti-cancer therapies. Co-chaperones regulate the ATPase-dependent Hsp90 activity and specifically, the co-chaperone Aha1 is the most robust stimulator of Hsp90 ATPase activity. Hch1p is a homologue of Aha1p and shares numerous conserved motifs. The conserved RKxK motif is involved in remodeling of the catalytic loop in Hsp90 and is required for Hch1p and Aha1p function. Surprisingly, the highly conserved *N* terminal peptide NxxNWHW is required for Hch1p activity *in vivo* but not for ATPase stimulation by either co-chaperone *in vitro*. Interestingly, Hch1p regulates sensitivity to Hsp90 inhibitor drugs *in vivo* whereas Aha1p does not. I propose that Hch1p regulates a step distinct than that of Aha1p which occurs early in the Hsp90 cycle and is sensitive to drug inhibition.

## TABLE OF CONTENTS

## LIST OF TABLES

**Title** **Page Number**

## LIST OF FIGURES

**Title** **Page Number**

## LIST OF ABBREVIATIONS

| | |
|---|---|
| *Δhch1* | Knock out of the *HCH1* gene in yeast |
| 5-FOA | 5-Fluoroorotic acid |
| Aha1p$^{1-156}$ | *N*-terminus of Aha1p |
| Aha1p$^{157-350}$ | *C*-terminus of Aha1p |
| AMP | Ampicillin |
| APS | Ammonium persulfate |
| βME | β-mercaptoethanol |
| BSA | Bovine serum albumin |
| CFTR | Cystic fibrosis transmembrane receptor |
| CYC | CYC terminator |
| DMSO | Dimethyl sulfoxide |
| DNA | Deoxyribonucleic acid |
| dNTP | Deoxyribonucleotide triphosphate |
| DPBS | Dulbecco's phosphate buffered saline |
| DTT | Dithiothreitol |
| ECL | Enhanced chemiluminescence |
| EDTA | Ethylenediamine-tetraacetic acid |
| FPLC | AKTA Explorer Fast Protein Liquid Chromatography |
| GA | Geldanamycin |
| GAL | Galactose |
| G418 | Geneticin |
| G418$^{R}$ | Geneticin resistance |
| GLU | Glucose |
| GPD | GPD promoter |
| GHKL | Gyrase, histidine kinase, and MutL proteins |
| HCl | Hydrochloric acid |
| HIC A | Hydrophobic interaction chromatography buffer A |
| HIC B | Hydrophobic interaction chromatography buffer B |

| | |
|---|---|
| HIS3 | Histidine biosynthesis 3 (imidazoleglycerol-phosphate dehydratase) |
| HexaHis | Histidine tag |
| HRP | Horseradish peroxidase |
| Hsp | Heat shock protein |
| Hsp100 | Heat shock protein 100 |
| Hsp90 | Heat shock protein 90 |
| Hsp70 | Heat shock protein 70 |
| Hsp60 | Heat shock protein 60 |
| Hsp40 | Heat shock protein 40 |
| sHsp | small Heat shock protein |
| Hsp90C | Heat shock protein 90 *C*-terminus |
| Hsp90M | Heat shock protein 90 Middle domain |
| Hsp90N | Heat shock protein 90 *N*-terminus |
| IgG | Immunoglobulin G |
| IMAC | Immobilized metal affinity chromatography |
| IMAC A | Immobilized metal affinity chromatography buffer A |
| IMAC B | Immobilized metal affinity chromatography buffer B |
| IPTG | Isopropyl-β-D-thiogalactopyranoside |
| IP | Immunoprecipitation |
| iT | Integrated at TRP1 locus |
| L-Arg | Arginine |
| L-Asp | Aspartic acid |
| L-Glu | Glutamic acid |
| L-Gly | Glycine |
| L-His | Histidine |
| L-Iso | Isoleucine |
| L-Leu | Leucine |
| L-Lys | Lysine |

| | |
|---|---|
| L-Met | Methionine |
| L-Phe | Phenylalanine |
| L-Ser | Serine |
| L-Thr | Threonine |
| L-Trp | Tryptophan |
| L-Tyr | Tyrosine |
| L-Val | Valine |
| LB | Luria broth |
| LiAc | Lithium acetate |
| LiAcTE | Lithium acetate, Tris base, EDTA solution |
| MIT | Massachusetts Institute of Technology |
| NADH | Nicotinamide adenine dinucleotide |
| NaOH | Sodium hydroxide |
| NEB | New England BioLabs |
| NVP | NVP-AUY922 |
| O.D. | Optical density |
| PCR | Polymerase chain reaction |
| PEG | Polyethylene glycol |
| PK/LDH | Pyruvate kinase/ lactate dehydrogenase |
| PMSF | Phenylmethanesulfonyl fluoride |
| RAF | Raffinose |
| RD | Radicicol |
| SDS | Sodium dodecyl sulfate |
| SDS-PAGE | Sodium dodecyl sulfate polyacrylamide gel electrophoresis |
| TAE | Tris base, acetic acid, EDTA solution |
| TBS | Tris-buffered saline solution |
| TCA | Trichloroacetic acid |
| TEF | TEF promoter |
| TEMED | Tetramethylethylenediamine |
| TPR | Tetratricopeptide repeat |

| | |
|---|---|
| *ts* | Temperature sensitive yeast mutant |
| Tris | Tris-(hydrocymethyl)aminomethane |
| TPR1 | Tryptophan biosynthesis 1 (Phosphoribosylanthranilate isomerise) |
| SC-URA | Synthetic complete lacking uracil |
| URA3 | Pyrimidine biosynthesis 3 (orotidine-5'-phosphate (OMP) decarboxylase) |
| WT | Wild-type |
| YPD | Yeast peptone dextrose media |

# Chapter One

## Introduction

## 1.1 Molecular chaperones are key players in maintaining cellular homeostasis

Cellular homeostasis is the ability to carry out cellular processes despite fluctuations in a cell's environment (Romero, 2004; Varela et al., 1974; Cannon, 1929). Almost all cellular processes require the function of complex molecular structures called proteins. The function of a protein is dependent on the acquisition a specific three-dimensional structure (Anfinsen, 1973). A linear polypeptide folds spontaneously into a specific structure through a process that is ultimately driven by intramolecular interactions between amino acids (Levinthal, 1968; Dill and Chan, 1997). The most powerful interactions that drive protein folding are hydrophobic in nature and very difficult to reverse (Bartlett and Radford, 2009; Felitsky et al., 2008; Dill, 1990; Tanford, 1978; Tanford, 1962). A stably folded protein is characterized by a desolvated, hydrophobic core because of the extremely high energetic cost of exposing hydrophobic moieties in an aqueous environment (Chandler, 2005; Dill, 1990; Ross and Subramanian, 1981; Kauzmann, 1959). Under stress, particularly thermal stress, proteins can misfold and expose their hydrophobic core, which is hazardous to surrounding proteins. Exposed hydrophobic amino acids can irreversibly interact with similar residues in other proteins, resulting in loss of function and the formation of toxic aggregates (Invernizzi et al., 2012; Pastore and Temussi, 2012; Kourtis and Tavernarakis, 2011; Vendruscolo et al., 2011; Kabakov and Gabai, 1993; Bensaude et al., 1990; Lepock et al., 1988). Because the cytosol is extremely crowded, with the protein concentration approximately 300 mg/mL (Frydman,

2001), cells must contain a mechanism to minimize inappropriate interactions between misfolded proteins and aggregation. Molecular chaperones are specialized proteins that shield misfolded proteins from interacting inappropriately with their neighbours (Hartl et al., 2011; Ellis, 2007; Lindquist and Craig, 1988; Lindquist, 1986). Through their ability to reversibly interact with misfolded proteins and prevent aggregation, chaperones maintain proteins in a functional state and allow cellular homeostasis to be maintained.

## 1.2 Heat shock proteins are molecular chaperones

Under conditions of thermal stress, cellular processes are at a greater risk of being disrupted because participating proteins are more likely to misfold, aggregate, and lose function (Chandler, 2005; Kabakov and Gabai, 1993; Bensaude et al., 1990; Dill, 1990; Lepock et al., 1988; Ross and Subramanian, 1981; Kauzmann, 1959). Cells compensate by employing the Heat Shock Response (HSR) which is a transcriptional program resulting in the up-regulation of numerous chaperones called Heat-shock proteins (Hsp) (Verghese et al., 2012; Kourtis and Tavernarakis, 2011; Lindquist, 1986). The induction of the HSR rapidly increases levels of cytosolic Hsps as studies have found some Hsp levels increase up to 10- to 15-fold after exposure to thermal stress conditions (Subjeck et al., 1982). Hsps are not only important during stress, as studies have shown basal levels of Hsps to be crucial at permissive temperatures (Feder and Hofmann, 1999; Nelson et al., 1992; Werner-Washburne et al., 1989; Lindquist and Craig, 1988; Lindquist, 1986). Hsps form a large, diverse group where many have

complex and specialized chaperone functions (Verghese et al., 2012). Although, they are not encoded with specific steric information for recognizing substrates (*i.e.* by specific amino acid sequence motifs), each group of Hsp has a specific set of substrate proteins that define their unique function within the cell.

## 1.3 Heat shock proteins

Hsps are divided according to their molecular size: Hsp100 group, Hsp90 group, Hsp70 group, Hsp60 chaperonin group, Hsp40 DnaJ group, and the small Hsp (sHsp) group (Verghese et al., 2012). The Hsp100 group is known to resolubilize aggregates and restore misfolded proteins to their respective pathways (Schirmer et al., 1996; Parsell et al., 1994). The Hsp60 chaperonin group works with Hsp70 to assist folding of nascent proteins (Heyrovská et al., 1998; Langer et al., 1992; Manning-Krieg et al., 1991). Other Hsp70s and sHsps have a variety of functions that include assisting non-nascent proteins achieve mature conformations, assembly of polypeptides into macromolecular structures and targeting proteins for degradation (Chen et al., 2011; Westhoff et al., 2005; Basha et al., 2004; Lee and Vierling, 2000; Haslbeck et al., 1999; Lee et al., 1997; Flynn et al., 1991; Landry and Gerasch, 1991; Nover et al., 1983). The Hsp40 DnaJ group assists chaperones and regulate the Hsp70 group by stimulating Hsp70 ATPase activity (Laufen et al., 1999; McCarty et al., 1995; Szabo et al., 1994). They assist by recruiting and stabilizing Hsp70 interaction with unfolded polypeptides. The Hsp70 group is the most studied group and participates in numerous processes within the cell, often in partnership with other chaperones,

such as Hsp90 (Proctor and Lorimer, 2011; Kampinga and Craig, 2010; Ran et al., 2008; Smith et al., 1993). The Hsp90 group assists non-nascent substrate proteins called 'clients' in their maturation, activation and assembly for such diverse cellular processes as signal transduction, cell cycle control, transcriptional regulation, and protein degradation (Taipale et al., 2010; Zhao et al., 2005; Prince and Matts, 2004; Scroggins et al., 2003; Basso et al., 2002; Pearl and Prodromou, 2000; Sato et al., 2000; Panaretou et al., 1998; Stancato et al., 1993). Eukaryotes have two isoforms of cytosolic Hsp90, a constitutive and an inducible isoform (in humans they are Hsp90β and Hsp90α, respectively, and in yeast they are Hsc82p and Hsp82p, respectively) (Csermely et al., 1998; Lindquist and Craig, 1988). Additionally, higher eukaryotes have two paralogues of Hsp90 located in the ER and mitochondria, known as Grp94 and TRAP1, respectively (Felts et al., 2000; Csermely et al., 1998; Shiu et al., 1977). The main focus of my thesis is on the inducible *Saccharomyces cerevisiae* isoform, Hsp82p.

## 1.4 The 90kDa Heat shock protein (Hsp90)

Hsp90 is essential for the maintenance of homeostasis because Hsp90 clients are key components in most cellular processes (Echeverría et al., 2011; Taipale et al., 2010). Due to the vast number of clients, Hsp90 is one of the most abundant proteins in the cytosol, often comprising 1-2% of the total cytosolic protein under normal conditions (Buchner, 1999; Panaretou et al., 1998; Nathan et al., 1997; Borkovich et al., 1989). Structurally, Hsp90 is a homodimer, with each monomer consisting of three domains: an *N*-terminal nucleotide binding ATPase

domain (Hsp90N), a client-binding middle domain (Hsp90M), and a *C*-terminal dimerization domain (Hsp90C) (Ali et al., 2006; Scheibel et al., 1998; Prodromou et al., 1997b) (Figure 1.1).

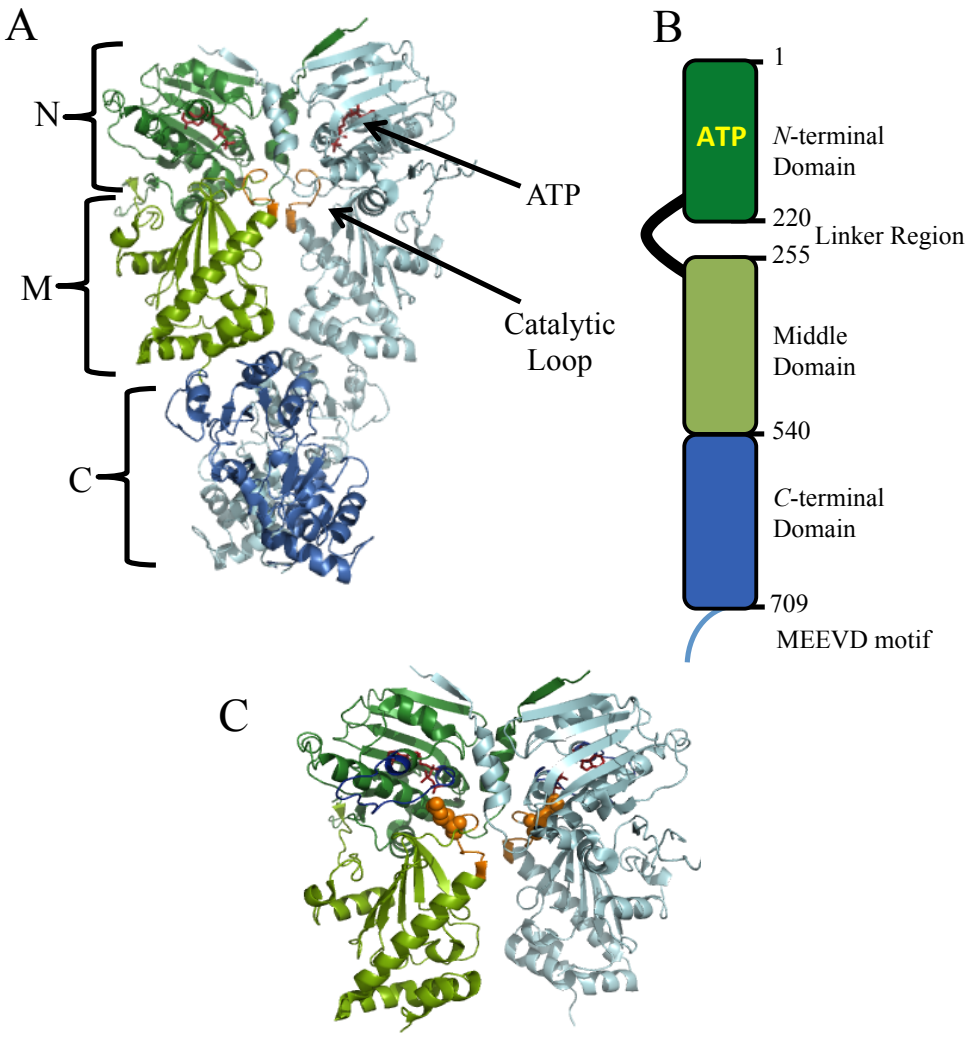


**Figure 1.1** **Structure of Hsp90.** A. Crystal structure of full length yeast Hsp90, Hsp82p, in an ATP-bound state, with the *N*-terminal domain (Hsp90N) in dark green, the middle domain (Hsp90M) in light green, and the *C*-terminal domain (Hsp90C) in blue. ATP is highlighted in red and the Hsp90 catalytic loop, residues 370-390, is highlighted in orange. B. A schematic Hsp90 monomer highlighting location and residue length of the *N*-terminal domain, non-conserved linker region, middle domain, *C*-terminal domain, and conserved MEEVD pentapeptide sequence. C. Hsp90N and Hsp90M with highlighted lid segment (blue) and catalytic loop (orange) with side chain of Arg380 in space filling model. (Crystal structure adapted from (Ali et al., 2006). PDB: 2CG9.)

The *N*-terminal domain of Hsp90 (Hsp90N) contains a non-canonical nucleotide-binding pocket (shared with gyrase, histidine kinase, and MutL proteins (GHKL)), which is essential for binding ATP (Prodromou et al., 1997a; Stebbins et al., 1997). Studies have shown that the ability of Hsp90 to bind and hydrolyze ATP is essential for client activation (Obermann et al., 1998; Panaretou et al., 1998; Sőti and Csermely, 1998). Within the Hsp90N, a ~30 amino acid fold forms a lid segment to stabilize bound nucleotides (Meyer et al., 2003). Additionally, the catalytic glutamate residue, E33, is required for the hydrolysis of ATP (Meyer et al., 2003; Richter et al., 2002; Prodromou et al., 2000; Panaretou et al., 1998; Prodromou et al., 1997b). While the Hsp90N has residues required for nucleotide binding, studies have shown isolated Hsp90N has negligible ATPase activity (Prodromou et al., 2000).

Hsp90M is the site of client binding as well as interaction with other proteins called co-chaperones (Hawle et al., 2006). Hsp90M is thought to discriminate binding and activation of various clients (Hawle et al., 2006; Meyer et al., 2003). The highly conserved motif, 377-N(L/I/V)SRExLQ-384 of yeast Hsp90M forms the critical catalytic loop necessary for ATPase activity (Meyer et al., 2003). Specifically, the residue, R380, within the catalytic loop is crucial for ATP hydrolysis. Hsp90M and Hsp90N are tethered together by a dispensable, relatively non-conserved linker region composed of ~30 highly charged amino acids and contributes flexibility to the Hsp90 structure (Tsutsumi et al., 2012; Ali et al., 2006; Pearl and Prodromou, 2006). Even though the charged linker has an obvious role in conformational flexibility, recent studies have shown that the

charged linker region is an important modulator of client activation and co-chaperone association (Tsutsumi et al., 2012).

Hsp90C is the main dimerization interface for the Hsp90 homodimer (Nemoto et al., 1995). It contains a conserved MEEVD pentapeptide sequence and is where co-chaperones containing tetracopeptide repeat (TPR) domains interact (Young et al., 1998). The MEEVD motif is bound by the 'two carboxylate' clamp structure of the TPR domain contained in many Hsp90 co-chaperones such as the co-chaperone **H**sp70-Hsp90 **O**rganizing **P**rotein (HOP), FKBP51, FKBP52 as well as others (Cliff et al., 2006; Scheufler et al., 2000).

The Hsp90 ATPase activity is dependent on the cooperation of the catalytic loop in Hsp90M and the lid segment from Hsp90N (Meyer et al., 2003; Prodromou and Pearl, 2003). In order to hydrolyze ATP, the Hsp90 *N*-terminal domains trap ATP by coming together, forming an ATP-bound, closed conformation (Ratzke et al., 2012; Pullen and Bolon, 2011; Richter et al., 2001; Prodromou et al., 2000). Upon ATP hydrolysis, Hsp90 monomers adopt an ADP-bound, open conformation (Richter et al., 2008; Mickler et al., 2009; Wegele et al., 2003). The complex process of ATP binding, *N* terminal dimerization, and hydrolysis of ATP occurs in a highly regulated cycle that is essential for Hsp90 activity (Richter et al., 2008; Prodromou et al., 2000; Weikl et al., 2000; Panaretou et al., 1998; Obermann et al., 1998).

## 1.5 Hsp90 clients

The list of Hsp90 clients is extensive and diverse consisting of over 200 proteins (Echeverría et al., 2011; Taipale et al., 2010). The majority of Hsp90 clients fall into two distinct groups: transcription factors, such as steroid hormone receptors, and signaling kinases, although recent studies have identified many others (Taipale et al., 2010; Wandinger et al., 2008). The structural determinants for recognition of clients by Hsp90 are not well understood, as no significant sequence homology between clients has been identified (Taipale et al., 2012; Citri et al., 2006; Xu et al., 2005; Nathan and Lindquist, 1995). It is thought that Hsp90 binds to specific secondary and tertiary structures of partially folded or fully folded proteins facilitating their stabilization and activation (Citri et al., 2006; Pearl and Prodromou, 2006). One example of the complexity of Hsp90 substrate specificity is the *src* kinase. The stable form of *src* - when phosphorylated at Tyr527 on the *C*-terminal segment - is inactive and does not require Hsp90 to avoid degradation. The viral form of *src* (v-src) is constitutively active due to the lack of the *C*-terminal segment and is highly unstable. Studies have shown its stability and maturation is dependent on Hsp90 as v-*src* rapidly degrades when Hsp90 is inhibited *in vivo* (Fabio Falsone et al., 2004; Xu et al., 1999; Whitesell et al., 1994; Xu and Lindquist, 1993). Other studies suggest that the thermal or conformational stability of a protein determines Hsp90 client recognition rather than a specific structural determinant (Taipale et al., 2012; Wandinger et al., 2008; Hartson et al., 1998; Schuh et al., 1985).

## 1.6 Hsp90 is important in cancer

Many Hsp90 clients are oncoproteins, which drive the aberrant signal transduction and cell growth observed in cancer (Trepel et al., 2010; Whitesell and Lindquist, 2005; Pratt and Toft, 2003). When hyperactivated, oncoproteins facilitate the transformation of normal cells into malignant cell types and thus cancer cells are highly dependent on Hsp90 activity (Whitesell and Lindquist, 2005; Neckers, 2002). Alternatively, high mutation rates associated with cancer can hyperactivate and destabilize clients, which can lead to higher requirements of Hsp90 (Whitesell et al., 1994). Compounds that specifically inhibit the ATPase activity of Hsp90 have potent anti-tumour effects as these compounds prevent Hsp90-mediated maturation and stabilization of oncoproteins, which results in their degradation (Tillotson et al., 2010; Neckers, 2002; Roe et al., 1999; Whitesell et al., 1994).

Hsp90 inhibitors compete for binding to the ATP binding pocket of the *N*-terminal domain (Grenert et al., 1997; Prodromou et al., 1997a; Stebbins et al., 1997). Naturally-occurring Hsp90 inhibitors, Geldanamycin (GM) and Radicicol (RD), were the first compounds to be used in clinical trials but their toxicity and poor solubility required the development of GM derivatives, 17-AAG and 17-DMAG, to solve those issues (Kelland et al., 1999). NVP-AUY922 is the product of a structure-based design strategy and is currently one of the most safe and effective Hsp90 inhibitors as it is showing promising anti-tumor effects in combination with other cancer therapies in phase II clinical trials (Jhaveri et al.,

2012; Neckers and Workman, 2012; Whitesell and Lindquist, 2005; Pearl et al., 2008; Brough et al., 2007).

## 1.7 Co-chaperones are regulators of Hsp90 activity

In order to facilitate the maturation of a client, Hsp90 must proceed through a conformationally dynamic cycle (Hessling et al., 2009). Hsp90 progresses through multiple states characterized by co-chaperone and nucleotide binding, and ultimately ATP hydrolysis, that results in client maturation (Krukenberg et al., 2011; Mickler et al., 2009; Hessling et al., 2009; Richter et al., 2008; Siligardi et al., 2004) (Figure 1.2). While the details are not known, each co-chaperone is associated with a specific conformation of Hsp90 at distinct stages of the cycle (Li et al., 2012; Li et al., 2010; Richter et al., 2004; Richter et al., 2003).

The early stage of the Hsp90 cycle involves delivery of clients such as steroid hormone receptors and kinases by the co-chaperones HOP and the **c**ell-**d**ivision **c**ycle 37 homologue (cdc37), respectively (Lee et al., 2004; Morishima et al., 2000). The steroid hormone receptor interaction with Hsp90 is one of the most well studied examples of client engagement (Pearl and Prodromou, 2006). Their delivery from the Hsp70/Hsp40 system is facilitated by the co-chaperone HOP or Sti1p in yeast (Johnson et al., 2007; Chadli et al., 2000; Chen and Smith, 1998; Smith et al., 1993). Sti1p contains three TPR domains, TPR1, TPR2A, and TPR2B, but only TPR1 and TPR2A are involved in binding to the EEVD peptide sequences of Hsp70 and Hsp90, respectively (Onuoha et al., 2008; Brinker et al.,

2002; Scheufler et al., 2000). The sequences upstream of the EEVD peptide motif differ slightly in Hsp90 (DDTSRMEEVD) from Hsp70 (GSGPTIEEVD) to provide specificity for Sti1p binding and allow efficient client transfer from Hsp70/Hsp40 to Hsp90 (Pearl and Prodromou, 2006; Wegele et al., 2006; Scheufler et al., 2000; Johnson et al., 1998). Cdc37 delivers kinases to Hsp90 and blocks ATPase activity of Hsp90 by binding to the ATP lid of Hsp90N and thus locking Hsp90 in the open conformation (Eckl et al., 2013; Siligardi et al., 2002). The interactions of Sti1p stabilize an ADP-bound open conformation of Hsp90, which inhibits Hsp90 ATPase activity (Richter et al., 2003; Siligardi et al., 2002; Prodromou et al., 1999). Previous reports suggest that the arrest of Hsp90 ATPase activity is important for loading clients and prior to the client maturation cycle (Pearl and Prodromou, 2006).

It is the concerted action of nucleotide binding as well as the co-chaperone p23, or Sba1p in yeast, that displace Sti1p and cause Hsp90 to adopt a closed, ATP bound state (Li et al., 2012; Li et al., 2010). Sba1p has been shown to bind to the dimerized interface of Hsp90 *N*-terminal domains and helps trap client proteins in between Hsp90M dimers (Li et al., 2012; McLaughlin et al., 2006; Richter et al., 2004; Chadli et al., 2000; Prodromou et al., 2000). Previous studies have shown that Sba1p inhibits the Hsp90 ATPase activity serving to prevent conformational changes associated with ATP hydrolysis. It may be that delaying hydrolysis and stabilizing the client-bound state may be required for the maturation of some or all clients (Ali et al., 2006; McLaughlin et al., 2006; Richter et al., 2004; Siligardi et al., 2004; Panaretou et al., 2002). The final stage

of the cycle is regulated by the co-chaperone **A**ctivator of **H**sp90 **A**TPase (Aha1) (Ali et al., 2006; Siligardi et al., 2004). Although both Sba1p and Aha1p recognize the ATP-bound, closed state of Hsp90, Aha1p robustly stimulates the Hsp90 ATPase activity and has been suggested that it assists in efficiency of activation and maturation of client proteins (Prodromou, 2012; Meyer et al., 2003; Lotz et al., 2003; Panaretou et al., 2002). The binding of Aha1p results in ATP hydrolysis, release of the mature or activated client, and return to the open, ADP-bound state (Obermann et al., 1998; Panaretou et al., 1998) (Figure 1.2).

ATP hydrolysis is essential for client maturation; consequently co-chaperones that regulate Hsp90 ATPase activity are very important in regulating Hsp90 client maturation. Aha1 is the only known co-chaperone to robustly stimulate the Hsp90 ATPase activity (Lotz et al., 2003; Meyer et al., 2003; Panaretou et al., 2002). Studies have shown that Aha1 plays a key role in the hyperactivation of oncoproteins by Hsp90 in malignant cell types while other studies have shown Aha1 to regulate sensitivity to Hsp90 inhibitors in cancer cells (Holmes et al., 2008; Panaretou et al., 2002). Conversely, silencing of Aha1 has been found to rescue a common mutant form of the Hsp90 client cystic fibrosis transmembrane receptor (CFTR) (Wang et al., 2006). Targeting co-chaperones that modulate the Hsp90 ATPase activity is important for understanding the role of Hsp90 in facilitating diseases such as cancer and cystic fibrosis (Koulov et al., 2010; Holmes et al., 2008; Panaretou et al., 2002). Further insights into the role of co-chaperones in regulating Hsp90 activity, particularly Aha1 in the context of disease states, as they are novel targets in the future of disease therapies.

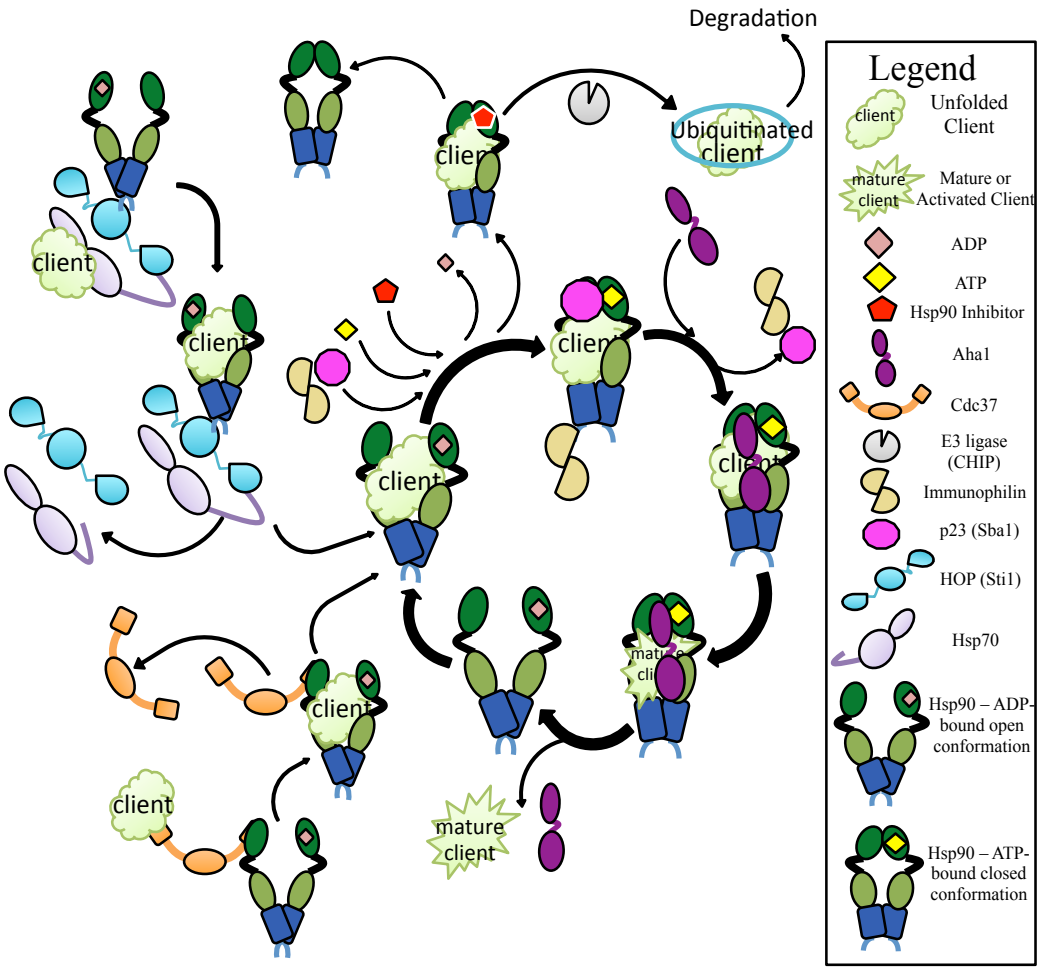


**Figure 1.2** **Simplified model of the Hsp90 Cycle.** There are two methods of client delivery to the Hsp90 system that involve the co-chaperones HOP (Sti1p) and Hsp70 or cdc37. HOP and cdc37 load clients onto an ADP-bound open state of Hsp90. Upon client binding, HOP or cdc37 are released as ATP and p23 (Sba1p) as well as immunophilins bind in a concerted fashion to facilitate an ATP-bound closed state of Hsp90. Aha1 binds and stimulates the Hsp90 ATPase activity and the mature or activated client is released. Hsp90-inhibitor drugs, such as NVP-AUY922, compete with ATP for binding to the nucleotide binding pocket of Hsp90N and inhibit ATP hydrolysis and client maturation. The Hsp90 client is targeted for degradation by the E3 ligase (CHIP) with ubiquitin.

## 1.8 Aha1p stimulates the Hsp90 ATPase activity and has a homologue Hch1p

Hsp90 has a very low intrinsic ATPase rate *in vitro* with the yeast Hsp90 ATPase rate being about ten-fold higher than that of human Hsp90 (McLaughlin et al., 2004; McLaughlin et al., 2002; Panaretou et al., 2002; Prodromou et al., 2000; Panaretou et al., 1998). The ATP hydrolysis rate is the rate-limiting step of the Hsp90 cycle and studies have shown that ATP is bound and released multiple times before hydrolysis occurs. Aha1 is the only co-chaperone that robustly, stimulates ATPase activity (up to ~12-fold) (Lotz et al., 2003; Panaretou et al., 2002). Human Aha1 and *S. cerevisiae* Aha1 are conserved as they share 23% amino acid sequence identity and 38% amino acid sequence similarity (Richter et al., 2008; Lotz et al., 2003). Aha1p is a 350 amino acid protein consisting of an *N*-terminal domain and a *C*-terminal domain joined by a 40 amino acid linker (Koulov et al., 2010) (Figure 1.3B). The Aha1p *N*-terminal domain binds to the Hsp90 middle domain and the Aha1p *C*-terminal domain binds to the Hsp90 *N*-terminal domain (Retzlaff et al., 2010; Lotz et al., 2003; Meyer et al., 2003) (Figure 1.3A).

The mechanism of stimulation of the Hsp90 ATPase activity by Aha1p has been partially elucidated (Meyer et al., 2004). Recent studies have shown that residues in the *N*-terminal domain of Aha1p remodel the Hsp90 catalytic loop (residues 370-390) in Hsp90M (Figure 1.4B) (Meyer et al., 2004). Specifically, residues Lys387 and Ile388 at the *C*-terminal end of the Hsp90 catalytic loop interact with residues in $Aha1p^{1-156}$ and move more than 15Å and 8Å,

respectively. This significant movement causes these residues to become incorporated into the alpha helix of Hsp90 that follows the catalytic loop (compare orientation of orange highlighted residues in Figure 1.4C with Figure 1.4B within the middle domain of Hsp82p). This results in a slight destabilization of the short helix within the catalytic loop of Hsp90 and releases Arg380 from interactions with surrounding Hsp90 residues. Arg380 therefore moves into an extended position that enables easier interaction with the γ phosphate of the bound ATP within the *N*-terminal domain of Hsp90. Even though the mechanism of ATPase stimulation has been partially elucidated, the Aha1p$^{1\text{-}156}$ cannot stimulate the Hsp90 ATPase rate as robustly as full length Aha1p suggesting that the *C*-terminus is integral to stimulation (Meyer et al., 2004; Lotz et al., 2003; Panaretou et al., 1998). Further studies are required to fully understand the mechanism of ATPase stimulation by Aha1p.

A similar but poorly studied co-chaperone, Hch1p, is only found in some fungi such as *S. cerevisiae* and shares 36.6% amino acid sequence identity to the 156 amino acid *N*-terminal domain of Aha1 (Lotz et al., 2003) (Figure 1.4A). Previous studies have shown that Hch1p can weakly stimulate the Hsp90 ATPase rate to a degree similar to Aha1p$^{1\text{-}156}$ (Lotz et al., 2003; Panaretou et al., 2002). Hch1p is a 153 amino acid protein that was first discovered as a suppressor of the *in vivo* defect of the temperature sensitive (*ts*) mutant Hsp82p$^{E381K}$. Over-expression of Hch1p restores growth at restrictive (35°C) temperatures to near wild-type levels in yeast expressing Hsp82p$^{E381K}$ (Nathan et al., 1999). Yeast two hybrid analysis shows that Hch1p binds to Hsp90M and previous work from our

lab suggests that Hch1p competes with Aha1p for binding to Hsp90 (Armstrong et al., 2012; Lotz et al., 2003) (Figure 1.3A). Interestingly, Hch1p shares highly conserved motifs with Aha1p, such as the NxxNWHW motif and RKxK loop, suggesting that Hch1p has the same function of Aha1p (Figure 1.4A – highlighted in red boxes). The similarity of Hch1p to Aha1p makes Hch1p very interesting for my studies.

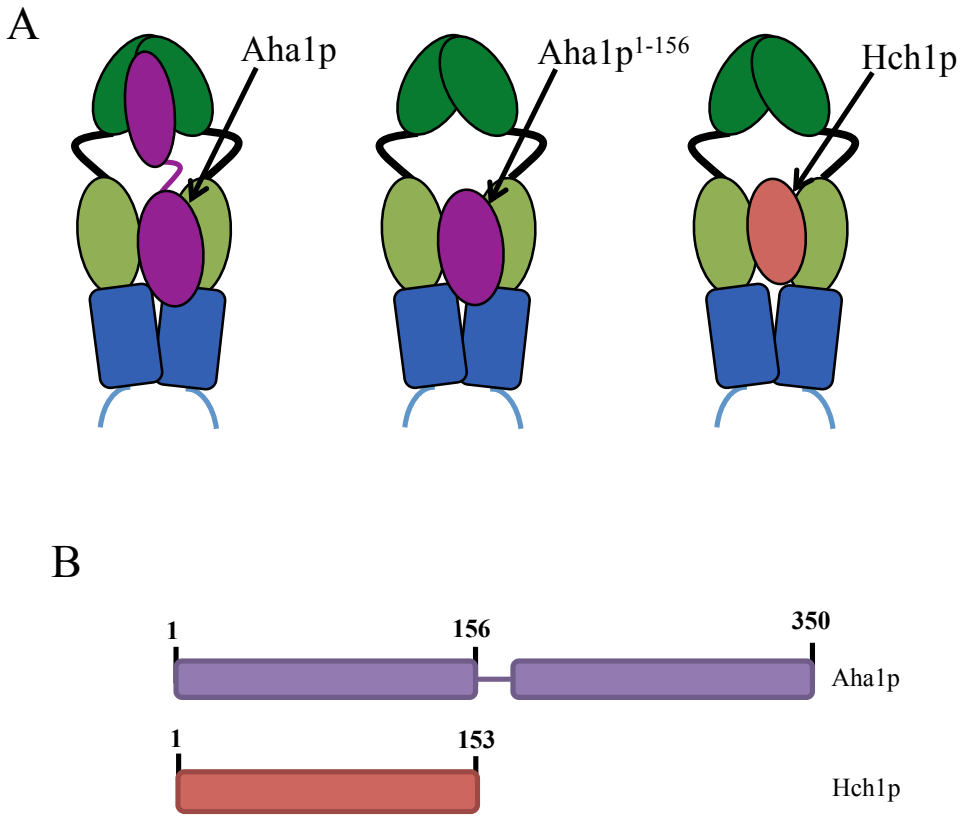


**Figure 1.3 Schematic of Aha1p and Hch1p with Hsp82p.** A. The *N*-terminal domain of the co-chaperone Aha1p binds to the middle domain of Hsp82p and the *C*-terminal domain of Aha1p binds to the *N*-terminal domain of Hsp82p in the closed conformation. The *N*-terminal domain of Aha1p, Aha1p$^{1-156}$, and Hch1p bind to the middle domain of Hsp82p. B. Domain structures illustrating the alignment of Aha1p, 350 amino acids in length, and Hch1p, 153 amino acids in length.

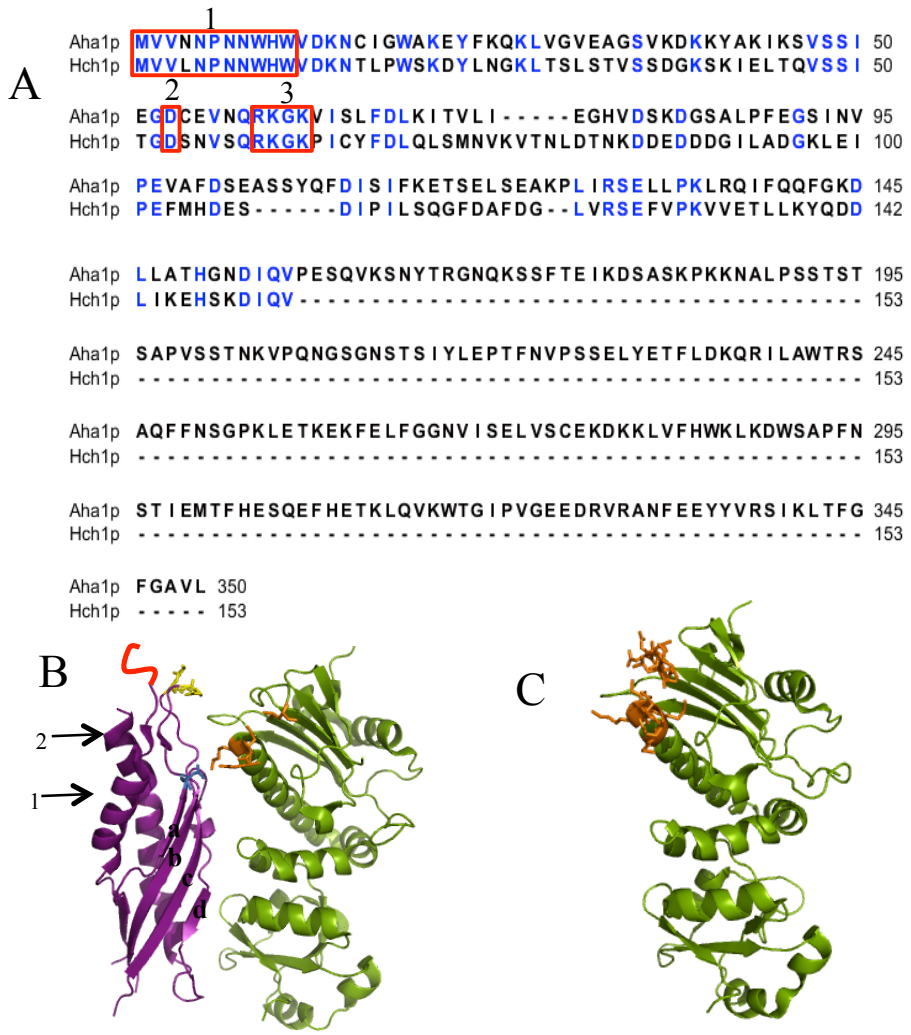


**Figure 1.4 Conserved motifs in Hch1p and Aha1p highlighted in sequence alignment and crystal structure.** A. Amino acid sequence alignment of Aha1p and Hch1p with conserved motifs used in our studies highlighted. NxxNWHW motif highlighted in box 1, D53 residue highlighted in box 2, and RKxK motif highlighted in box 3. B. Crystal structure of Aha1p$^{1\text{-}156}$ (purple) bound to the middle domain of Hsp82p (green) with the D53 residue (blue), RKxK loop highlighted in Aha1p$^{1\text{-}156}$ (yellow), schematic representation of unstructured NxxNWHW motif (red), and the catalytic loop in Hsp82p (orange). Alpha helices and β sheets strands are labeled 1, 2 and a, b, c, d, respectively. (Crystal structure adapted from (Meyer et al., 2004). PDB:1USU). C. Crystal structure of middle domain of Hsp82p with highlighted catalytic loop (orange) without Aha1p (Crystal structure adapted from (Meyer et al., 2003). PDB:1HK7).

## 1.9 Yeast as a model system

Studying the Hsp90 system in mammalian cells is difficult because mammalian cells contain multiple Hsp90 isoforms and immortalized cell lines undergo many genetic alterations that complicate studies (*i.e.* copy number variants of Hsp90 system components). In humans, the inducible isoform, Hsp90α, shares 60% amino acid identity with the *S. cerevisiae* inducible isoform, Hsp82p (Prodromou et al., 1997b). Due to the high degree of conservation, isoforms of Hsp90 can be replaced within organisms and support viability as Hsp90α can sustain growth of yeast when expressed as the sole source of Hsp90 (Minami et al., 1994; Picard et al., 1990). Many of the components of the human Hsp90 system are functionally interchangeable as the human co-chaperones p23 and HOP can replace yeast co-chaperones Sba1p and Sti1p, respectively, in yeast (Carrigan et al., 2004; Nelson et al., 2004; Bohen, 1998). Moreover, mammalian Hsp90 client proteins such as the glucocorticoid hormone receptor and the kinase src can be activated by the yeast Hsp90 system (Bohen and Yamamoto, 1993; Xu and Lindquist, 1993; Picard et al., 1990). Therefore, *S. cerevisiae* is a useful model organism that serves as a valuable tool in understanding the Hsp90 system. Since yeast are a genetically tractable model organism and Hsp90 is essential for cell survival, yeast expressing Hsp82p temperature sensitive (*ts*) mutants as the sole source of Hsp82p have provided key mechanistic and structural insights of the Hsp90 system (Nathan et al., 1999; Nathan and Lindquist, 1995; Nathan et al., 1997). In contrast to classical *ts* mutants, Hsp90 *ts* mutants do not misfold at restrictive temperatures but rather they have specific impairments that are

revealed by the higher substrate burden associated with elevated temperature. In this way they provide a means to dissect individual steps of the Hsp90 cycle (Nathan et al., 1999; Nathan et al., 1997).

## 1.10 Hsp82p temperature sensitive (*ts*) mutants are tools to study the Hsp90 cycle

To investigate specific aspects of the Hsp90 cycle, my studies involved the use of the *ts* mutants Hsp82p$^{E381K}$, Hsp82p$^{V391E}$, and Hsp82p$^{A587T}$. Yeast strains expressing the Hsp82p$^{E381K}$ mutant grow at half the rate of wild type yeast strains at 25°C but growth is restored to near wild-type levels when Hch1p is over-expressed (Nathan et al., 1999; Nathan and Lindquist, 1995). In contrast, yeast-expressing Hsp82p$^{A587T}$ is significantly impaired when Hch1p is over-expressed (Armstrong et al., 2012; Nathan et al., 1999). Moreover, our group found that growth of yeast expressing Hsp82p$^{A587T}$ is restored to near-wild-type levels when *HCH1* is deleted (Armstrong et al., 2012). Yeast expressing wild-type Hsp82p become resistant to the Hsp90 inhibitor drug, NVP-AUY922, when *HCH1* is deleted (Armstrong et al., 2012). Importantly, neither of these phenomena occur when *AHA1* is deleted. Other studies have shown that introducing a mutation V391E into Hsp82p to construct the mutant Hsp82p$^{V391E}$ blocks the binding of Aha1p to the middle domain of Hsp82p. As my studies focus on determining the function of Hch1p and its relationship with Aha1p, I chose these three mutations in Hsp82p to interrogate the role of Hch1p within the Hsp90 system (Figure 1.5).

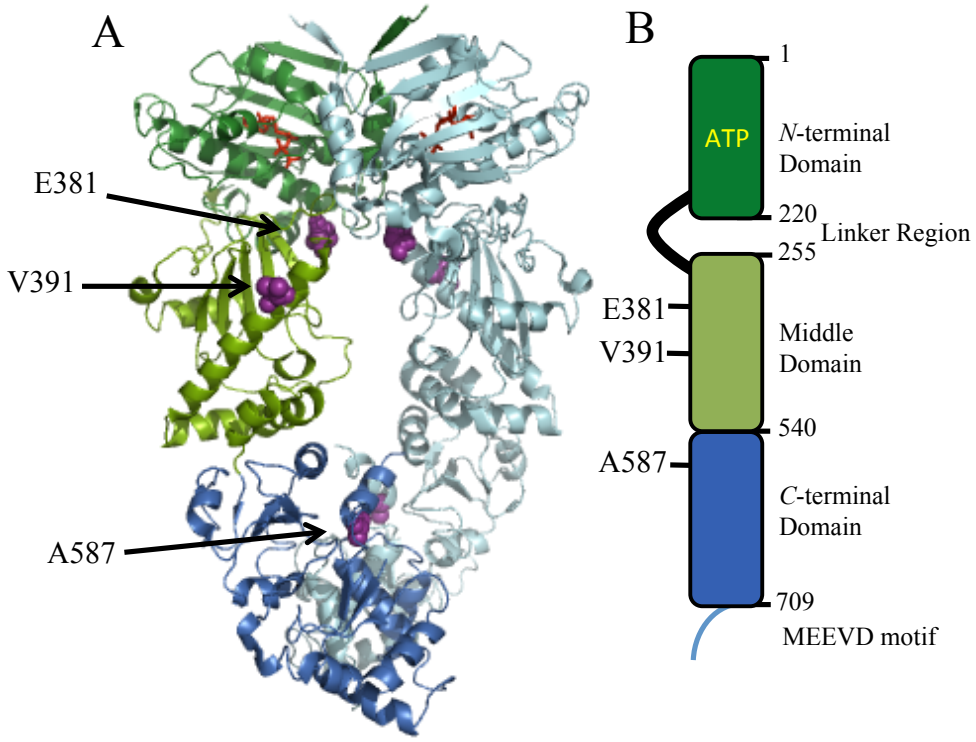


**Figure 1.5 Identification of Hsp82p mutants used in this study.** A. Crystal structure of mutated residues, E381, V391 and A587, highlighted in purple to construct Hsp82p mutants, Hsp82p$^{E381K}$, Hsp82p$^{V391E}$, and Hsp82p$^{A587T}$. B. Schematic of Hsp82p monomer with highlighted mutations to make Hsp82p mutants. (Crystal structure adapted from (Ali et al., 2006). PDB: 2CG9.)

## 1.11 Rationale and thesis objectives

Despite recent advancements, there remains much to be elucidated about the Hsp90 cycle. Studies have shown Hsp90 to be a key player in malignant cell types by supporting aberrant or increased client protein activation (Taipale et al., 2010; Trepel et al., 2010; Whitesell and Lindquist, 2005). More importantly, the role of Hsp90 in regulating oncoproteins such as Akt, BCR-ABL, Cdk4, HER2, and Raf-1 identifies Hsp90 as a target for cancer therapies (Basso et al., 2002; Gorre et al., 2002; Münster et al., 2002; Schulte et al., 1996; Stepanova et al., 1996). The maintenance of aberrant client protein activation in malignant cell states requires altered or increased Hsp90 function (Xu and Neckers, 2007). Hsp90 co-chaperones are crucial components as they regulate Hsp90 ATPase-driven activity (Li et al., 2012; Koulov et al., 2010; Li et al., 2010; McLaughlin et al., 2006; McLaughlin et al., 2004; Siligardi et al., 2004; Lotz et al., 2003; Panaretou et al., 2002; Panaretou et al., 1998; Obermann et al., 1998). Co-chaperones, such as Aha1, have been found to mediate altered Hsp90 function in malignant cell types (Holmes et al. 2008). Aha1 levels are upregulated in human cancer cell lines after being treated with Hsp90 inhibitors drugs and silencing Aha1 levels in human cancer cell lines increases sensitivity to Hsp90 inhibitor drugs (Panaretou et al., 2002; Holmes et al., 2008). The role of Aha1 in regulating the Hsp90 system is crucial for Hsp90 activity however the exact mechanism of how Aha1 regulates Hsp90 activity remains largely unknown. More specifically, it is thought that Aha1p regulates Hsp90 function by robustly stimulating ATPase activity. The *C*-terminal domain of Aha1p is required to stimulate the Hsp90

ATPase activity to very high levels (Meyer et al., 2004; Lotz et al., 2003; Panaretou et al., 1998). However, its homologue, Hch1p, does not contain such a *C*-terminal domain and has an interesting biological role in suppressing the Hsp82p$^{E381K}$ defect *in vivo* (Nathan et al., 1999). Due to the sequence similarity with the *N*-terminal domain of Aha1p, I hypothesize that the mechanism of Hch1p to interact *in vivo* and stimulate yeast Hsp90, Hsp82p, *in vitro* is similar to Aha1p. In order to investigate this hypothesis, I used *S. cerevisiae* to examine the functional differences of Hch1p and Aha1p *in vitro* and *in vivo*. I carried out structural and functional analysis to determine the structural motifs that are linked to Hch1p and Aha1p function to better understand the mechanisms of the biology of this co-chaperone family.

# Chapter Two

## Materials and Methods

## 2.1 Materials

### 2.1.1 Reagents

According to the Environmental Health and Safety protocols of the University of Alberta and Workplace Hazardous Materials Information System (WHIMIS), reagents below were used following the appropriate outlined procedures.

**Table 2.1** Chemicals and other materials

| Material | Producer/Supplier |
|---|---|
| β-Mercaptoethanol (βMe) | BioShop Canada Inc. |
| Acetone | Fisher Chemicals |
| Acrylamide (30%; 29:1) | Bio-Rad Laboratories |
| Agar | Fisher Chemicals |
| Agarose (UltraPure™) | Fisher Chemicals |
| Amino Acids | MP BioChemicals, LLC |
| Ammonium Sulphate | Fisher Chemicals |
| Ammonium Persulphate (APS) | Life Technologies Inc. |
| Ampicillin | Sigma-Aldrich Life Sciences |
| Adenosine Tri-Phosphate (ATP) | Fisher BioReagents |
| Adenylyl-imidodiphosphate (AMP-PNP) | Sigma-Aldrich Life Sciences |

| | |
|---|---|
| Adenosine Di-Phosphate (ADP) | MP Biomedicals, LLC |
| Bovine serum albumin (BSA) | Sigma-Aldrich Life Sciences |
| Butanol | Fisher Scientific Canada |
| Bromophenol Blue | BDH Laboratory Sciences |
| Brilliant Blue R-250 | Fisher BioReagents |
| Coomassie Blue Stain | BioRad Laboratories |
| Dextrose (D-Glucose) | Fisher Brand BioReagents |
| Dimethyl Sulfoxide (DMSO) | Fisher Chemicals |
| Dithiothreitol (DTT) | Roche Diagnostics |
| Deoxyribonucleotide triphosphate (dNTP) | Roche Diagnostics |
| Ethanol | Fisher Chemicals |
| Ethylenediamine-tetraacetic acid (EDTA) | Fisher Chemicals |
| Filter Paper | Munktel |
| Galactose | Fisher BioReagents |
| GeneRuler 1 kb DNA Ladder | Fermentas – Thermo Fisher Scientific |
| Geneticin (G418) | Life Technologies Inc. |
| Glacial Acetic Acid | Fisher Brand BioReagents |
| Glycerol | Fisher Brand BioReagents |
| Glycine | MP Biomedicals, LLC |

| | |
|---|---|
| HALT protease inhibitor Cocktail | ThermoScientific |
| Hepes | Brand BioReagents |
| Hydrogen Chloride (HCl) | Fisher Brand BioReagents |
| Hydrogen Peroxide ($H_2O_2$) | Fisher Brand BioReagents |
| Imidazole | Fisher Brand BioReagents |
| Isopropyl-β-D-thiogalactopyranoside (IPTG) | OmniPur |
| Isopropanol | Fisher Brand Chemicals |
| Luria Broth (LB), Miller | Fisher Brand BioReagents |
| Lithium Acetate | Acros Organics |
| Magnesium Chloride ($MgCl_2$) | Fisher Brand Chemicals |
| Methanol | Fisher Brand BioReagents |
| Milk protein | Carnation |
| Nitrocellulose Membranes | BioRad Laboratories |
| Nickel Sulphate | Fisher Scientific Canada |
| Nicotinamide Adenine Dinucleotide (NADH) | Sigma-Aldrich Life Sciences |
| NVP-AUY922 | Chemie Tek |
| PCR Primers | Integrated DNA Technology |
| PEG3550 | Fisher Scientific Canada |
| Peptone | Becton, Dickinson and Company (BD) |

| | |
|---|---|
| PfuTurbo DNA Polymerase | Agilent Technologies |
| Pfu Buffer | Agilent Technologies |
| Phosphoenol pyruvate (PEP) | Sigma-Aldrich Life Sciences |
| Phenylmethylsulfonylfluoride (PMSF) | ThermoScientific |
| Ponceau S | MP Biomedicals, LLC |
| Potassium Acetate | Fisher Chemicals |
| Pyruvate Kinase/Lactate Dehydrogenase enzyme from Rabbit muscle (PK/LDH) | Sigma-Aldrich Life Sciences |
| Sodium Dodecyl Sulphate (SDS) | Fisher Scientific Canada |
| Sodium Acetate | EMD Millipore |
| Sodium Chloride (NaCl) | Fisher Scientific Canada |
| Sodium Hydroxide (NaOH) | Fisher Scientific Canada |
| Sodium Phosphate ($NaH_2PO_4$) | Fisher Scientific Canada |
| Sodium Molybdate | Acros Organics |
| Sorbitol | Fisher Scientific Canada |
| SYBR Safe DNA gel stain | Invitrogen – Life Technologies |
| Raffinose | MP Biomedicals, LLC |
| Restriction Digest Enzymes | New England Biolabs (NEB) |
| Restriction Digest Enzyme Buffers | New England Biolabs (NEB) |

| | |
|---|---|
| T4 Ligase | New England Biolabs (NEB) |
| T4 Ligase Buffer | New England Biolabs (NEB) |
| Trichloroacetic Acid (TCA) | Fisher Scientific Canada |
| Tetramethylethylenediamine (TEMED) | Fisher Scientific Canada |
| TopTaq DNA Polymerase | QIAGEN |
| TopTaq Buffer | QIAGEN |
| Tris-(hydroxymethyl)aminomethane (Tris-Base) | Fisher Scientific Canada |
| Triton X-100 | Fisher Scientific Canada |
| Tween 20 | Fisher BioReagents |
| Xylene Cyanol | Becton, Dickinson and Company (BD) |
| Yeast Nitrogen Base | Becton, Dickinson and Company (BD) |
| Yeast Extract | Becton, Dickinson and Company (BD) |

**Table 2.2** Commercial kits

| Kit | Supplier |
|---|---|
| QIAGEN Plasmid Midiprep Kit | QIAGEN |
| QIAGEN PCR Purification Kit | QIAGEN |
| QIAprep Spin Miniprep Kit | QIAGEN |
| QIAquick Gel Extraction Kit | QIAGEN |
| QuikChange$^{TM}$ Mutagenesis | Agilent Technologies |

### 2.1.2 General laboratory media and buffers

**Table 2.3** Media and buffers

| Buffer | Contents |
|---|---|
| 4X ATPase Assay Reaction Buffer | 11 mM Hepes<br>4 mM PEP |
| 1X Coomassie Stain | 25 g Brilliant Blue R-250<br>500 mL Methanol |
| Destain | 2.105 L 95 % Ethanol<br>15.895 L $ddH_2O$<br>2.0 L Glacial Acetic Acid |
| 6X DNA Loading Dye | 0.3 % (w/v) Bromophenol Blue<br>30 % (v/v) Glycerol<br>0.3 % (w/v) Xylene cyanol<br>Q.S. 10 mL $ddH_2O$ |
| ECL #1 and #2 | Solution #1<br>0.45 mM p-Coumaric Acid<br>3.75 mL DMSO<br>2.5 mM Luminol<br>Q.S. 250 mL 0.1 M Tris pH 8.8<br>Solution #2<br>0.02 % (v/v) Hydrogen Peroxide<br>250 mL 0.1 M Tris Base pH 8.8 |
| 10X Electrode | 2880 g Glycine<br>600 g Tris Base<br>200 g SDS<br>Q.S. 20 L $ddH_2O$ |
| Gel Filtration Buffer (Co-Chaperone) | 25 mM Hepes<br>50 mM NaCl<br>5 mM β-Mercaptoethanol<br>Q.S. 1 L $ddH_2O$, pH 7.2 |
| Gel Filtration Buffer (Hsp90) | 25 mM Hepes<br>10 mM NaCl<br>5 mM β-Mercaptoethanol<br>Q.S. 1 L $ddH_2O$, pH 7.2 |
| Hydrophobic Ionic Buffer A | 25 mM Hepes |

| | |
|---|---|
| | 3 M Ammonium Sulphate<br>5 mM β-Mercaptoethanol<br>Q.S. 1 L $ddH_2O$, pH 7.2 |
| Hydrophobic Ionic Buffer B | 10 mM Hepes<br>5 mM β-Mercaptoethanol<br>Q.S. 1 L $ddH_2O$, pH 7.2 |
| Immobilized Metal Ion Affinity Chromatography (IMAC) Buffer A | 1 mM $MgCl_2$<br>25 mM $NaH_2PO_4$<br>500 mM NaCl<br>5 mM β-Mercaptoethanol<br>Q.S. 1 L $ddH_2O$, pH 7.2 |
| Immobilized Metal Ion Affinity Chromatography (IMAC) Buffer B | 1 mM $MgCl_2$<br>25 mM $NaH_2PO_4$<br>500 mM NaCl<br>1 M Imidazole<br>5 mM β-Mercaptoethanol<br>Q.S. 1 L $ddH_2O$, pH 7.2 |
| LiAcTE | 100 mM LiAc<br>10 mM Tris Base, pH 7.2<br>1 mM EDTA<br>Q.S. 500 mL $ddH_2O$ |
| Luria Broth, Miller's | 25 g LB powder<br>1 L ddH20 |
| Lysis Buffer (yeast) | 2.2 M NaOH<br>β-Mercaptoethanol<br>200 mM PMSF<br>550 μL $ddH_2O$ |
| PEG | 10 mM Tris Base pH 7.2<br>100 mM LiAc<br>1 mM EDTA + 40 % (v/v) PEG 3550<br>Q.S. 125 mL $ddH_2O$ |
| Ponceau stain | 1 g Ponceau S<br>50 mL Acetic acid<br>Q.S. 1 L $ddH_2O$ |
| 10X PBS | 1600 g NaCl<br>40 g KCl<br>48 g $KH_2PO_4$<br>432 g $Na_2HPO_4$<br>Q.S. 20 L $ddH_2O$ |

| | |
|---|---|
| Resuspension Buffer | 25 mM Hepes<br>1 mM $MgCl_2$<br>500 mM NaCl<br>20 mM Imidazole<br>5 mM β-Mercaptoethanol<br>Q.S. 1 L $ddH_2O$, pH 7.2 |
| 4X Running Gel Buffer | 363.4 g Tris Base<br>1600 mL $ddH_2O$<br>8 g SDS<br>Q.S. 2 L $ddH_2O$<br>pH 8.8 |
| 6X SDS-PAGE Sample Buffer | 30 % (v/v) Glycerol<br>120 mM Tris Base pH 7.0<br>6 % (w/v) SDS<br>0.6 % (w/v) Bromophenol Blue |
| Drop Out Yeast Medium | 2 % (w/v) Carbon Source (Galactose or Glucose or Raffinose) where indicated<br>1.75 g Yeast Nitrogen Base<br>5 g Ammonium Sulphate<br>Amino Acids:<br>2 mg/mL Adenine Sulphate<br>4 mg/mL Arginine<br>10 mg/mL Aspartate<br>10 mg/mL Glutamic Acid<br>6 mg/mL Isoleucine<br>10 mg/mL Leucine<br>5 mg/mL Lysine<br>2 mg/mL Methionine<br>5 mg/mL Phenylalanine<br>40 mg/mL Serine<br>20 mg/mL Threonine<br>2 mg/mL Tyrosine<br>15 mg/mL Valine<br>The following were added unless omitted for drop out media:<br>33 mg/mL Histidine<br>10 mg/mL Tryptophan<br>2 mg/mL Uracil<br>Q.S. 1 L $ddH_2O$<br>For Solid Media:<br>20 g Agar |
| Stacking Gel Buffer | 33.92 g Tris Base<br>1800 mL $ddH_2O$, pH 6.8 |

| | |
|---|---|
| | 2.2 g SDS<br>Q.S. 2 L dd$H_2O$ |
| 50X TAE | 242 g Tris Base<br>57.1 mL Glacial Acetic Acid<br>100 mL 0.5 M EDTA<br>Q.S. 1 L dd$H_2O$, pH 8.0 |
| 10X TBS (tris-buffered saline) | 320 g NaCl<br>8 g KCl<br>120 g Tris Base<br>Q.S. 4 L dd$H_2O$, pH 8.0 |
| 10X Western Transfer Buffer | 605 g Tris Base<br>2880 g Glycine<br>Q.S. 20 L dd$H_2O$ |
| YPD | 10 g Yeast Extract<br>10 g Peptone<br>20 g Agar<br>2 % (w/v) Galactose or Glucose<br>Q.S. 1 L dd$H_2O$ |

*Q.S. – quantum sufficit

### 2.1.3 Plasmid vectors and yeast strains

Plasmid vectors constructed, or used from other studies, containing selectable markers and primers used to construct genes of interest, are outlined in Table 2.4. Yeast strains outlined in Table 2.5 were constructed by integration of plasmids or used from other studies are outlined in Table 2.5 and include site of integration, variant of Hsp82p expressed, and any genes deleted.

**Table 2.4** Plasmids

| Plasmid Name | Derived From | Selection marker or epitope tag | Primers |
|---|---|---|---|
| pET11dhisHsp82 | | $Amp^r$, HexaHis | |
| pET11dhisHsp82$^{E381K}$ | pET11dhisHsp82 | $Amp^r$, HexaHis | 123[2], 124[2] |
| pET11dhisAha1 | | $Amp^r$, HexaHis | |
| pET11dhisHch1 | | $Amp^r$, HexaHis | |
| pET11dhisSba1 | | $Amp^r$, HexaHis | |
| pET11dhisSti1 | | $Amp^r$, HexaHis | |
| pET11dhisHch1Aha1 chimera | pET11dhisAha1, pET11dhisHch1 | $Amp^r$, HexaHis | 026[3], 467[3], 468[3], 029[3] |
| pET11dhisNterminalAha1 | pET11dhisAha1 | $Amp^r$, HexaHis | 013[1], 217[1] |
| pET11dhisAha1$^{D53K}$ | pET11dhisAha1 | $Amp^r$, HexaHis | 550[2], 551[2] |
| pET11dhisAha1$^{R59A}$ | pET11dhisAha1 | $Amp^r$, HexaHis | 558[2], 599[2] |
| pET11dhisAha1$^{K60A}$ | pET11dhisAha1 | $Amp^r$, HexaHis | 560[2], 561[2] |
| pET11dhisAha1$^{K62A}$ | pET11dhisAha1 | $Amp^r$, HexaHis | 562[2], 563[2] |
| pET11dhisAha1Δ11 | pET11dhisAha1 | $Amp^r$, $HexaHis_6$ | 572[1], 029[1] |
| pET11dhischimera DomainSwap2 | pET11dhisAha1, pET11dhisHch1 | $Amp^r$, HexaHis | 028[3], 497[3], 498[3], 029[3] |
| pET11dhischimera | pET11dhisAha1, | $Amp^r$, HexaHis | 026[3], |

| | | | |
|---|---|---|---|
| DomainSwap3 | pET11dhisHch1 | | 500[3], 499[3], 502[3], 506[3], 029[3] |
| pET11dhischimera DomainSwap5 | pET11dhisAha1, pET11dhisHch1 | Amp$^r$, HexaHis | 026[3], 503[3], 504[3], 029[3] |
| pET11dhis1b | pET11dhisAha1, pET11dhisHch1 | Amp$^r$, HexaHis | 508[3], 509[3] |
| pET11dhis2b | pET11dhisAha1, pET11dhisHch1 | Amp$^r$, HexaHis | 510[3], 511[3] |
| pET11dhis3b | pET11dhisAha1, pET11dhisHch1 | Amp$^r$, HexaHis | 512[3], 513[3] |
| pET11dhis4b | pET11dhisAha1, pET11dhisHch1 | Amp$^r$, HexaHis | 514[3], 515[3] |
| pET11dhisAha1loop6swap | pET11dhisAha1, pET11dhisHch1 | Amp$^r$, HexaHis | 495[4], 496[4] |
| pET11dhisHch1Chimera loop6swap | pET11dhisAha1, pET11dhisHch1 | Amp$^r$, HexaHis | 493[4], 494[4] |
| p404GPDhisHsp82 | | TRP1, HexaHis | |
| p404GPDhisHsp82$^{E381K}$ | p404GPDhisHsp82 | TRP1, HexaHis | 123[2], 124[2] |
| p404GPDhisHsp82$^{V391E}$ | p404GPDhisHsp82 | TRP1, HexaHis | 289[2], 290[2] |
| p404GPDhisHsp82$^{A587T}$ | p404GPDhisHsp82 | TRP1, HexaHis | 99[2], 100[2] |
| p404GPDhisHsp82$^{E381K/A587T}$ | p404GPDhisHsp82 | TRP1, HexaHis | 99[2], 100[2], 123[2], 124[2], |
| pRS426854 vc | | URA3 | |
| pRS426854Aha1myc | pRS426854 | URA3, myc | |

| | | | |
|---|---|---|---|
| pRS426854Hch1myc | pRS426854 | URA3, myc | |
| pRS426854Hch1Aha1 chimeramyc | pRS426854Aha1 myc, pRS426854Hch1 myc | URA3, myc | 026[3], 029[3], 468[3], 467[3] |
| pRS426854NterminalAha1 myc | pRS426854Aha1 myc | URA3, myc | 026[1], 193[1] |
| pRS426854Hch1myc$^{D53K}$ | pRS426854Hch1 myc | URA3, myc | 548[2], 549[2] |
| pRS426854Hch1myc$^{R59A}$ | pRS426854Hch1 myc | URA3, myc | 552[2], 553[2] |
| pRS426854Hch1myc$^{K60A}$ | pRS426854Hch1 myc | URA3, myc | 554[2], 555[2] |
| pRS426854Hch1myc$^{K62A}$ | pRS426854Hch1 myc | URA3, myc | 556[2], 557[2] |
| pRS426854Hch1Δ11myc | pRS426854Hch1 myc | URA3, myc | 017[1], 571[1] |
| pRS426854Aha1p$^{1-156}$ DomainSwap1myc | pRS426854Aha1 myc, pRS426854Hch1 myc | URA3, myc | 017[3], 500[3], 499[3], 193[3] |
| pRS426854Hch1Domain Swap2myc | pET11dhisDomain Swap2 | URA3, myc | 013[3], 090[3] |
| pRS426853Hch1pDomain Swap3myc | pET11dhisDomain Swap3 | URA3, myc | 013[3], 090[3] |
| pRS426854Aha1p$^{1-156}$ DomainSwap4myc | pRS426854Aha1 myc, pRS426854Hch1 myc | URA3, myc | 13[3], 498[3], 497[3], 504[3], 503[3], 193[3] |
| pRS426854Hch1Domain Swap5myc | pET11dhisDomain Swap5 | URA3, myc | 013[3], 090[3] |
| pRS426854Aha1p$^{1-156}$ DomainSwap6myc | pRS426854Aha1 myc, pRS426854Hch1 | URA3, myc | 013[3], 502[3], 506[3], |

| | | | |
|---|---|---|---|
| | myc | | 090[3] |
| pRS426854-1amyc | pRS426854Aha1 myc, pRS426854Hch1 myc | URA3, myc | 508[3], 509[3] |
| pRS426854-2amyc | pRS426854Aha1 myc, pRS426854Hch1 myc | URA3, myc | 510[3], 511[3] |
| pRS426854-3amyc | pRS426854Aha1 myc, pRS426854Hch1 myc | URA3, myc | 512[3], 513[3] |
| pRS426854-4amyc | pRS426854Aha1 myc, pRS426854Hch1 myc | URA3, myc | 514[3], 515[3] |
| pRS426854Aha1$^{1\text{-}156}$loop6 swapmyc | pRS426854Aha1 myc, pRS426854Hch1 myc | URA3, myc | 495[4], 496[4] |
| pRS426854Hch1loop6swap myc | pRS426854Aha1 myc, pRS426854Hch1 myc | URA3, myc | 493[4], 494[4] |
| pRS41KanTef | p424TEF into p41Kan | G418$^{R}$ | |
| pRS41KanTefHch1myc | pRS41KanTef | G418$^{R}$, myc | |
| pRS41KanTefHch1myc$^{D53K}$ | pRS41KanTefHch1 myc | G418$^{R}$, myc | 548[2], 549[2] |
| pRS41KanTefHch1myc$^{R59A}$ | pRS41KanTefHch1 myc | G418$^{R}$, myc | 552[2], 553[2] |
| pRS41KanTefHch1myc$^{K60A}$ | pRS41KanTefHch1 myc | G418$^{R}$, myc | 554[2], 555[2] |
| pRS41KanTefHch1myc$^{K62A}$ | pRS41KanTefHch1 myc | G418$^{R}$, myc | 556[2], 557[2] |

| | | | |
|---|---|---|---|
| pRS41KanTefHch1$^{\Delta 11}$myc | pRS41KanTefHch1 myc | G418$^{R}$, myc | 017[1], 571[1] |

[1]- primers were used in PCR reaction to amplify gene sequence, see Section 2.2.1

[2]- Quikchange$^{TM}$ Mutagenesis reaction to insert mutation, see Section 2.2.2

[3]- primer pairs were used in PCR reactions, the products of which were used in a gene synthesis reaction

[4]- Megaprimers used to insert large gene sequence, see Section 2.2.3

**Table 2.5** Yeast strains

| Yeast Strain | Genotype | Source |
|---|---|---|
| ΔPCLD82a | *MATa ade2-1 leu2-3,112 his3-11,15 trp1-1 ura3-1 can1-100 hsc82::LEU2 hsp82::LEU2 pKAT6* | Nathan and Lindquist (1995) |
| iP82a | *MATa ade2-1 leu2-3,112 his3-11,15 trp1-1 ura3-1 can1-100 hsc82::LEU2 hsp82::LEU2 pTGPD-HSP82* | Nathan and Lindquist (1995) |
| iP82a *Δhch1* | *MATa ade2-1 leu2-3,112 his3-11,15 trp1-1 ura3-1 can1-100 hch1::URA3 hsc82::LEU2 hsp82::LEU2 pTGPD-HSP82* | Armstrong (2012) |
| iP82a *Δaha1* | *MATa ade2-1 leu2-3,112 his3-11,15 trp1-1 ura3-1 can1-100 aha1::URA3 hsc82::LEU2 hsp82::LEU2 pTGPD-HSP82* | Armstrong (2012) |
| iE381Ka | *MATa ade2-1 leu2-3,112 his3-11,15 trp1-1 ura3-1 can1-100 hsc82::LEU2 hsp82::LEU2 pTGPD-HSP82* | Nathan and Lindquist (1995) |
| iE381Ka *Δhch1* | *MATa ade2-1 leu2-3,112 his3-11,15 trp1-1 ura3-1 can1-100 hch1::URA3 hsc82::LEU2* | Armstrong (2012) |

| | | |
|---|---|---|
| | *hsp82::LEU2 pTGPD-HSP82* | |
| iE381Ka *Δaha1* | *MATa ade2-1 leu2-3,112 his3-11,15 trp1-1 ura3-1 can1-100 aha1::URA3 hsc82::LEU2 hsp82::LEU2 pTGPD-HSP82* | Armstrong (2012) |
| iTGPD HisHsp82 | *MATa ade2-1 leu2-3,112 his3-11,15 trp1-1 ura3-1 can1-100 hsc82::LEU2 hsp82::LEU2 p404GPD-HisHSP82* | Armstrong (2012) |
| iTGPD HisHsp82 *Δhch1* | *MATa ade2-1 leu2-3,112 his3-11,15 trp1-1 ura3-1 can1-100 hch1::HIS3 hsc82::LEU2 hsp82::LEU2 p404GPD-HisHSP82* | Armstrong (2012) |
| iTGPD HisHsp82 *Δaha1* | *MATa ade2-1 leu2-3,112 his3-11,15 trp1-1 ura3-1 can1-100 aha1::HIS3 hsc82::LEU2 hsp82::LEU2 p404GPD-HisHSP82* | Armstrong (2012) |
| iTGPD HisE381K | *MATa ade2-1 leu2-3,112 his3-11,15 trp1-1 ura3-1 can1-100 hsc82::LEU2 hsp82::LEU2 p404GPD-HisHSP82$^{E381K}$* | This study |
| iTGPD HisE381K *Δhch1* | *MATa ade2-1 leu2-3,112 his3-11,15 trp1-1 ura3-1 can1-100 hch1::HIS3 hsc82::LEU2 hsp82::LEU2 p404GPD-HisHSP82$^{E381K}$* | This study |
| iTGPD HisE381K *Δaha1* | *MATa ade2-1 leu2-3,112 his3-11,15 trp1-1 ura3-1 can1-100 aha1::HIS3 hsc82::LEU2 hsp82::LEU2 p404GPD-HisHSP82$^{E381K}$* | This study |
| iTGPD HisA587T | *MATa ade2-1 leu2-3,112 his3-11,15 trp1-1 ura3-1 can1-100 hsc82::LEU2 hsp82::LEU2 p404GPD-HisHSP82$^{A587T}$* | Armstrong (2012) |
| iTGPD HisA587T *Δhch1* | *MATa ade2-1 leu2-3,112 his3-11,15 trp1-1 ura3-1 can1-100 hch1::HIS3 hsc82::LEU2 hsp82::LEU2 p404GPD-* | Armstrong (2012) |

| | | |
|---|---|---|
| | *HisHSP82$^{A587T}$* | |
| iTGPD HisA587T/E381K | *MATa ade2-1 leu2-3,112 his3-11,15 trp1-1 ura3-1 can1-100 hsc82::LEU2 hsp82::LEU2 p404GPD-HisHSP82$^{A587T/E381K}$* | This study |
| iTGPD HisA587T/E381K *Δhch1* | *MATa ade2-1 leu2-3,112 his3-11,15 trp1-1 ura3-1 can1-100 hch1::HIS3 hsc82::LEU2 hsp82::LEU2 p404GPD-HisHSP82$^{A587T/E381K}$* | This study |

### 2.1.4 Primers

Primers were used in a Polymerase Chain Reaction following procedure outlined by QIAGEN TopTaq protocol to generate specific genes, add tags or insert mutations are outlined in Table 2.6.

**Table 2.6** Primers used for molecular cloning

| Primer ID | Name | Sequence |
|---|---|---|
| 009 | senseScHsp82BamHI | gagagaggatccatggctagtgaaacttttgaatttcaagc |
| 012 | antisenseScHsp82mycXhoI | gagagactcgagtcactacaaatcttcttcagaaatcaatttttgttcatctacctcttccatttcg |
| 022 | NScHsp82NdeI | gagagacatatggctggtgaaacttttg |
| 023 | CScHsp82BamHI | gagagaggatcctcactaatctacctcttccatttcggtg |
| 017 | senseScHch1BamHI | gagagaggatccatggttgtcttgaatccaaataactg |
| 026 | NScHch1NdeI | gagagacatatgggtgtcttgaatcc |
| 090 | antisenseHch1mycSacI | gagagagagctctcactacaaatcttcttcagaaatcaatttttgttccataacttgtatatccttttgagtgttc |

| | | |
|---|---|---|
| 013 | senseScAha1BamHI | gagagaggatccatggtcgtgaataacccaaataactg |
| 126 | antisensemycAHA1NotI | gagagagcggccgctcactacaaatcttcttcagaaatcaatttttgttccattaatacggcaccaaagccg |
| 028 | NScAha1NdeI | gagagacatatggtcgtgaataacccaaataactggc |
| 029 | CScAha1 BamHI | gagagaggatcctcactataatacggcaccaaagccg |
| 193 | antisenseAHA1Nterm156mycNotI | gagagagcggccgctcactacaaatcttcttcagaaatcaatttttgttccatcacctgaatgtcattaccatgggtggccagc |
| 217 | antisenseSCAha1BamH1 (stop@156aa) | gagagaggatcctcactataatacggcaccaaagccgaatg |
| 044 | NScSba1NdeI | gagagacatatgtccgataaagttattaaccc |
| 045 | CScSba1BamHI | gagagaggatcctcactaagctttcacttccggctc |
| 046 | NScSti1NdeI | gagagacatatgtcattgacagccgatg |
| 047 | CScSti1BamHI | gagagaggatcctcactagcggccagtccggatgataccagcagcgatc |
| 123 | sQCHsp82E381KXbaI | gactctgaggatttaccattgaatttgtctagaaaaatgttacaacaaaataagatcatg |
| 124 | aQCHsp82E381KXbaI | catgatcttattttgttgtaacatttttctagacaaattcaatggtaaatcctcagagtc |
| 289 | sQCHsp82V391E | gttacaacaaaataagatcatgaaggagattagaaagaacattgtcaaaaag |
| 290 | aQCHsp82V391E | ctttttgacaatgttctttctaatctccttcatgatcttatttttgttgtaac |
| 099 | sQCHsp82T587AwtAfeI | cagaactggtcaatttggttggagcgctaacatggaaagaatcatgaaggc |
| 100 | aQCHsp82T587AwtAfeI | gccttcatgattctttccatgttagcgctccaaccaaattgaccagttctg |
| 467 | schimerantermhch1aha1 | ctcaaaggatatacaagttcccgaatctcaggtg |
| 468 | achimerantermhch1aha1 | cacctgagattcgggaacttgtatatcctttgag |

| | | |
|---|---|---|
| 493 | sQCVLHchtoGPAha | cagttgtcgatgaacgtcaaaggacacgtggactctaaggacggatcggcattgccagcggacgggaaactagaaattccag |
| 494 | aQCVLHchtoGPAha | ctggaatttctagtttcccgtccgctggcaatgccgatccgtccttagagtccacgtgtcctttgacgttcatcgacaactg |
| 495 | sQCGPAhatoVLHch | gaaaatcacggtgttaatagaggtgacaaatttggatactaataaggacgacgaggatgatgacggcatacttttcgagggtagcattaacgttcctg |
| 496 | aQCGPAhatoVLHch | caggaacgttaatgctaccctcgaaaagtatgccgtcatcatcctcgtcgtccttattagtatccaaatttgtcacctctattaacaccgtgattttc |
| 497 | sA12H | gaaggtgattgtgaagttaatcaaaggaagggcaagccg |
| 498 | aA12H | cggcttgcccttcctttgattaacttcacaatcaccttc |
| 499 | sH12A | caccggtgactccaacgtatctcagcgtaaggggaaggttatatc |
| 500 | aH12A | gatataaccttcccccttacgctgagatacgttggagtcaccggtg |
| 501 | sA23H | ctaaggacggatcggcattgccagcggacgggaaactag |
| 502 | aA23H | ctagtttcccgtccgctggcaatgccgatccgtccttag |
| 503 | sH23A | cgaggatgatgacggcatacttttcgagggtagcattaacgttcctg |
| 504 | aH23A | caggaacgttaatgctaccctcgaaaagtatgccgtcatcatcctcg |
| 508 | sQCAha1V98toF109intoHch1 | cgggaaactagaaattccagaggttgccttcgatagcgaggcctcaagctatcaatttgatattccgattttgtcgcaagggtttg |
| 509 | aQCAha1V98toF109intoHch1 | caaacccttgcgacaaaatcggaatatcaaattgatagcttgaggcctcgctatcgaaggcaacctctggaatttctagtttcccg |

| | | |
|---|---|---|
| 510 | sQCHch1F103toS108intoAha1 | cgagggtagcattaacgttcctgaatttatgcatgacgagtctgacatatctatatttaaggagac |
| 511 | aQCHch1F103toS108intoAha1 | gtctccttaaatatagatatgtcagactcgtcatgcataaattcaggaacgttaatgctaccctcg |
| 512 | sQCAha1F114toP125intoHch1 | gacgagtctgatattccgatttttaaggagactagcgaattgagtgaagccaagccattggttaggtctgaatttgtccctaaag |
| 513 | aQCAha1F114toP125intoHch1 | ctttagggacaaattcagacctaaccaatggcttggcttcactcaattcgctagtctccttaaaaatcggaatatcagactcgtc |
| 514 | sQCHch1L113toG122intoAha1 | gctatcaatttgacatatctatattgtcgcaagggtttgatgcttttgatggactaattagatccgagttattgcccaag |
| 515 | aQCHch1L113toG122intoAha1 | cttgggcaataactcggatctaattagtccatcaaaagcatcaaacccttgcgacaatatagatatgtcaaattgatagc |
| 548 | sD53KHCH1QC | gttaacccaggtgagtagcatcaccggtaaatccaacgtatctcaaaggaagggc |
| 549 | aD53KHCH1QC | gcccttcctttgagatacgttggatttaccggtgatgctactcacctgggttaac |
| 550 | sD53KAHA1QC | gccaaaatcaagtctgtttcgtccattgaaggtaaatgtgaagttaatcagcgtaaggggaaggt |
| 551 | aD53KAHA1QC | accttcccttacgctgattaacttcacatttaccttcaatggacgaaacagacttgattttggc |
| 552 | sR59AHCH1QC | caccggtgactccaacgtatctcaagcgaagggcaagccgatttgctactttgacttacagttgtcg |
| 553 | aR59AHCH1QC | cgacaactgtaagtcaaagtagcaaatcggcttgccctcgcttgagatacgttggagtcaccggtg |
| 554 | sK60AHCH1QC | caccggtgactccaacgtatctcaaagggcgggcaagccgatttgctactttgacttacagttgtcg |
| 555 | aK60AHCH1QC | cgacaactgtaagtcaaagtagcaaatcggcttgcccgcccttgagatacgttggagtcaccggtg |
| 556 | sK62AHCH1QC | caccggtgactccaacgtatctcaaaggaagggcgcgccgatttgctactttgacttacagttgtcg |

| | | |
|---|---|---|
| 557 | aK62AHCH1QC | cgacaactgtaagtcaaagtagcaaatcggcgcgcc cttcctttgagatacgttggagtcaccggtg |
| 558 | sR59AAHA1QC | gtccattgaaggtgattgtgaagttaatcaggcgaagg ggaaggttatatctttgtttgatttgaaaatcacggtg |
| 559 | aR59AAHA1QC | caccgtgattttcaaatcaaacaaagatataaccttccc cttcgcctgattaacttcacaatcaccttcaatggac |
| 560 | sK60AAHA1QC | gtccattgaaggtgattgtgaagttaatcagcgtgcgg ggaaggttatatctttgtttgatttgaaaatcacggtg |
| 561 | aK60AAHA1QC | caccgtgattttcaaatcaaacaaagatataaccttccc cgcacgctgattaacttcacaatcaccttcaatggac |
| 562 | sK62AAHA1QC | gtccattgaaggtgattgtgaagttaatcagcgtaagg gggcggttatatctttgtttgatttgaaaatcacggtg |
| 563 | aK62AAHA1QC | caccgtgattttcaaatcaaacaaagatataaccgccc ccttacgctgattaacttcacaatcaccttcaatggac |
| 571 | senseBamHIHch1del11 | gagagaggatccatggtggataaaaacaccttacctt ggtc |
| 572 | senseNdeIAha1del11 | gagagacatatggtcgataagaactgcatc |

### 2.1.5 Antibodies

Primary antibodies, listed in Table 2.7, used for western blotting experiments, were acquired from various sources. Secondary antibodies were acquired from Jackson Labs and used at a dilution of 1:2000.

**Table 2.7** Primary antibodies

| Primary Antibody | Dilution | Type | Secondary | Supplier |
|---|---|---|---|---|
| Anti-Actin | 1:2000 | Polyclonal | Goat α Rabbit | Dr. Gary Eitzen |
| Anti-HexaHis | 1:1000 | Monoclonal | Goat α Mouse | EMD Millipore Corporation |
| Anti-Hsp82 (K41220A) | 1:1000 | Monoclonal | Goat α Mouse | StressMarq BioSciences Inc. |
| C-Myc Antibody (9E10) | 1:1000 | Monoclonal | Goat α Mouse | Prepared from the 9E10 hybridoma |

## 2.2 Methods

### 2.2.1 Polymerize Chain Reaction (PCR)

Genes of interest were generated using a PCR reaction from a Qiagen TopTaq Polymerase PCR kit with template and primers used listed in Table 2.4. Detailed construction found in Section 2.2.3.

### 2.2.2 QuikChange™ Mutagenesis (QC)

Site directed mutations were introduced using QuikChange™ Mutagenesis protocol from Agilent Technologies. Reactions contained 100ng template DNA along with 4 mMol dNTP, 5 µL 10X Pfu Buffer, 1 µL Pfu, 10 pmol/µL of sense and antisense primer and distilled water to a total volume of 50 µL. Reactions carried out with a PCR protocol on an Eppendorf Mastercyler

machine. 50 µL QC reactions were digested with 2 µL of *Dpn*1 enzyme and incubated for four hours at 37°C.

### 2.2.3 Plasmid construction and isolation

Bacterial expression plasmids were constructed using pET11dhis. Using primers designed to introduce *Nde*I and *Bam*HI restriction sites at the 5' and 3' respectively, *HSP82*, *HCH1* and *SBA1* coding sequences were amplified using PCR. *AHA1* and *STI1* coding sequences were similarly amplified using primers that introduce *Nde*I and *Not*I restriction sites at the 5' and 3' ends respectively. These gene products were digested with either *Nde*I and *Bam*HI or *Nde*I and *Not*I and cloned into the similarly digest pET11his vector. All coding sequences for bacterial expression contained an *N*-terminal HexaHis-tag upstream of the *Nde*I site (Armstrong et al., 2012). Quikchange$^{TM}$ site-directed mutagenesis was used to introduce a lysine mutation in place of E381 residue into pET11dhisHsp82 generating pET11dhisHsp82$^{E381K}$.

*HA$^{chimera}$* coding sequence was constructed in a two-step PCR process. The first PCR amplified *HCH1* coding sequence using primers sense 026 and antisense 468, where the primer 468 contained the first 20 nucleotides of *AHA1* codons 157-350 downstream of *HCH1*. *AHA1$^{157-350}$* coding sequence using primers sense 467 and antisense 029, where primer 467 contained the last 20 nucleotides of *HCH1* coding sequence upstream of *AHA1* codons 157-350. The second PCR step used the two overlapping gene fragments as template with primers sense 026, which is complementary to the 5' end of *HCH1*, and antisense

029, which is complementary to the 3' end of *AHA1*. Other *HCH1* and *AHA1* domain swap variants were constructed similarly using primers listed in Table 2.4 and cloned into pET11dhis vector as described above.

Mutations and loop swaps were introduced into either *HCH1* or *AHA1* coding sequences using QuikChange™ Mutagenesis Protocol. Primers used to introduce mutations for each variant is listed in Table 2.4. Mutations D53K, R59A, K60A, and K62A, were introduced into template plasmids pET11dhisAha1 and pRS426854Hch1myc. Loop swap variants were generated by using megaprimer PCR method to construct plasmids pET11dhisAha1loop6swap, pET11dhisHch1Chimeraloop6swap, pRS426854Hch1loop6swapmyc, and pRS426854Aha1p$^{1\text{-}156}$loop6swapmyc by replacing residues 77 to 95 from *HCH1* with residues 77 to 88 in *AHA1* or *AHA1*$^{1\text{-}156}$ or replacing residues 77 to 88 from *AHA1* with residues 77 to 95 in *HCH1* or *HA*$^{chimera}$ using primers listed in Table 2.4.

Variants *AHA1*$^{1\text{-}156}$ and *AHA1*$^{\Delta 11}$ were amplified using primers 013 and 217, and 572 and 029, respectively by PCR and cloned into pET11dhis as described above.

Galactose-inducible over-expression plasmid, pRS426854, was constructed by cloning the GAL1/10 promoter into pRS426 using *Eco*RI-*Bam*HI (Armstrong et al., 2012). PCR was used to amplify *HCH1*, all *HCH1* mutants and variants or *AHA1*$^{1\text{-}156}$ with restriction sites for *Bam*HI-*Sac*I at the 5' and 3' ends, respectively, from pET11dhis vectors. For *AHA1*, all *AHA1* mutants and variants as well as *HA*$^{chimera}$ and *HA*$^{chimera}$ variants, PCR was used to amplify coding

sequences with *Bam*HI-*Not*I sites at the 5' and 3' ends, respectively, from pET11dhis vectors. All coding sequences were generated with a *C*-terminal myc tag and coding sequences were cloned into similarly digested pRS426854 downstream of the GAL1 promoter.

The yeast integrating plasmid, pRS404GPD, was generated by cloning GPD promotor and CYC terminator from p414GPD into pRS404. *HCH1* coding sequence was amplified by PCR with primers that introduce a *Bgl*II site with a HexaHis-tag at the 5' end and an *Xho*I site at the 3' end, along with nested *Nde*I and *Bam*HI restriction sites were contained at the 5' and 3' end, respectively. *HCH1* PCR product was digested with *Bgl*II and *Xho*I and cloned into pRS404GPD generating pRS404GPDhisHCH1. *HSP82* and mutant $HSP82^{E381K}$, $HSP82^{A587T}$, and $HSP82^{V391E}$ were cloned as *Nde*I and *Bam*HI fragments into similarly cut pRS404GPD to generate the plasmids, pRS404GPDhisHsp82, $pRS404GPDhisHsp82^{E381K}$, $pRS404GPDhisHsp82^{A587T}$, and $pRS404GPDhisHsp82^{V391E}$ (Armstrong et al., 2012). QuikChange Mutagenesis was used to introduce a second mutation, E381K, into the $pRS404GPDhisHsp82^{A587T}$ plasmid, constructing $pRS404GPDhisHsp82^{E381K/A587T}$.

The $G418^{R}$ over-expression plasmids were constructed by cloning the TEF2 promoter into pRS41Kan using *Kpn*I and *Sac*I digest to generate pRS41KanTef (Armstrong et al., 2012; Taxis and Knop, 2006; Mumberg et al., 1995). *HCH1myc* and *HCH1myc* mutants were amplified using PCR from pRS426854Hch1myc and pRS426854Hch1myc variants vectors with *Bam*HI and

*Xho*I sites. PCR products and pRS41KanTef were digested with *Bam*HI and *Xho*I and cloned downstream of the TEF promoter.

### 2.2.4 Restriction endonuclease digestion

Following New England Biolabs protocols, restriction endonuclease reactions were assembled with 1 µg of DNA, 2.5 µL of NEB restriction digestive enzyme, 5 µL enzyme specific NEB 10X reaction buffer, 5 µL of 10X BSA and distilled water to a total of 50 µL. Reaction was incubated at 37°C for four hours. For diagnostic purposes used to verify successful subcloning of PCR products into vector backbones, 0.5 µg of DNA was digested with 0.5 µL of NEB restrictive digestive enzyme, 2 µL of enzyme specific NEB 10X reaction buffer, 2 µL of 10X BSA and distilled water to a total of 20 µL volume. Reaction was incubated at 37 °C for one hour. Yeast integrating p404 plasmids were linearized using *Hind*III prior to integration by plasmid shuffling.

**Table 2.8** Restriction endonucleases

| Restriction Endonuclease | Buffers Etc. | Application |
|---|---|---|
| *Bam*HI-*Nde*I | NEB #4 + BSA | Plasmid Isolation |
| *Bam*HI-*Not*I | NEB #3 + BSA | Plasmid Isolation |
| *Bam*HI-*Sac*I | NEB #4 + BSA | Plasmid Isolation |
| *Bam*HI-*Xho*I | NEB #3 + BSA | Plasmid Isolation |
| *Bgl*II-*Xho*I | NEB #3 + BSA | Plasmid Isolation |
| *Dpn*I | NEB #4 + BSA | QC Mutagenesis |
| *Hind*III | NEB #2 | p404GPD linearization |
| *Kpn*I-*Sac*I | NEB #1 + BSA | Plasmid Isolation |
| *Nde*I-*Not*I | NEB #3 + BSA | Plasmid Isolation |

### 2.2.5 Agarose gel electrophoresis

PCR DNA products and digested DNA products were visualized and separated by agarose gel electrophoresis. 0.8 % agarose gels were used to run sample and 1 Kb DNA ladder and visualized using Cell Biosciences FluorChemQ system. Entire PCR samples or restriction endonuclease digests were run on agarose gel and bands were excised followed by purification. Diagnostic endonuclease digests were run on agarose gels to verify successful cloning.

### 2.2.6 DNA purification

PCR products were purified following PCR Purification Kit Protocol from QIAGEN. PCR product sample was diluted into five times volume of Buffer PB, placed in a QIAquick spin column and centrifuged using an Eppendorf 5417C centrifuge with an F45-30-11 rotor set at 14,000 rpm for one minute. 750 µL Buffer PE was added and spin column was centrifuged using same centrifuge for one minute. Another spin for two minutes was done to dry sample of ethanol and DNA was eluted in a clean 1.5 mL microcentrifuge tube using 50 µL $dH_2O$ and centrifuged again under same conditions for one minute.

Agarose gel purifications were carried out according to QIAGEN QIAquick gel extraction kit Protocol. Following DNA band excision from agarose gel, bands were melted in five times volume of Buffer QG at 50 °C for ten to fifteen minutes. Melted sample was centrifuged through a QIAquick spin column using an Eppendorf 5417C centrifuge with an F45-30-11 rotor set at 14,000 rpm for one minute, flowthrough was discarded and 500 µL of Buffer QG was

centrifuged through spin column again for one minute. 750 µL of Buffer PE was added to column and centrifuged again for one minute followed by a 2-minute dry spin. DNA sample was eluted in 30 µL of $dH_2O$ and centrifuged again for one minute.

### 2.2.7 Ligation

NEB ligase kit was used to combine digested PCR products to vector DNA using 3:1 molar ratio, with 2 µl of 10X Ligase Buffer, 0.75 µl Ligase enzyme and distilled water to a total of 20 µl volume. Control reactions contained only cut vector DNA. Reactions were incubated at room temperature for one hour.

### 2.2.8 *Escherichia coli* transformation

After ligation incubation of one hour, 2 µl of ligation reactions were added to 50 µl of DH5α competent *Escherichia coli* cells. Reactions were incubated on ice for ten minutes, heat shocked at 42 °C for 42 seconds, then incubated on ice for two minutes. 1 mL of LB was added to cell/DNA mixture and were incubated at 37 °C for a one hour recovery. Following incubation, cells were centrifuged for 15 seconds in an Eppendorf 5417C centrifuge with an F45-30-11 rotor set at 14,000 rpm and plated on LB Agar plates containing 100 µg/ml ampicillin, and incubated at 37 °C overnight. Plasmids isolated for protein expression were transformed into BL21(DE3) competent *Escherichia coli* strain following the same procedure as outlined for DH5α competent *Escherichia coli* cells.

### 2.2.9 *Saccharomyces cerevisiae* transformation

To begin the lithium acetate transformation protocol, yeast cells were first grown overnight spinning at 30 °C in 5 mL of YPD and diluted to $OD_{600}$ of 0.3 followed by a spinning incubation for four hours (Ito et al., 1983). Cells were then centrifuged in an Eppendorf 5417C centrifuge with an F45-30-11 rotor set at 3,000 rpm for two minutes and resuspended with 1 mL of sterile $ddH_2O$, centrifuged again at 3,000 rpm for two minutes to pellet washed cells. $ddH_2O$ supernatant was decanted and pelleted cells were resuspended in 1mL solution of Li/Ac. After another spin of 3000, for two minutes and Li/Ac supernatant was decanted, cells were then resuspended in 50 µl of Li/Ac. Cells were resuspended with 10 µl of salmon sperm DNA, 1 µg of DNA, 300 µl of PEG solution (LiAcTE and 40 % PEG3550), and 6 µl of DMSO. Transformations were then incubated for sixty minutes in a 30 °C water bath for recovery, followed by a 42 °C heat shock for fifteen minutes. Cells were then centrifuged for two minutes at 3,000 rpm to pellet yeast cells and supernatant was decanted. Pellets were resuspended in 1 mL of 1 M sorbitol and 1 mL of YPD. Resuspended transformants were incubated in sterile glass tubes while spinning at 30 °C overnight. Following overnight incubation, cells were centrifuged for two minutes at 3,000 rpm and plated on either YPD or selectable media agar plates. Transformed yeast were grown at 30 °C for two days.

### 2.2.10 Protein expression and purification

Following *E. coli* transformation protocol in Section 2.2.8 with BL21(DE3) *E. coli* competent cells, multiple colonies are picked and grown in 5 mL LB cultures containing 0.5 mg ampicillin overnight at 37 °C. Glycerol stocks are prepared from overnight cultures, comprising of 750 µl 30 % glycerol and 750 µl culture, and stored at -80 °C. Multiple colonies are picked to test protein expression and ensure efficient expression of clone. Following this, a 50 mL LB cultures containing 5 mg ampicillin overnight is inoculated with clone from glycerol stock and grown overnight at 37 °C. 10 mL of the initial 50 mL LB culture is used to seed a 750 mL LB culture containing 75 mg ampicillin. 750 mL cultures are grown to an $OD_{600}$ of 1 for Hsp90 and Hsp90 mutants, $OD_{600}$ of 2.0 for Hch1p, or $OD_{600}$ of 0.8 for all other co-chaperones. Once optimal density was reached, gene expression is induced using 1 mM isopropyl-beta-thiogalactopyranoside (IPTG). Cultures were incubated at 37 °C for a time specific to protein being expressed and 100 µl samples were taken of pre-induced cultures and post induced cultures for visualization of protein expression on 10 % SDS-PAGE followed by coomassie blue staining (Section 2.2.19) (Laemmli, 1970; Shapiro and Viñuela, 1967). Following required incubation time, cultures were centrifuged in a Beckman Coulter Avanti J-26XP1 with a JLA-8.1 rotor for twelve minutes at 7,500 rpm. Pellets were resuspended with 1X PBS and transferred to 50 mL falcon tubes, where they were centrifuged for fifteen minutes at 4,150 rpm using a Thermo Scientific Sorval Legend T+ with multiple carrier

swinging bucket 7500 6445 rotor. Lastly, supernatant was decanted and pellets were stored at -80 °C.

### 2.2.11 Mechanical lysis for bacterial cultures

Frozen pellets were resuspended in Resuspension Buffer (Table 2.3) to a total volume of 50 mL. 100 µL of HALT protease inhibitor and 19 µl of β-ME was added to resuspended cells. Cells were then lyzed 5-10 times using an Avestin Emulsiflex C3 until sample turned thick and very viscous. Lyzed sample was pelleted for thirty minutes by ultracentrifugation in a Beckman Coulter Optima L-100K using a Ti60 rotor at 36,000 rpm. Following ultracentrifugation, the clear supernatant was separated from pellet and placed in a new falcon tube.

### 2.2.12 Immobilized Metal Affinity Chromatography (IMAC)

Supernatant from Section 2.2.11 was injected into an AKTA Explorer Fast Protein Liquid Chromatography (FPLC) system with a Frac-950 collector where sample was injected onto a 5 mL HisTrap FastFlow (FF) Nickel ($Ni^{+}$) column from GE Healthcare Life Sciences. Running a gradient of 5-100 % IMAC B containing imidazole over thirteen column volumes in three steps eluted protein samples into 1mL fractions. The first step involved a 5 % IMAC B concentration for two column volumes, the second step involved 5-100 % IMAC B gradient for five column volumes and the last step was 100 % IMAC B for six column volumes. Absorbance chromatogram was used to determine location of sample in eluted fractions and 10 µl of those fractions were run on a 10 % SDS-PAGE to

ascertain concentration and clarity of protein samples. Samples were pooled and concentrated in a 15 mL Amicon Ultra Centrifugal Filter Device by centrifugation in a Thermo Scientific Sorvall Legend T + with a multiple carrier swinging bucket 7500 6445 rotor at 4,150 rpm for fifteen minutes. Concentrated samples were placed in a 1.5 mL microcentrifuge tube and centrifuged in an Eppendorf Centrifuge 5417C with an F45-30-11 rotor set at 14,000 rpm and 4 °C for one minute to pellet any insoluble particulates.

### 2.2.13 Hydrophobic Interaction Chromatography (HIC)

Hsp82 samples were pooled after IMAC runs and total sample volume was diluted with HIC A (Table 2.3). Sample was injected over a 5 mL butyl column from GE Healthcare Life Sciences and Hsp82p proteins were eluted using 0-100 % gradient in eight column volumes of HIC B (Table 2.3). 10 µl of fractionated eluted samples were run on 10 % SDS PAGE to determine clarity and concentration (Laemmli, 1970; Shapiro and Viñuela, 1967). Samples were then pooled and concentrated in 15 mL Amicon Ultra Centrifugal Filter Device in a Thermo Scientific Sorvall Legend T + Centrifuge with a multiple carrier swinging bucket 7500 6445 rotor at 4,150 rpm for fifteen minutes.

### 2.2.14 Gel Filtration Chromatography (GF)

Concentrated 100 µl, 250 µl, or 500 µl samples were injected into FLPC loading port. Hsp82 samples were injected onto a Superose 6 Gel Filtration column (GE Healthcare Life Sciences) using Hsp82 Gel Filtration Buffer (Table

2.3). Co-chaperones were injected on a Superdex 75 Gel Filtration column using CoChaperone Gel Filtration Buffer (Table 2.3). 0.5 mL fractions were eluted and 10 μL of samples were run on 10 % SDS-PAGE to determine clarity and concentration of eluted samples. Following gel filtration, samples were pooled and prepared for measurement with a NanoDrop Spectrophotometer. Multiple readings of protein absorbance at 280 nm ($A_{280}$) were taken and averages were calculated. To determine the final concentration of protein sample purified, the protein's extinction coefficient (ε) was used in the following formula:

Concentration (μM) = (Absorbance at 280 nm ($A_{280}$) / extinction coefficient of protein (ε)) x 1,000,000

Finally, samples were prepared with a calculated concentration and run on a 10 % SDS PAGE to verify concentration and clarity of samples. Pooled protein sample was then divided into either 50 μL or 100 μL fractions and flash frozen using liquid nitrogen and stored at -80 °C.

### 2.2.15 ATPase assay

Hsp82p ATPase activity was analyzed by using a PK/LDH regenerated system and were implemented in triplicate using a 96 well plate with a prepared 4X Reaction Buffer (Table 2.3) or 384 well plate with a prepared 10X Reaction Buffer (Table 2.3) *(Panaretou et al., 1998)*. Absorbance at 340 nm was read every minute for ninety minutes at 30 °C in a BioTek Synergy Plate Reader.

Absorbance values were normalized to a 1 cm pathlength and data exported to Excel by the Gen5 software program. Data was then analyzed and graphed using Prism GraphPad with the values of triplicates shown as averages and standard error of the mean expressed as error. Experiments done in triplicate were averaged and errors of averages are expressed as standard error of the mean. Reaction components were verified by running 10 µL samples on 10 % SDS PAGE and coomassie blue stained.

### 2.2.16 Yeast strain construction

#### 2.2.16.1 iT Hsp82$^{E381K/A587T}$ strains

For iT strains, iTGPD HisA587T/E381K and iTGPD HisA587T/E381K *Δhch1*, plasmid pRS404GPDhisHsp82$^{E831K/A587T}$ was linearized by a HindIII digest and was then shuffled into ΔPCLDa and ΔPCLDa *Δhch1*. The linearized pRS404GPD plasmid contains a functional TRP1 locus that when shuffled, integrates into the non-functional TRP locus on the chromosome of the ΔPCLDa strain using Lithium Acetate Transformation. To select for successful plasmid shuffling, transformations were plated on SC-TRP plates with 1 g/L 5-fluoroorotic acid (5-FOA) *(Boeke et al., 1984)*. All other iT strains were obtained from previous performed experiments in (Armstrong et al., 2012).

#### 2.2.16.2 MIT strains

MIT strains used in experiments were obtained from Dr Susan Lindquist from previously preformed experiments in (Nathan and Lindquist,

1995). Δ galactose-inducible expression system was used in ip82a and iE381Ka strains. Lithium Acetate Transformation was used to transform pRS426854 over-expression plasmids listed in Table 2.4. To ensure the pRS426854 galactose-inducible plasmids were retained in ip82a and iE381Ka strains, the cultures were grown on SC-Ura plates.

#### 2.2.16.3 iT and MIT drug-selectable over-expression strains

Lithium Acetate Transformation was used to transform pRS41KanTef, pRS41KanTefHch1myc,pRS41KanTefHch1myc$^{D53K}$, pRS41KanTefHch1myc$^{R59A}$, pRS41KanTefHch1myc$^{K60A}$, pRS41KanTefHch1myc$^{K62A}$, and pRS41KanTefHch1myc$^{\Delta 11}$ over-expression plasmids into the strains ip82a and iE381Ka, and strain iTGPD hisHsp82. The transformed *S. cerevisiae* cells were plated on YPD + 200 mg/L G418 agar plates following transformation to ensure G418$^{R}$ plasmids were successfully incorporated.

### 2.2.17 Yeast growth assay

Yeast strains were grown in either 5 mL YPD for iT strains, 5 mL SC-URA + RAF for galactose-inducible over-expression system, or 5 mL YPD + 200 mg/L of G418 for G418$^{R}$ strains spinning overnight at 30 °C. All yeast cultures were then diluted to an initial $OD_{600}$ of 0.1 in distilled water and followed by three 10-fold serial dilutions. 5 μL aliquots of iT culture dilutions were plated on YPD medium agar plates or YPD + NVP-AUY922 (50 μM, 200 μM, and 400 μM NVP). YPD dilution assays were grown overnight at room temperature, 30 °C,

34.5 °C and 37 °C, whereas YPD + NVP-AUY922 plates were grown overnight at 30 °C. Galactose-inducible over-expression strains were plated in 5 µL aliquots on galactose vs glucose SC-Ura media plates and grown overnight at 30 °C. The $G418^R$ over-expression strains from both MIT series and iTGPDhisHsp82 were plated in 5 µL aliquots on YPD + 200 mg/L G418 agar plates and YPD + 200 mg/L G418 + NVP-AUY-922 agar plates (50 µM, 200 µM, 400 µM NVP) and were grown overnight at 30 °C.

### 2.2.18 Alkaline lysis for yeast cultures

Galactose-inducible over expression strain were grown overnight spinning, at 30 °C, in 5 mL SC-Ura+GAL cultures. iT yeast strains were grown in 5 mL YPD medium overnight spinning at 30 °C. iT $G418^R$ over-expression strains were grown overnight spinning at 30 °C in YPD + 200 mg/L G418 medium. Following overnight incubation, all strains were diluted to $OD_{600}$ of 5. Yeast cells pelleted by a two minute spin in an Eppendorf 5417C centrifuge with an F45-30-11 rotor set at 3,000 rpm. Pellets were then washed with 1 mL of distilled water, followed by another spin for two minutes, and pellets were resuspended with 500 µL $ddH_2O$ and 90 µL of NaOH Lysis Buffer (Table 2.3). Samples were incubated on ice for ten minutes, followed by the addition of 250 µL 100 % TCA, vortexed for thirty seconds, and incubated for an additional ten minutes on ice. Samples were centrifuged in an Eppendorf 5417C centrifuge with an F45-30-11 rotor set at 14,000 rpm for ten minutes at 4 °C. Pellets were washed with 500 µL of 80 % Acetone. Pellets were then incubated for ten minutes on ice followed by a spin at

14,000 rpm for ten minutes at 4 °C. Supernatant was decanted and pellets were washed with 500 µL 80 % acetone followed by incubation on ice for ten minutes, and centrifuged for ten minutes at 14,000 rpm at 4 °C. Supernatant was removed and pellets were left to dry at room temperature for twenty minutes. Pellets were suspended in 50 µL 2X Sample Buffer (Table 2.3). Samples were then boiled at 100 °C for ten minutes and run on a 10 % SDS-PAGE.

### 2.2.19 Sodium Dodecyl Sulfate Polyacrylamide Gel Electrophoresis (SDS-PAGE) and coomassie blue staining

To verify bacterial protein expression, 100 µL pre- and post-induction culture samples from Section 2.2.10 were prepared by the addition of 20 µL 6X Sample Buffer (Table 2.3) and boiled at 100 °C for fifteen to twenty minutes and then centrifuged using an Eppendorf Centrifuge 5417C with an F45-30-11 rotor set at 14,000 rpm for one minute. 15 µL of sample was separated on 10 % SDS-PAGE running gel (Laemmli, 1970; Shapiro and Viñuela, 1967). Gels were then stained with coomassie blue stain (Table 2.3) to visualize the correct size and amount of protein.

Following alkaline lysis of yeast cultures from Section 2.2.18, samples were resuspended in 50 µL of 2X Sample Buffer (Table 2.3) and boiled for ten minutes at 100 °C. Samples were then centrifuged using an Eppendorf Centrifuge 5417C with an F45-30-11 rotor set at 14,000 rpm for one minute. 15 µL of sample was separated on 10 % SDS-PAGE gel followed by western analysis (Laemmli, 1970; Shapiro and Viñuela, 1967).

### 2.2.20 Western blot analysis

After SDS PAGE, samples are transferred to pure nitrocellulose membrane (BIO RAD) using 1X western buffer + 20 % Methanol (Table 2.3). Membranes were blocked for non-specific binding in 2 % BSA-0.1 % TBS-tween (Tris-buffered saline (TBS), 0.1 % Tween, and 2 % Bovine Serum Albumin). HexaHis-tagged Hsp82p and myc tagged co-chaperone proteins were detected by immunoblotting. Anti-HexaHis Rabbit (1:1000 dilution) antibody was used to probe for Hsp82p overnight at 4 °C, which was then followed by HRP-conjugated anti-rabbit IgG (1:2000 dilution). Anti-myc tag (9E10) mouse (1:1000 dilution) antibody was used to probe for co-chaperone proteins overnight at 4 °C and was followed by HRP-conjugated anti-mouse IgG (1:2000). Actin loading control was probed for with Anti-Actin (1:2000 dilution) antibody overnight at 4 °C followed by HRP conjugated anti-rabbit IgG. Bands were visualized using Enhanced ChemiLuminescence (ECL) and membranes were imaged using the Cell BioSciences FluorChemQ system.

# Chapter Three

## Results – Characterization of the motif requirements for Aha1p function and its homologue Hch1p

## 3.1 A motif specific to the *N*-terminal domain of Aha1p (Aha1p$^{1-156}$) and not shared with Hch1p is required to robustly stimulate the Hsp90 ATPase activity

The Hsp90 co-chaperone Hch1p shares 36% amino acid sequence identity with the 156 amino acid *N*-terminus of Aha1p (Figure 1.3). Previous studies have shown Aha1p stimulates the Hsp82p ATPase activity by up to ~12-fold whereas Hch1p can only weakly stimulate the Hsp82p ATPase rate above the intrinsic rate (Armstrong et al., 2012; Panaretou et al., 2002; Lotz et al., 2003). The weak stimulation of the Hsp82p ATPase activity by Hch1p is thought to be due to the absence of the Aha1p *C*-terminal domain, Aha1p$^{157-350}$. This part of Aha1p interacts with the Hsp82p *N*-terminal domain and is necessary for robust ATPase stimulation. I hypothesized that Hch1p fused to Aha1p$^{157-350}$, HA$^{chimera}$, would stimulate the Hsp82p ATPase rate to the same extent as Aha1p (Figure 3.1A). Surprisingly, the HA$^{chimera}$ was no more effective than unmodified Hch1p in stimulating the Hsp82p ATPase rate (Figure 3.1B). This suggests that robust ATPase stimulation by Aha1p requires a motif or sequence element that is not shared with Hch1p.

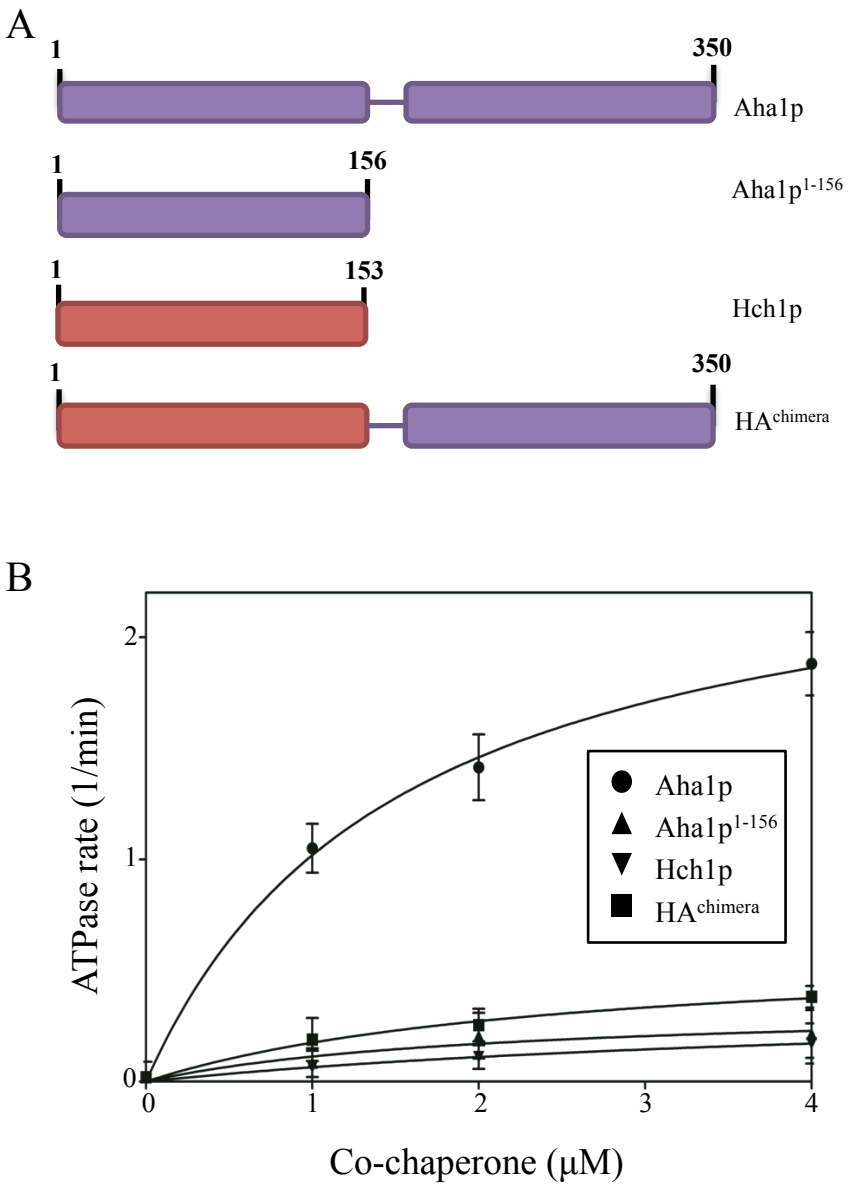


**Figure 3.1 Hch1p cannot fulfill the role of Aha1p$^{1-156}$ in stimulating the Hsp82p ATPase activity.** A. Schematic representation of full length Aha1p, *N*-terminal domain of Aha1p (Aha1p$^{1-156}$), Hch1p and HA$^{chimera}$. B. Stimulation of the Hsp82p ATPase rate by increasing concentrations of Aha1p (circles), Aha1p$^{1-156}$ (up triangles), Hch1p (down triangles), or the HA$^{chimera}$ (squares). Reactions contain 1 μM Hsp82p, and indicated co-chaperone concentrations. ATPase rate shown in μM ATP hydrolyzed per minute per μM of enzyme (1/min).

## 3.2 Hch1p, but not Aha1p$^{1-156}$, suppresses the Hsp82p$^{E381K}$ defect *in vivo*

Previous studies have shown that Hch1p over-expression rescues growth of yeast expressing the Hsp82p *ts* mutant Hsp82p$^{E381K}$ at restrictive temperatures (Nathan et al., 1999). Since the HA$^{chimera}$ did not stimulate the Hsp90 ATPase rate to the same extent as Aha1p, I hypothesize that Aha1p$^{1-156}$ would not suppress the *in vivo* defect of Hsp82p$^{E381K}$. In order to test this, I transformed yeast expressing either wild-type Hsp82p or Hsp82p$^{E381K}$ (obtained from Dr. Susan Lindquist (Nathan and Lindquist, 1995)) with plasmids that over-express *C*-terminally myc tagged Aha1p, Hch1p, Aha1p$^{1-156}$ or HA$^{chimera}$ in a galactose-inducible fashion. Consistent with previous reports, over-expression of Hch1p rescues growth of yeast expressing Hsp82p$^{E381K}$ to near wild- type levels (Figure 3.2A). However, while the HA$^{chimera}$ rescued Hsp82p$^{E381K}$ yeast strains, neither Aha1p nor Aha1p$^{1-156}$ had this effect (Figure 3.2A). Co-chaperone expression was confirmed by probing yeast lysates with anti-myc antibodies by western blot (Figure 3.2B). To verify that the rescue of yeast was not due to differences in Hsp82p expression, Hsp82p levels were verified as compared to actin loading control by probing western blots with anti-Hsp90 and anti-actin antibodies (Figure 3.2B). Hch1p and the HA$^{chimera}$, but not Aha1p or Aha1p$^{1-156}$, were able to rescue growth of yeast expressing Hsp82p$^{E381K}$ suggesting that the effect is mediated by a structural or sequence feature of Hch1p that is not shared with the *N*-terminal domain of Aha1p.

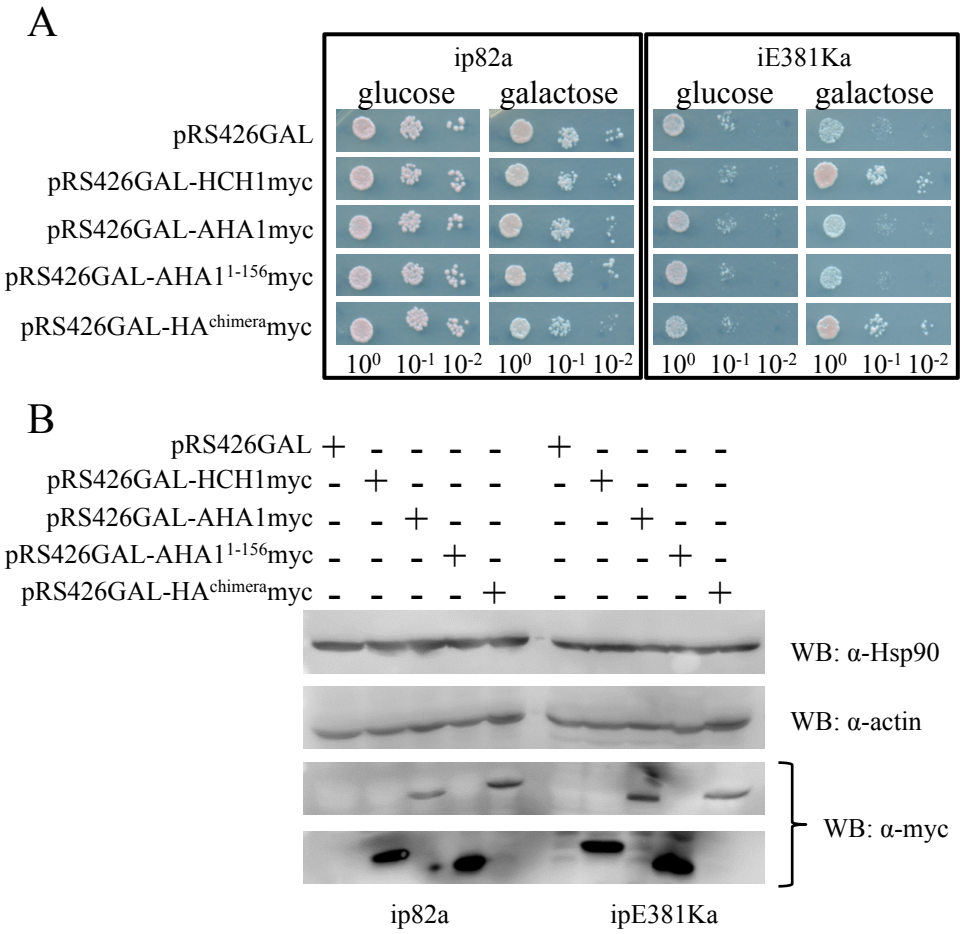


**Figure 3.2 Hch1p, but not Aha1p$^{1-156}$, is required for rescue of *S. cerevisiae* yeast strain expressing Hsp82p$^{E381K}$ as their sole source of Hsp90.** A. Viability of yeast strains ip82a and iE381Ka containing GAL-driven overexpression of myc-tagged Hch1p, the HA$^{chimera}$, Aha1p and Aha1p$^{1-156}$. Cells were grown overnight in SC media lacking uracil (SC-Ura) 2 % raffinose and followed by a dilution to 1 x $10^8$ cells per ml. 10-fold serial dilutions were prepared and 5 µl aliquots were spotted on SC-Ura agar plates supplemented with either 2 % glucose or galactose. B. Western analysis of yeast shown in A with anti-Hsp90, anti-actin, and anti-myc antibodies.

### 3.3 Swap mutations compromise Hch1p and Aha1p folding

The results summarized in Figures 3.1 and 3.2 show the specific properties of Hch1p and Aha1p are linked to some unique sequence or structure in these related co-chaperones. I hypothesized that regions of Hch1p and Aha1p$^{1-156}$ not shared between them are responsible for their unique properties. Candidate regions were identified by sequence alignment and structural modeling based on the known structure of the Aha1p *N*-terminal domain in complex with the middle domain of Hsp82p (Meyer et al., 2004). I selected the sixth loop (between the strands b and c of the β sheet, shown in Figure 3.3C), which is not conserved and located in proximity to the *C*-terminal domain of Hsp90. I hypothesized that this loop in Hch1p is involved in suppressing *in vivo* defect of Hsp82p$^{E381K}$. I employed Quikchange$^{TM}$ mutagenesis to construct my mutants as described in Materials and Methods Section 2.2.3 and the resultant plasmids pET11dhisAha1loop6swap, pET11dhisHch1Chimeraloop6swap were constructed for *in vitro* expression and pRS426854Hch1loop6swapmyc, and pRS426854Aha1p$^{1-156}$loop6swapmyc were constructed for *in vivo* expression. Aha1p and Aha1p$^{1-156}$ residues 77 to 88 replaced with Hch1p residues 77 to 95 or Hch1p and HA$^{chimera}$ residues 77 to 95 replaced with Aha1p residues 77 to 88 (Figure 3.3B). If the 6$^{th}$ loop in Aha1p is required for maximal stimulation of Hsp90 ATPase activity then the HA$^{chimera}$ loop 6 swap mutant would stimulate the Hsp90 ATPase rate *in vitro* to the same extent as Aha1p. Similarly, over-expression of the Aha1p$^{1-156}$ loop 6 swap mutant would overcome the defect in Hsp82p$^{E381K}$ *in vivo*. Unfortunately, loop 6 swap mutants were insoluble when I

attempted to express and purify these mutants from *E. coli*. Aha1p is a soluble and efficiently expressed protein and yields an extremely large absorbance peak during imidazole elution. Figure 3.4B is a representative gel of Aha1p purified following immobilized metal affinity chromatography (IMAC). Although the swap mutants had efficient expression, as represented by Aha1 loop 6 swap mutant expression levels (Figure 3.4A), I did not detect the loop swap mutants during imidazole elution (Figure 3.4B – red box). Since my loop 6 swap mutants were insoluble *in vitro*, and preliminary tests done by a different student in our lab with the loop 6 swap mutants did not rescue growth of yeast expressing Hsp82p$^{E381K}$ (data not shown), I did not pursue rigorous studies with these mutants. The sequence conservation between Hch1p and Aha1p is very poor in strands proximal to the *C*-terminal domain of Hsp90 so it is likely that I did not select the appropriate boundaries for these regions.

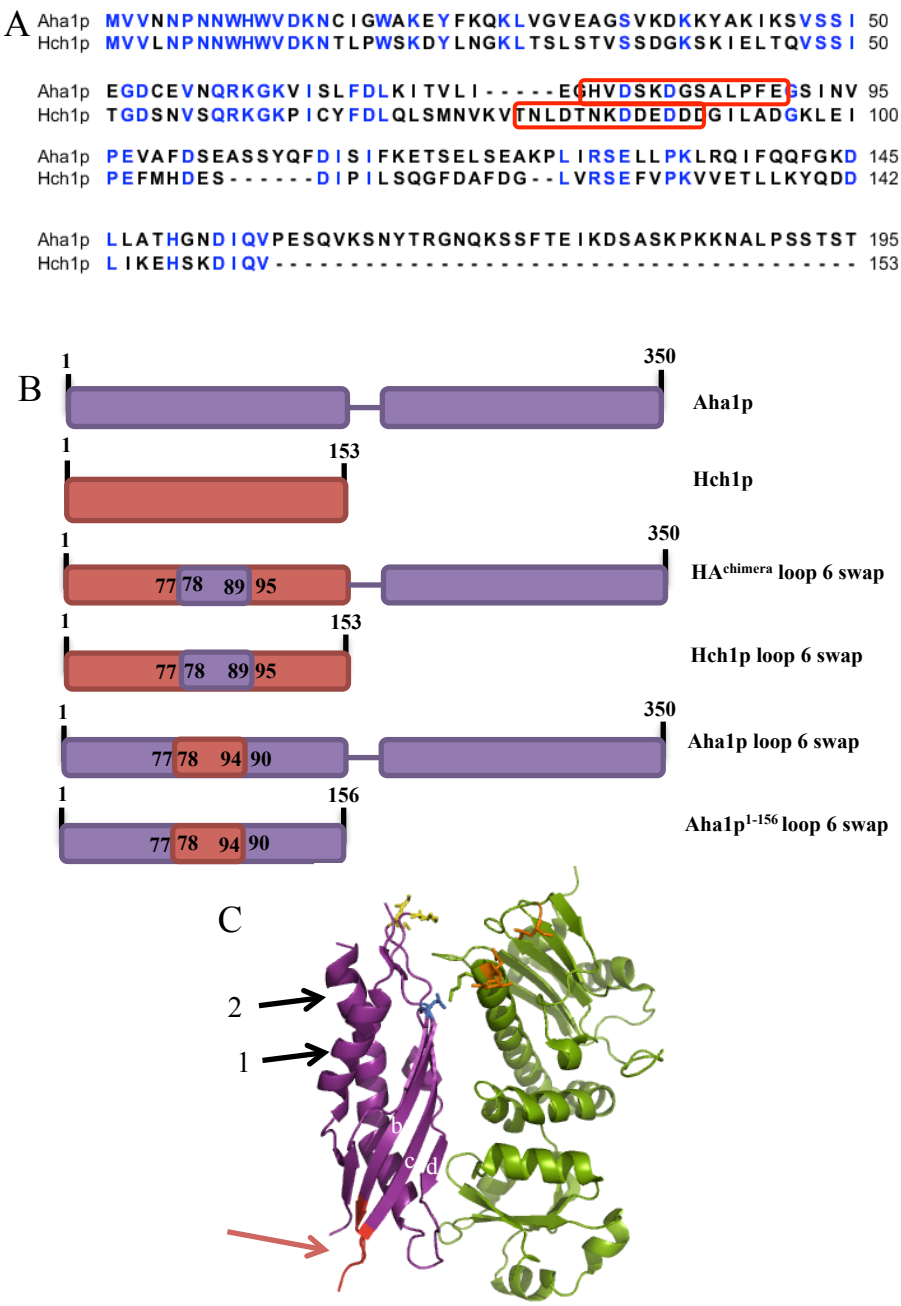


**Figure 3.3 Hch1p Aha1p loop 6 swap construction.** A. Amino acid sequence alignment highlighting loop swapped between Hch1p and Aha1p$^{1-156}$. B. Schematic representation of loop 6 swap mutants created. C. Crystal structure of Aha1p$^{1-156}$ with loop residues (red arrow) between strands labeled b and c of the β sheet are substituted with Hch1p residues to construct loop 6 swap mutants. (Crystal structure adapted from (Meyer et al., 2004).

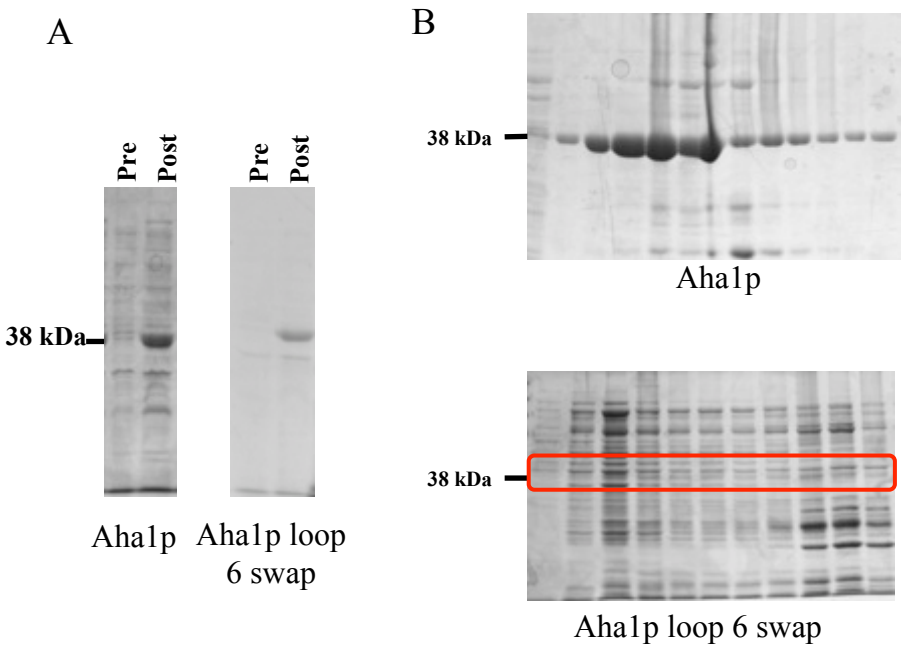


**Figure 3.4** ***In vitro*** **purification of loop 6 swap mutants.** A. Pre and post IPTG induction of Aha1p and Aha1 loop 6 swap mutant. Cultures were grown to an 0.8 $OD_{600}$ and gene expression was induced with 1 mM IPTG and incubated for 4 hours. B. Representative gels of flow through protein levels following an IMAC purification by imidazole elution of Aha1p and Aha1p loop 6 swap mutant and red box highlights expected location of purified mutant protein.

Since changes in the residues of the 6th loop of Hch1p and Aha1p compromised protein folding, I decided to take a more general approach by swapping larger sequences. Hch1p was divided into three sections that were delimited by highly conserved sequences. I hypothesized that substituting larger sections between conserved regions of Aha1p and Hch1p would allow the resultant hybrid proteins to fold into soluble structures (Figure 3.5A, B, C). Constructs containing $HA^{chimera\ DS2}$, $HA^{chimera\ DS3}$, and $HA^{chimera\ DS5}$ were generated for expression and purification from *E. coli* (Figure 3.5B). $Aha1p^{1\text{-}156\ DS1}$, $Hch1p^{DS2}$, $Hch1p^{DS3}$, $Aha1p^{1\text{-}156\ DS4}$, $Hch1p^{DS5}$, and $Aha1p^{1\text{-}156\ DS6}$ were constructed for galactose-inducible over-expression in yeast (Figure 3.5C). $HA^{chimera\ DS2}$, $HA^{chimera\ DS3}$, and $HA^{chimera\ DS5}$ were expressed in *E. coli* (Figure 3.5E) but insoluble when I attempted to purify them (Figure 3.5F). The growth assays with iE381Ka yeast strain over-expressing $Aha1p^{1\text{-}156\ DS1}$, $Aha1p^{1\text{-}156\ DS4}$, and $Aha1p^{1\text{-}156\ DS6}$ as well as $Hch1p^{DS2}$, $Hch1p^{DS3}$, and $Hch1p^{DS5}$, showed no signs of yeast growth rescue as compared to strains over-expressing wild-type Hch1p (Figure 3.6A and Figure 3.6C, respectively). Co-chaperone accumulation was not detected in lysates when probed by western blot with anti-myc antibodies as compared to unmodified Hch1p, Aha1p, $Aha1p^{1\text{-}156}$ or the $HA^{chimera}$ (Figure 3.6B and Figure 3.6D). Exchanging large sections of $Aha1p^{1\text{-}156}$ and Hch1p apparently disrupts the overall folding of each co-chaperone, which suggests that while the conserved sections of Hch1p and Aha1p may fold into similar structures, the residues that comprise similar structures are not compatible between the two co-chaperones. I concluded that either the Hch1p and Aha1p protein structures differ

significantly despite their high degree of conservation, or that they fold into similar structures, but there are strict local requirements to maintain folding in the context of each protein.

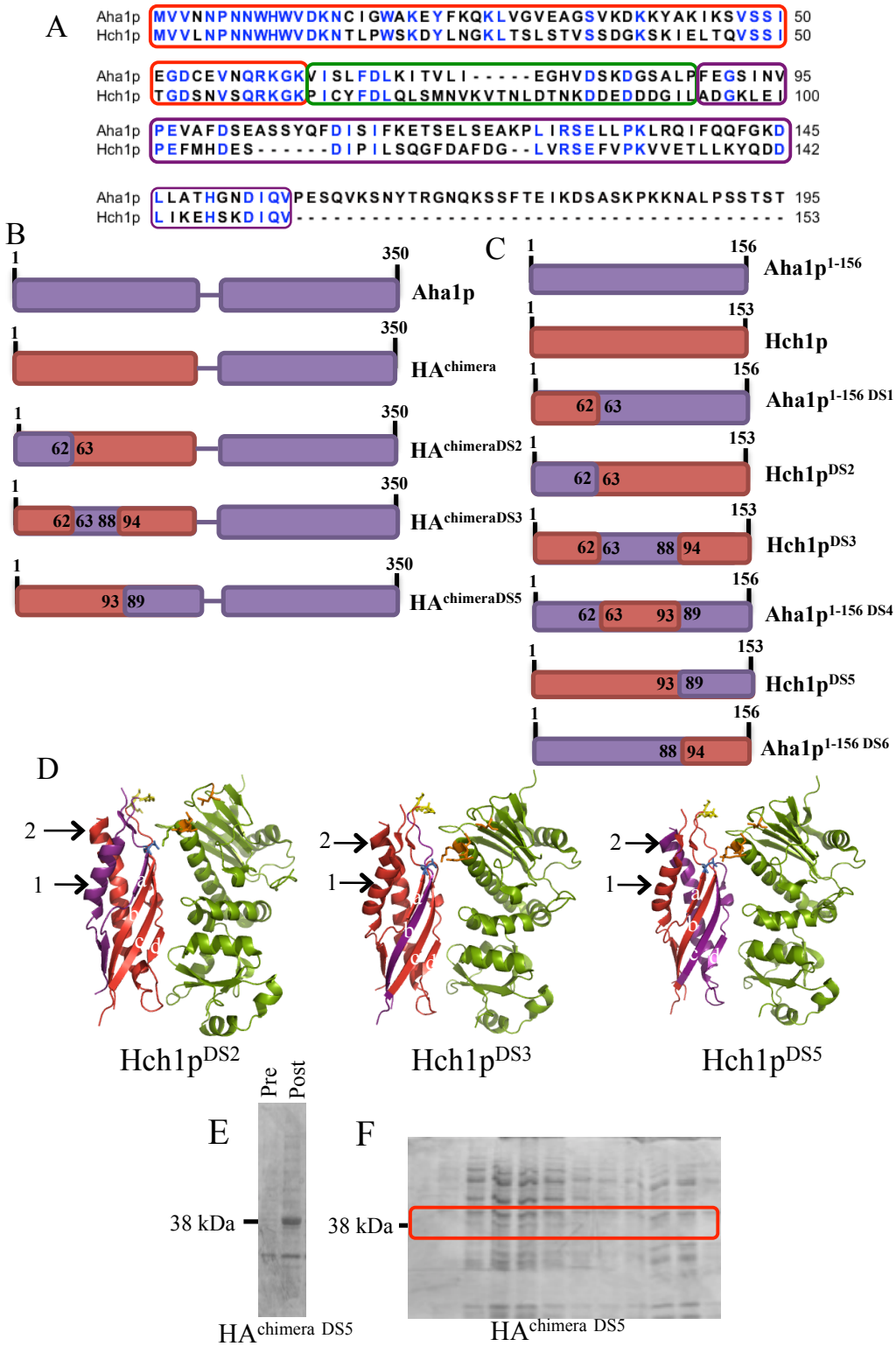
A
Aha1p MVVNNPNNWHWVDKNCIGWAKEYFKQKLVGVEAGSVKDKKYAKIKSVSSI 50
Hch1p MVVLNPNNWHWVDKNTLPWSKDYLNGKLTSLSTVSSDGKSKIELTQVSSI 50
Aha1p EGDCEVNQRKGKVISLFDLKITVLI-----EGHVDSKDGSALPFEGSINV 95
Hch1p TGDSNVSQRKGKPICYFDLQLSMNVKVTNLDTNKDDEDDDGILADGKLEI 100
Aha1p PEVAFDSEASSYQFDISIFKETSELSEAKPLIRSELLPKLRQIFQQFGKD 145
Hch1p PEFMHDES------DIPILSQGFDAFDG--LVRSEFVPKVVETLLKYQDD 142
Aha1p LLATHGNDIQVPESQVKSNYTRGNQKSSFTEIKDSASKPKKNALPSSTST 195
Hch1p LIKEHSKDIQV----------153
B
Aha1p
HAchimera
HAchimeraDS2
HAchimeraDS3
HAchimeraDS5
C
Aha1p1-156
Hch1p
Aha1p1-156 DS1
Hch1pDS2
Hch1pDS3
Aha1p1-156 DS4
Hch1pDS5
Aha1p1-156 DS6
D
Hch1pDS2
Hch1pDS3
Hch1pDS5
E
Pre
Post
38 kDa
HAchimera DS5
F
38 kDa
HAchimera DS5

**Figure 3.5 Domain Swap mutants are insoluble *in vitro*.** A. Alignment of Aha1p and Hch1p highlighting swapped sections in red, green and purple, to construct swap mutants. B. Schematic representation of Aha1p, $HA^{chimera}$, and $HA^{chimera\ DS2}$, $HA^{chimera\ DS3}$, and $HA^{chimera\ DS5}$ constructed for *in vitro* testing. C. Schematic representation of Hch1p, $Aha1p^{1-156}$, $Aha1p^{1-156\ DS1}$, $Hch1p^{DS2}$, $Hch1p^{DS3}$, $Aha1p^{1-156\ DS4}$, $Hch1p^{DS5}$, $Aha1p^{1-156\ DS6}$ constructed for *in vivo* testing. D. Crystal structure of $Aha1p^{1-156}$ highlighting residues (red) replaced with residues of Hch1p to construct $Hch1p^{DS2}$, $Hch1p^{DS3}$, and $Hch1p^{DS5}$. E. Pre and post $HA^{chimera\ DS5}$ protein levels following induction with 1 mM IPTG. Cultures were grown to an 0.8 $OD_{600}$ and induced for 4 hours. F. Representative gel of $HA^{chimera\ DS5}$ flow through protein levels following IMAC purification. (Crystal structure adapted from (Meyer et al., 2004).

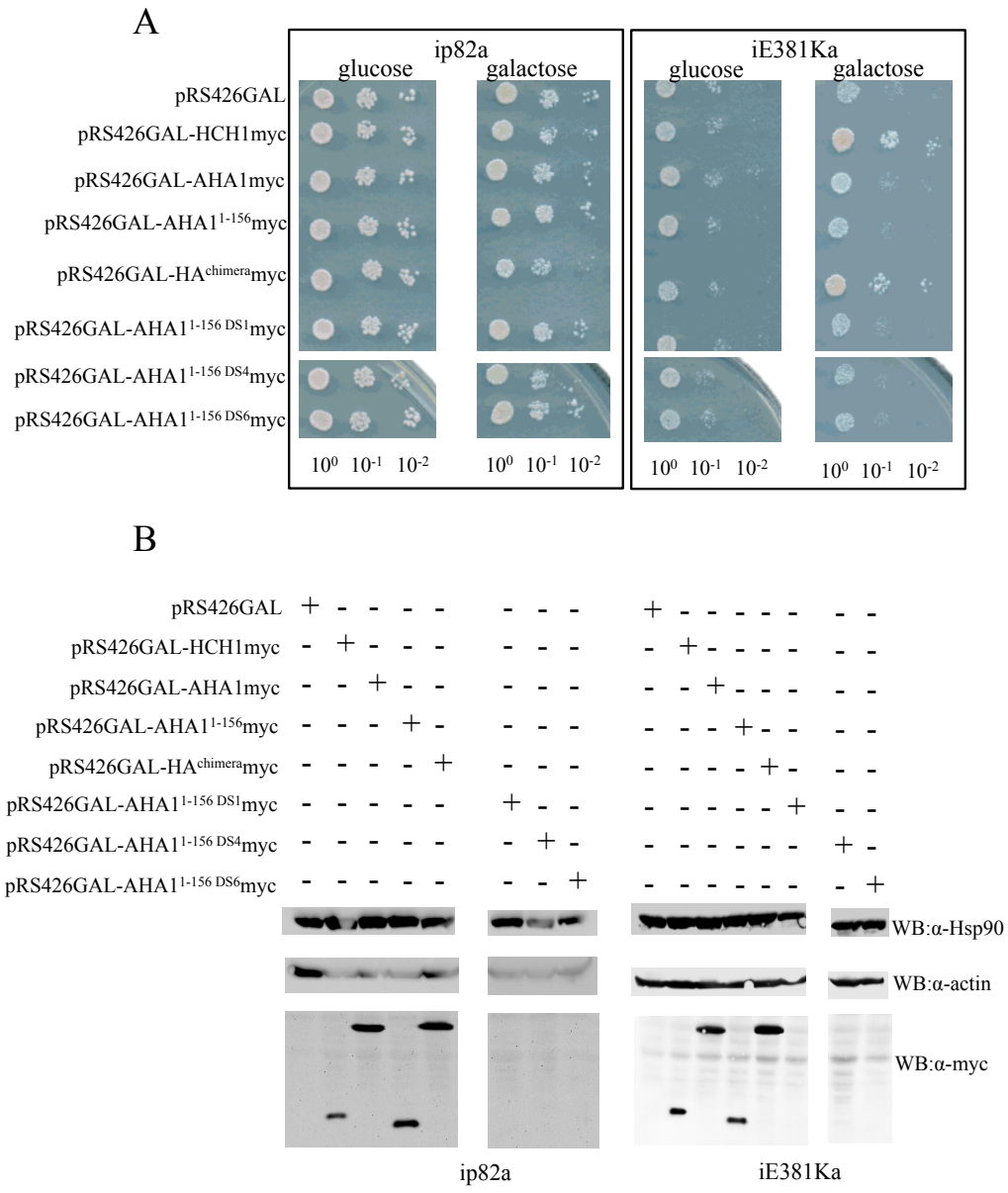
A
ip82a
iE381Ka
glucose
galactose
pRS426GAL
pRS426GAL-HCH1myc
pRS426GAL-AHA1myc
pRS426GAL-AHA1 1-156 myc
pRS426GAL-HA chimera myc
pRS426GAL-AHA1 1-156 DS1 myc
pRS426GAL-AHA1 1-156 DS4 myc
pRS426GAL-AHA1 1-156 DS6 myc
10 0 10 -1 10 -2
B
WB:α-Hsp90
WB:α-actin
WB:α-myc
ip82a
iE381Ka

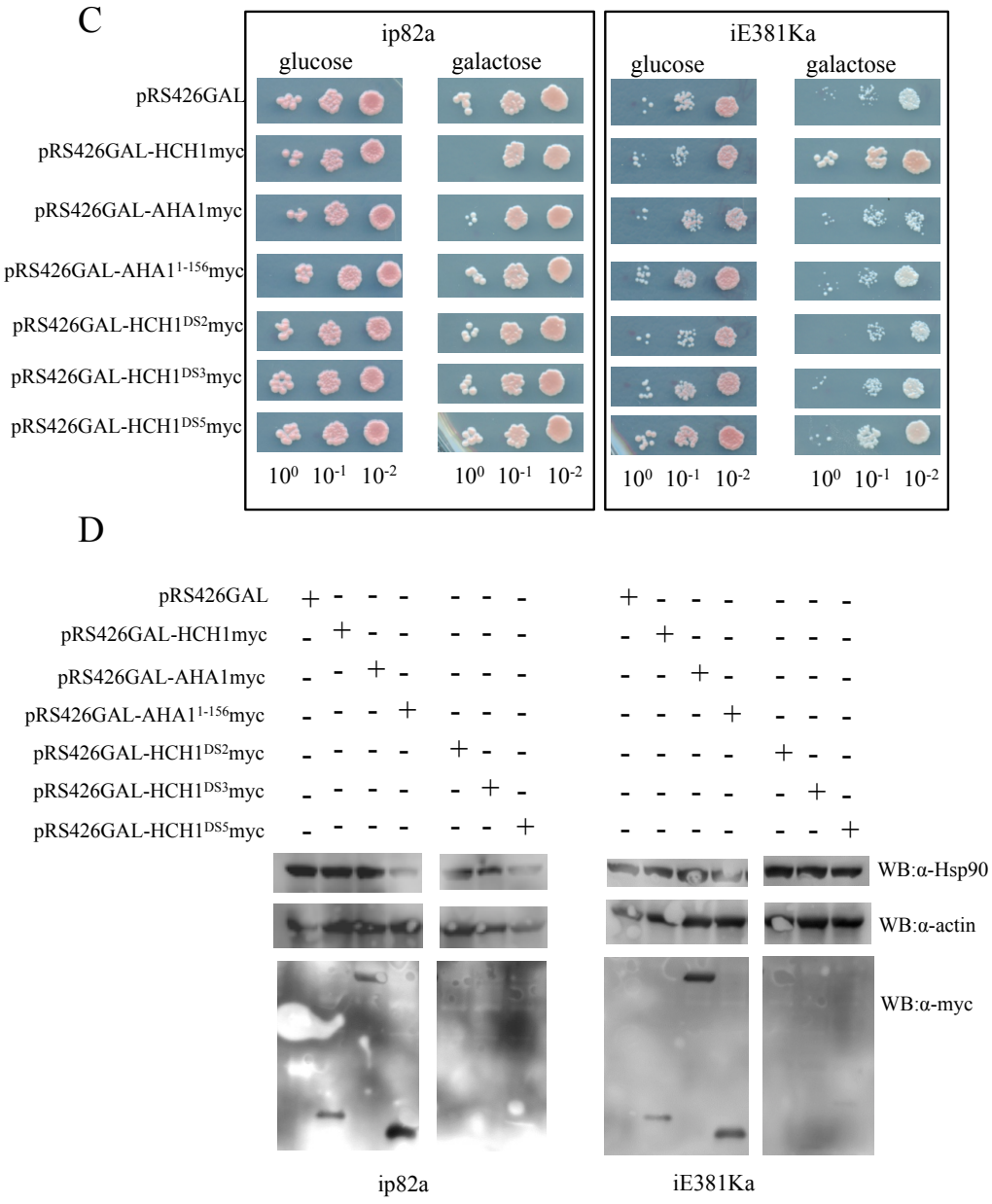
C
ip82a
iE381Ka
glucose
galactose
pRS426GAL
pRS426GAL-HCH1myc
pRS426GAL-AHA1myc
pRS426GAL-AHA1^1-156myc
pRS426GAL-HCH1^DS2myc
pRS426GAL-HCH1^DS3myc
pRS426GAL-HCH1^DS5myc
10^0 10^-1 10^-2
D
WB:α-Hsp90
WB:α-actin
WB:α-myc
ip82a
iE381Ka

**Figure 3.6 Domain Swap mutants are insoluble *in vivo*.** Cells were grown overnight at 30 °C in SC media lacking uracil (SC-Ura) and containing 2 % raffinose and followed by a dilution to 1 x $10^8$ cells per ml. 10-fold serial dilutions were prepared and 5 µl aliquots were spotted on SC-Ura agar plates supplemented with either 2 % glucose or galactose. A. Viability of yeast strain ip82a and iE381Ka containing GAL-driven overexpression of myc-tagged Hch1p, Aha1p, Aha1p$^{1\text{-}156}$, the HA$^{chimera}$, Aha1p$^{1\text{-}156\ DS1}$, Aha1p$^{1\text{-}156\ DS4}$, and Aha1p$^{1\text{-}156\ DS6}$. B. Western analysis of yeast shown in A with anti-Hsp90, anti-actin and anti-myc antibodies. C. Viability of yeast strain ip82a and iE381Ka containing GAL-driven overexpression of myc-tagged Hch1p, Aha1p, Aha1p$^{1\text{-}156}$, Hch1p$^{DS2}$, Hch1p$^{DS3}$, Hch1$^{DS5}$. D. Western analysis of yeast shown in C with anti-Hsp90, anti-actin and anti-myc antibodies.

The next strategy of substitutions used three criteria. First, they were to be non-conserved, and second, they are not a part of large secondary structures (*i.e.* strands and helices), in order to minimize disruptive interactions from substituted residues and prevent disruption of folding of the entire protein. Lastly, the sections selected were to be proximal to the Aha1p-Hsp90 middle domain interface. I hypothesized that non-conserved sections in Aha1p$^{1\text{-}156}$ interact with the Hsp90 catalytic loop differently than Hch1p. I constructed an extensive list of swap mutants for both *in vitro* and *in vivo* analysis by replacing either Hch1p residues 103 to 108 with Aha1p residues 98 to 109 or Hch1p residues 113 to 122 with Aha1p residues 114 to 125. Alignment of selected amino acid sections and schematic representations of the swap mutants are shown in Figure 3.7A, B, as well as a crystal structure highlighting residues substituted in Aha1p$^{1\text{-}156}$ are shown in red shown in Figure 3.7C. All 'a' swap mutants were constructed in galactose-inducible over-expression plasmids for *in vivo* analysis. I hypothesized that the Aha1p$^{1\text{-}156}$ mutants (mutants 2a or 4a) would gain the ability to rescue yeast growth in strains expressing Hsp82p$^{E381K}$ or Hch1p mutants (mutants 1a or 3a) would lose the ability to suppress the *in vivo* defect of Hsp82p$^{E381K}$. All 'b' swap mutants were constructed for *in vitro* purification. I hypothesized that replacing residues in the Hch1p portion of the HA$^{chimera}$ with Aha1p residues (mutants 1b or 3b) would confer the ability to robustly stimulate the Hsp82p ATPase activity. Growth assays over-expressing 'a' mutants showed that none of the mutants rescued growth of yeast expressing Hsp82p$^{E381K}$ (Figure 3.8A). Surprisingly, mutant 1a and 4a were detected by western blot with anti-myc

antibodies (Figure 3.8B) suggesting that these constructs were accumulating but were not able to suppress Hsp82p$^{E381K}$ defect *in vivo*. However, all the mutants for *in vitro* analysis were insoluble despite efficient expression (Figure 3.8C – representative gel). Mutant 1b was pursued with more rigorous purification methods, as mutant 1a was soluble *in vivo* (Figure 3.8B). I examined 1b mutant within the supernatant following lysis. Unfortunately, a HexaHis signal of the mutant was not detected in the supernatant sample when probed by western blot with an anti-HexaHis antibody as compared to the extremely soluble Aha1p (Figure 3.8D) suggesting that 1b was not soluble and was pelleted out of the supernatant during ultracentrifugation. As all of my mutants were insoluble during purification and the soluble mutants detected by western blot from *in vivo* analysis did not impart any properties to suppress Hsp82p$^{E381K}$ defect *in vivo*, I concluded that a new strategy was needed to focus on conserved residues rather than non-conserved residues of Hch1p and Aha1p.

A

```
Aha1p  MVVNNPNNWHWVDKNCIGWAKEYFKQKLVGVEAGSVKDKKYAKIKSVSSI  50
Hch1p  MVVLNPNNWHWVDKNTLPWSKDYLNGKLTSLSTVSSDGKSKIELTQVSSI  50

Aha1p  EGDCEVNQRKGKVISLFDLKITVLI-----EGHVDSKDGSALPFEGSINV  95
Hch1p  TGDSNVSQRKGKPICYFDLQLSMNVKVTNLDTNKDDEDDDGILADGKLEI  100

Aha1p  PEVAFDSEASSYQFDISIFKETSELSEAKPLIRSELLPKLRQIFQQFGKD  145
Hch1p  PEFMHDES------DIPILSQGFDAFDG--LVRSEFVPKVVETLLKYQDD  142

Aha1p  LLATHGNDIQVPESQVKSNYTRGNQKSSFTEIKDSASKPKKNALPSSTST  195
Hch1p  LIKEHSKDIQV-----------------------------------------  153
```

B

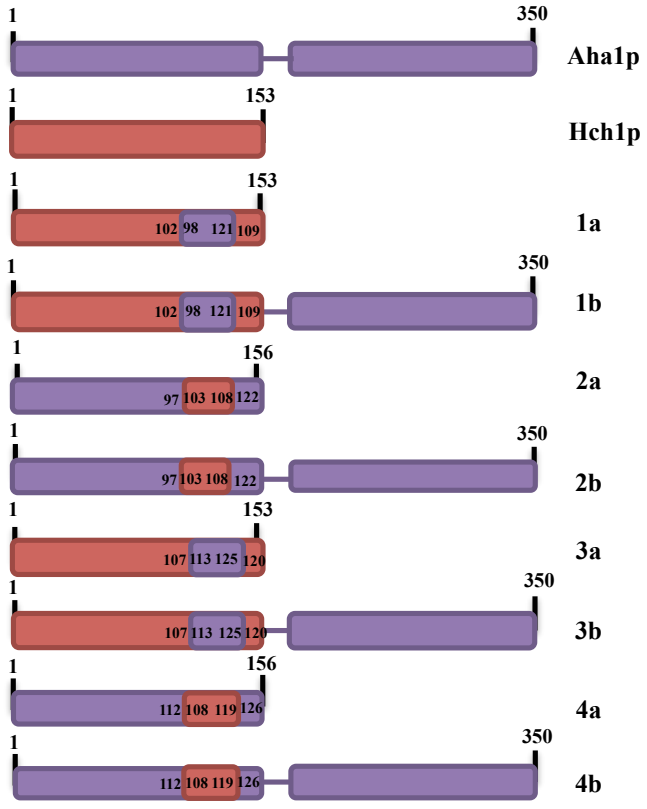


C

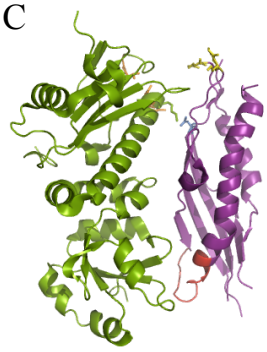

2a mutant

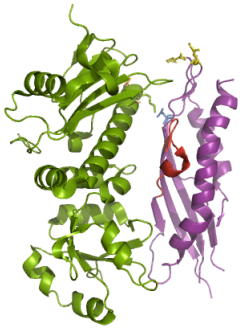

4a mutant

**Figure 3.7 Construction of loop swaps.** A. Alignment of Hch1p and Aha1p with orange box highlighting section swapped to construct mutant series 1 and 2 and green box highlighting section swapped to construct mutant series 3 and 4. B. Schematic representation of mutants constructed. 'a' mutants were constructed for *in vivo* analysis and 'b' mutants were constructed for *in vitro* analysis. C. Crystal structures of Aha1p$^{1-156}$ highlighting residues in red that were replaced with Hch1p residues to generate hybrid constructs. (Crystal structure adapted from (Meyer et al., 2004).

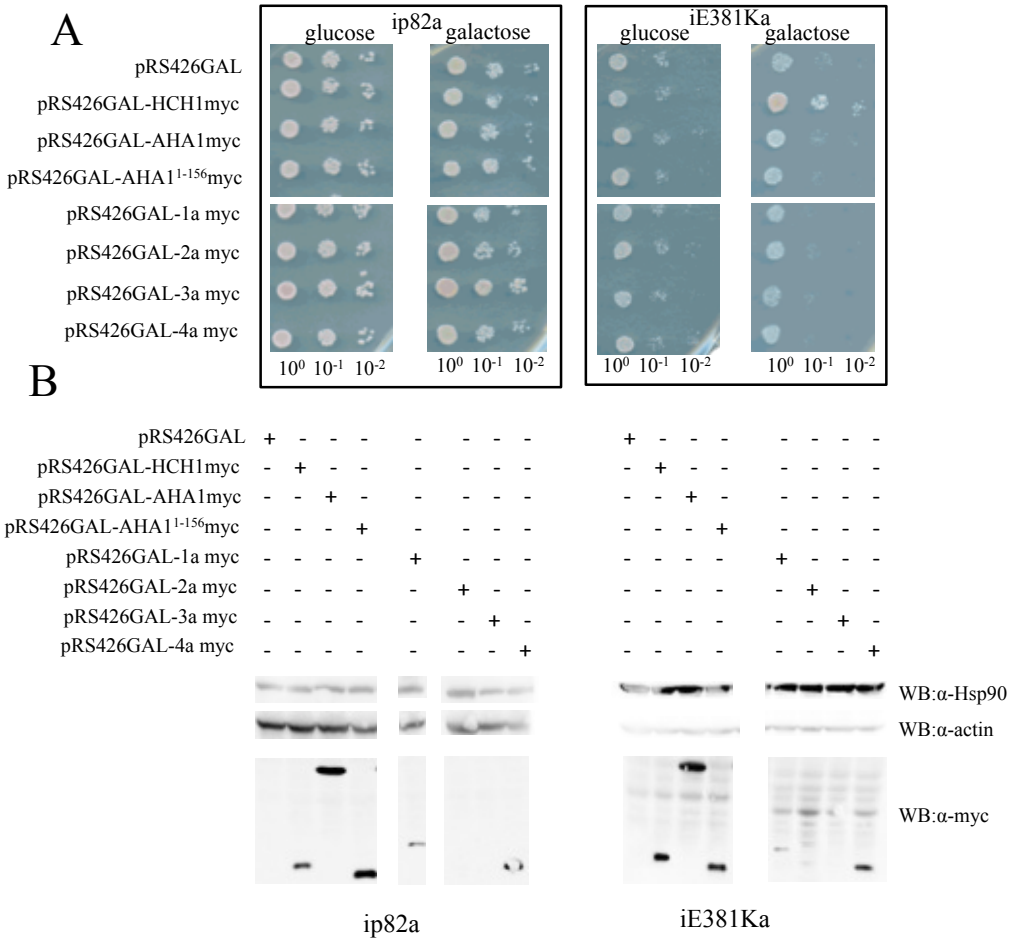
A
ip82a
iE381Ka
glucose
galactose
glucose
galactose
pRS426GAL
pRS426GAL-HCH1myc
pRS426GAL-AHA1myc
pRS426GAL-AHA1 1-156 myc
pRS426GAL-1a myc
pRS426GAL-2a myc
pRS426GAL-3a myc
pRS426GAL-4a myc
10^0 10^-1 10^-2
10^0 10^-1 10^-2
10^0 10^-1 10^-2
10^0 10^-1 10^-2
B
pRS426GAL
pRS426GAL-HCH1myc
pRS426GAL-AHA1myc
pRS426GAL-AHA1 1-156 myc
pRS426GAL-1a myc
pRS426GAL-2a myc
pRS426GAL-3a myc
pRS426GAL-4a myc
WB:α-Hsp90
WB:α-actin
WB:α-myc
ip82a
iE381Ka
C
Pre
Post
38 kDa
D
Pre lysis
Post lysis
Post spin
38 kDa
Aha1p
Pre lysis
Post lysis
Post spin
38 kDa
Mutant 1b

**Figure 3.8 Loop swaps are insoluble *in vivo* and *in vitro*.** A. Viability of yeast strain ip82a and iE381Ka containing GAL-driven overexpression of myc-tagged Hch1p, Aha1p, Aha1p$^{1-156}$, loop swaps 1a, 2a, 3a, and 4a. Cells were grown overnight in SC media lacking uracil (SC-Ura) containing 2 % raffinose and followed by a dilution to 1 x $10^8$ cells per ml. 10-fold serial dilutions were prepared and 5 µl aliquots were spotted on SC-Ura agar plates supplemented with either 2 % glucose or galactose. B. Western analysis of yeast shown in A with anti-Hsp90, anti-actin, and anti-myc antibodies. C. Representative gel of 1b mutant pre and post IPTG induction. Cultures were grown to an $OD_{600}$ of 0.8 and induced with 1 mM IPTG for 4 hrs. D. Representative western of Aha1 and 1b protein levels before lysis, after lysis and after ultracentrifugation probed with anti-HexaHis antibody.

## 3.4 Hch1p-mediated growth rescue in yeast expressing Hsp82p$^{E381K}$ requires specific motifs shared with Aha1p

My previous construction of Hch1p and Aha1p swap mutants focused on non-conserved amino acid sequences substitutions. Due to the fact that substituting non-conserved several residues disrupted folding, my approach was altered to examine the role of several conserved motifs between Hch1p and Aha1p. I considered three motifs that have been previously studied in Aha1p-mediated ATPase stimulation assays (Figure 1.4). The first motif, NxxNWHW (Figure 1.4 – first red box), is highly conserved in both Aha1p and Hch1p and previous studies have shown that deletion of the NxxNWHW motif, to construct a Aha1p$^{\Delta 11}$ mutant, did not impair Aha1p-mediated ATPase stimulation *in vitro* (Meyer et al., 2004). Other studies have shown another conserved residue, D53 (Figure 1.4 – second red box), is required for Aha1p to bind to the Hsp90 middle domain and a charge reversal (D53K) mutation at this site severely impairs the Aha1p-Hsp90 interaction (Meyer et al., 2004). Lastly, the RKxK motif (Figure 1.4 – third red box) is highly conserved between Hch1p and Aha1p and is involved in stabilizing the catalytic loop (residues 370-390) in Hsp90. Previous reports have shown that alanine mutations within the RKxK loop (R59A, K60A, and K62A) decrease the ability of Aha1p$^{1-156}$ to stimulate the Hsp82p ATPase rate (Meyer et al., 2004). I constructed expression plasmids encoding Aha1p with each of the mutations, R59A, K60A, and K62A. I then purified them to homogeneity for *in vitro* testing. Consistent with previous results, Aha1p$^{\Delta 11}$ was not impaired in its ability to stimulate the Hsp82p ATPase rate indicating that this motif is not

required for Aha1p-mediated ATPase stimulation (Figure 3.9A, B). Aha1p$^{D53K}$ was severely impaired in Hsp82p ATPase stimulation in a fashion consistent with reduced binding affinity (Figure 3.9B). Aha1p$^{R59A}$ and Aha1p$^{K60A}$ stimulated the Hsp82p ATPase activity less than wild-type Aha1p (Figure 3.9B). Interestingly, the Aha1p$^{D53K}$, Aha1p$^{R59A}$, and Aha1p$^{K60A}$ mutants stimulated the Hsp90 ATPase activity to a similar fashion as compared to previous results with Aha1p$^{1\text{-}156\ D53K}$, Aha1p$^{1\text{-}156\ R59A}$, and Aha1p$^{1\text{-}156\ K60A}$ (Meyer et al., 2004). Aha1p mediated stimulation of Hsp82p ATPase activity does not involve the NxxNWHW but requires the RKxK to remodel the Hsp90 catalytic loop and D53 for middle domain binding.

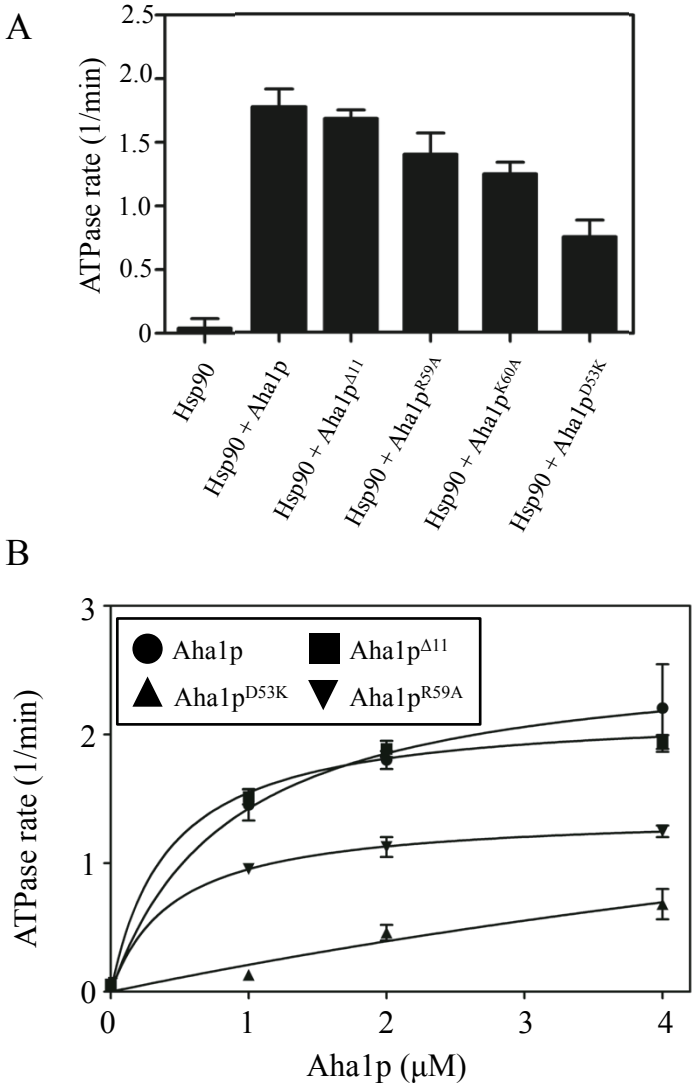


**Figure 3.9 Aha1p function requires two conserved motifs to stimulate the Hsp90 ATPase activity.** ATPase rate shown in uM ATP hydrolyzed per uM of enzyme (1/min). A. Stimulation of Hsp82p ATPase activity by Aha1p, Aha1p$^{\Delta 11}$, Aha1p$^{K60A}$, Aha1p$^{R59A}$, and Aha1p$^{D53K}$. Reactions contain 2 μM Hsp82p and 4 μM co-chaperone. B. Stimulation of Hsp82p ATPase activity with increasing concentrations of Aha1p (circles), Aha1p$^{D53K}$ (up triangles), Aha1p$^{R59A}$ (down triangles), or Aha1p$^{\Delta 11}$ (squares). Reactions contain 1 uM Hsp82p and indicated co-chaperone concentrations.

Since the D53K mutation severely affected the binding affinity of Aha1p to Hsp82p(Meyer et al., 2004), I hypothesized that Hch1p$^{D53K}$ would not suppress Hsp82p$^{E381K}$ *in vivo*. Yeast over-expressing Hch1p$^{D53K}$ did not rescue yeast growth in strains expressing Hsp82$^{E381K}$ suggesting that, similar to Aha1p, the Hch1p mediated rescue of Hsp82p$^{E381K}$ requires interaction to the Hsp82p middle domain (Figure 3.10A). The deletion of the NxxNWHW motif in Aha1p did not impair the Hsp82p ATPase stimulation; therefore I hypothesized that this motif would not be required for Hch1p-mediated rescue of Hsp82p$^{E381K}$ *in vivo*. Hch1p $^{\Delta 11}$ did not rescue yeast growth in yeast strains expressing Hsp82p$^{E381K}$ suggesting that the conserved *N*-terminal motif is necessary for Hch1p function *in vivo* (Figure 3.10A). To rule out the possibility that Hch1p$^{D53K}$ and Hch1p $^{\Delta 11}$ were unable to rescue yeast growth of Hsp82p$^{E381K}$ yeast strains due to lack of expression of co-chaperone, lysates were probed by western blot with anti-myc antibodies to verify co-chaperone over-expression (Figure 3.10B). Hsp82p levels were confirmed according to the actin loading control by probing lysates by western blots with anti-Hsp90 and anti-actin antibodies (Figure 3.10B). Finally, I wanted to determine the role of R59A, K60A, and K62A mutations in Hch1p suppression of the Hsp82$^{E381K}$ defect *in vivo*. Hch1p$^{K60A}$ was not able to rescue growth of yeast expressing Hsp82p$^{E381K}$ when compared to wildtype Hch1p suggesting that Hch1p$^{K60A}$ contributes the most to remodeling of the Hsp82p catalytic loop (Figure 3.10C). Hch1p$^{R59A}$ had minor impairments in its ability to rescue growth in yeast strains expressing Hsp82p$^{E381K}$ suggesting that this residue also contributes, but to a lesser extent than K60, in suppressing the defect of

Hsp82p$^{E381K}$ *in vivo*. The K62A mutation did not disrupt Hch1p suppression of Hsp82p$^{E381K}$ *in vivo* (Figure 3.10C). Expressions of all constructs in lysates were verified by western blot by probing with anti-myc antibodies (Figure 3.10D). The results show that Hch1p function involves the D53, NxxNWHW, and most of the RKxK motif. The residues of RKxK in Hch1p do not contribute equally to Hch1p function, as K60 is the most important for Hch1p activity *in vivo,* R59 is less important and K62 is not important for Hch1p activity.

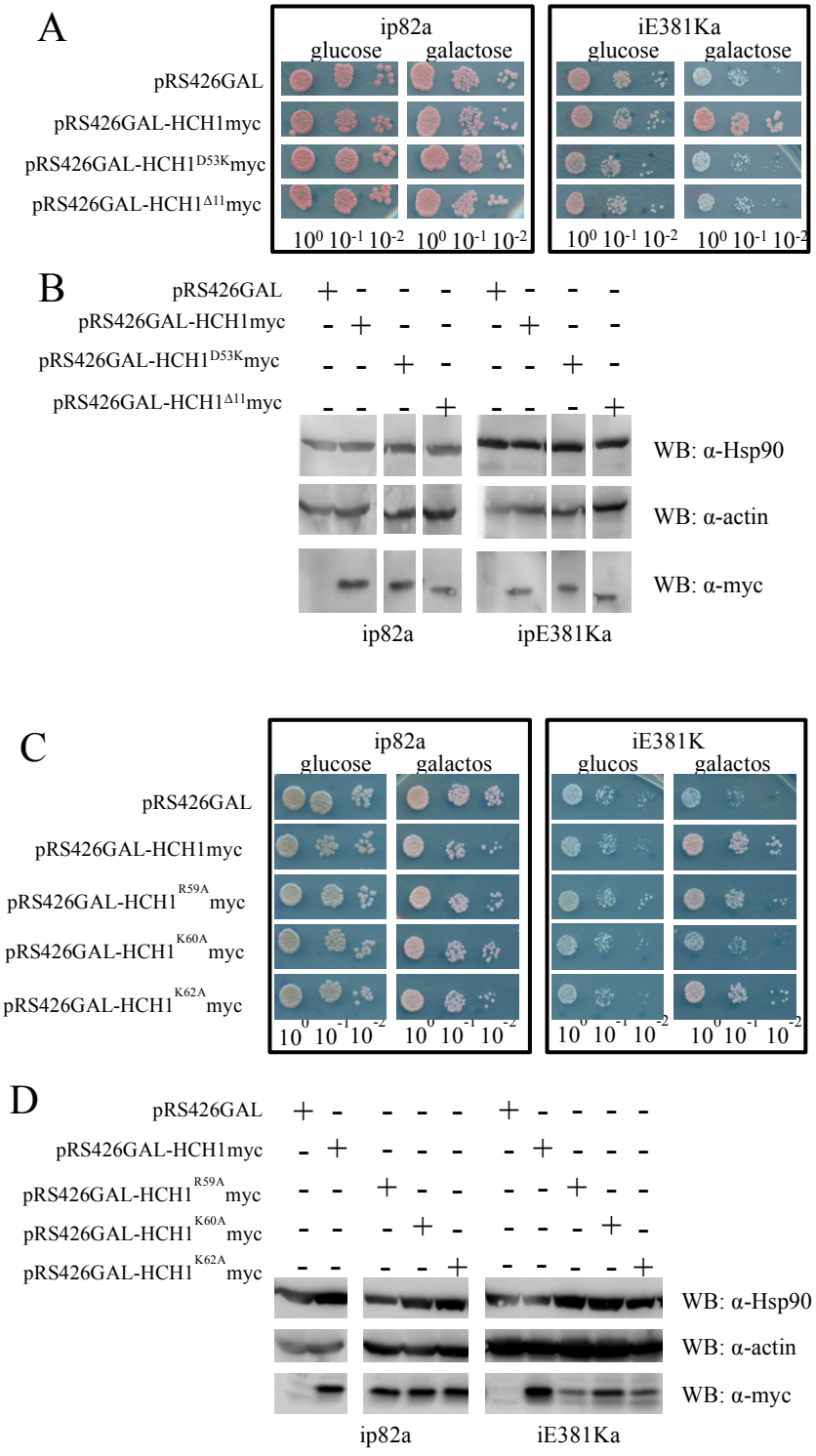
A
ip82a
glucose
galactose
iE381Ka
glucose
galactose
pRS426GAL
pRS426GAL-HCH1myc
pRS426GAL-HCH1D53Kmyc
pRS426GAL-HCH1Δ11myc
10^0 10^-1 10^-2 10^0 10^-1 10^-2
10^0 10^-1 10^-2 10^0 10^-1 10^-2
B
pRS426GAL
pRS426GAL-HCH1myc
pRS426GAL-HCH1D53Kmyc
pRS426GAL-HCH1Δ11myc
WB: α-Hsp90
WB: α-actin
WB: α-myc
ip82a
ipE381Ka
C
ip82a
glucose
galactos
iE381K
glucos
galactos
pRS426GAL
pRS426GAL-HCH1myc
pRS426GAL-HCH1R59Amyc
pRS426GAL-HCH1K60Amyc
pRS426GAL-HCH1K62Amyc
10^0 10^-1 10^-2 10^0 10^-1 10^-2
10^0 10^-1 10^-2 10^0 10^-1 10^-2
D
pRS426GAL
pRS426GAL-HCH1myc
pRS426GAL-HCH1R59Amyc
pRS426GAL-HCH1K60Amyc
pRS426GAL-HCH1K62Amyc
WB: α-Hsp90
WB: α-actin
WB: α-myc
ip82a
iE381Ka

**Figure 3.10 Hch1p mediated rescue of growth of yeast expressing Hsp82p$^{E381K}$ requires three conserved motifs.** Cells were grown overnight at 30 °C in SC media lacking uracil (SC-Ura) containing 2 % raffinose and followed by a dilution to 1 x $10^8$ cells per ml. 10-fold serial dilutions were prepared and 5 µl aliquots were spotted on SC-Ura agar plates supplemented with either 2 % glucose or galactose. Plates were grown at 30 °C for 2 days. A. Viability of yeast strain ip82a and iE381Ka containing GAL-driven overexpression of myc-tagged Hch1p, Hch1p$^{\Delta 11}$, and Hch1p$^{D53K}$. B. Western analysis of yeast shown in A with anti-Hsp90, anti-actin, and anti-myc antibodies. C. Viability of yeast strain ip82a and iE381Ka containing GAL-driven overexpression of myc-tagged Hch1p, Hch1p$^{R59A}$, Hch1p$^{K60A}$, and Hch1p$^{K62A}$. D. Western analysis of yeast shown in C with anti-Hsp90, anti-actin, and anti-myc antibodies.

### 3.5 Hch1p requires three conserved motifs to confer sensitivity to the Hsp90 inhibitor drug NVP-AUY922 in yeast strains expressing wild type Hsp82p

Previous studies have shown that the over-expression of Hch1p confers sensitivity to the Hsp90 inhibitor drug, NVP-AUY922, in yeast expressing wild type Hsp82p (Armstrong et al. 2012). My results show that the function of Hch1p *in vivo* is dependent on three motifs. Since Hch1p confers sensitivity to NVP-AUY922 in yeast expressing wild-type Hsp82p, I hypothesized that Hch1p requires the same motifs for the induction of drug sensitivity. Consistent with previous results (Armstrong et al., 2012), wild-type Hsp82p containing yeast strains over-expressing myc tagged Hch1p show hypersensitivity to NVP-AUY922 at 400µM (Figure 3.11A). Yeast strains over-expressing Hch1p $^{\Delta 11}$, Hch1p$^{D53K}$, Hch1p$^{K60A}$, and Hch1p$^{R59A}$ were resistant to NVP-AUY922 up to 400µM (Figure 3.11A) suggesting that these residues required for *in vivo* rescue of Hsp82p$^{E381K}$ are also required for the induction of drug sensitivity. As expected, yeast expressing Hch1p$^{K62A}$ induced sensitivity to NVP-AUY922 up to 400µM, which confirms that K62 residue is not required for Hch1p function *in vivo* (Figure 3.11A). Co-chaperone expression levels and Hsp82p expression levels were confirmed by probing lysates by western blot with anti-myc and anti-Hsp90 antibodies as compared to the actin loading control (Figure 3.11B). Thus the mechanism of Hch1p function *in vivo* requires D53 interaction with the Hsp90M, remodeling of the Hsp90 catalytic loop by the RKxK loop and the *N*-terminal peptide of Hch1p.

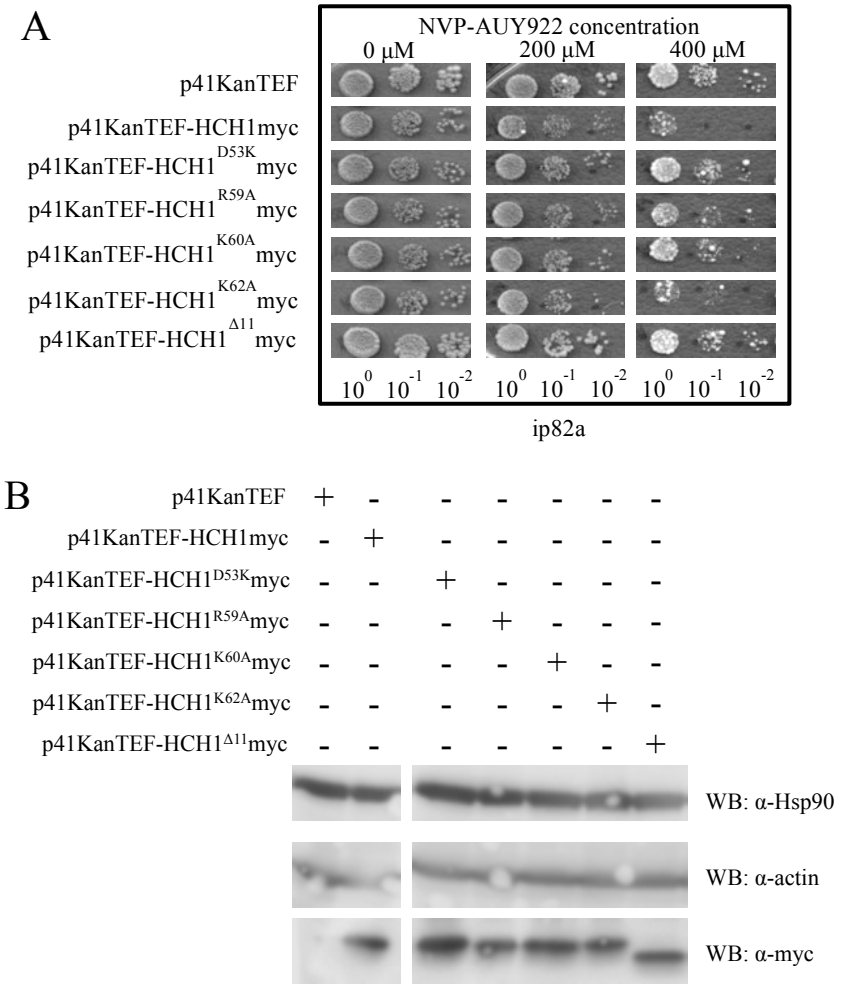


**Figure 3.11 The same motifs of Hch1p required for Hsp82p$^{E381K}$ rescue *in vivo* also confer sensitivity to Hsp90 inhibitor drugs in yeast expressing wildtype Hsp82p.** A. Viability of yeast strains ip82a with the constitutively overexpressed of myc-tagged Hch1p, Hch1p$^{D53K,}$ Hch1p$^{R59A}$, Hch1p$^{K60A}$, Hch1p$^{K62A}$, Hch1p$^{\Delta 11}$ or vector control. Cells were grown overnight at 30 °C in YPD media containing 200 mg/L G418 and followed by a dilution to 1 x $10^8$ cells per ml. 10-fold serial dilutions were prepared and 5 μl aliquots were spotted on YPD agar plates supplemented 200 mg/L G418 and indicated concentrations of NVP-AUY922. Plates were grown for two days at 30 °C. B. Western analysis of yeast shown in A with anti-Hsp90, anti-actin, and anti-myc antibodies.

## 3.6 Hsp82p$^{E381K}$ induces resistance to the Hsp90 inhibitor drug NVP-AUY922 *in vivo* but not *in vitro*

Previous studies have shown that yeast strains expressing a different Hsp82p *ts* mutant, Hsp82p$^{A587T}$, grow very slowly and are hypersensitive to the Hsp90 inhibitor NVP-AUY922 (Armstrong et al., 2012). When *HCH1* is deleted, yeast strains expressing Hsp82p$^{A587T}$ are resistant to NVP-AUY922 (Armstrong et al., 2012). Preliminary results by another student in our lab have shown that yeast strains expressing Hsp82p$^{E381K}$ are not viable without Hch1p (Heather Armstrong - unpublished data). The Hsp90 cycle contains steps that are sensitive to drug inhibition and co-chaperones, such as Hch1p, cause a drug sensitive step be more prominent *in vivo* as yeast expressing wild-type Hsp82p are hypersensitive to NVP-AUY922 when Hch1p is over-expressed (Armstrong et al., 2012). Because yeast expressing Hsp82p$^{E381K}$ are dependent on Hch1p *in vivo*, I wanted to determine whether Hsp82p$^{E381K}$ confers sensitivity to NVP-AUY922 when expressed in yeast. Yeast-expressing wild-type Hsp82p or Hsp82p$^{E381K}$ were transformed with an over-expression plasmid encoding Hch1p or a control vector. Similar to previous results (Armstrong et al., 2012), yeast expressing wild-type Hsp82p are more sensitive to NVP-AUY922 when Hch1p was over-expressed as compared to the control (Figure 3.12A). Yeast expressing Hsp82p$^{E381K}$ were resistant to NVP-AUY922 up to 200μM and drug sensitivity was not apparent when Hch1p was over-expressed (Figure 3.12A). Levels of co-chaperone expression as well as Hsp82p levels were verified by probing lysates by western blot with anti-Hsp90 and anti-myc antibodies (Figure 3.12B).

In order to rule out whether the resistance to NVP-AUY922 in yeast expressing Hsp82$^{E381K}$ was due to the inability to bind to the Hsp90 inhibitor drug, I tested whether the intrinsic ATPase activity of Hsp82p$^{E381K}$ is susceptible to inhibition *in vitro*. NVP-AUY922 was titrated into ATPase reactions containing wild-type Hsp82p or Hsp82p$^{E381K}$. The ATPase activity of Hsp82p$^{E381K}$ was inhibited by NVP-AUY922 to a similar degree as wild-type Hsp82p (Figure 3.12C). This suggests that yeast expressing Hsp82p$^{E381K}$ induce drug resistance *in vivo* not due to the inability to bind to Hsp90 inhibitor drug, NVP-AUY922 but due to the formation of an Hch1p-Hsp82p$^{E381K}$ complex that is resistant to NVP-AUY922.

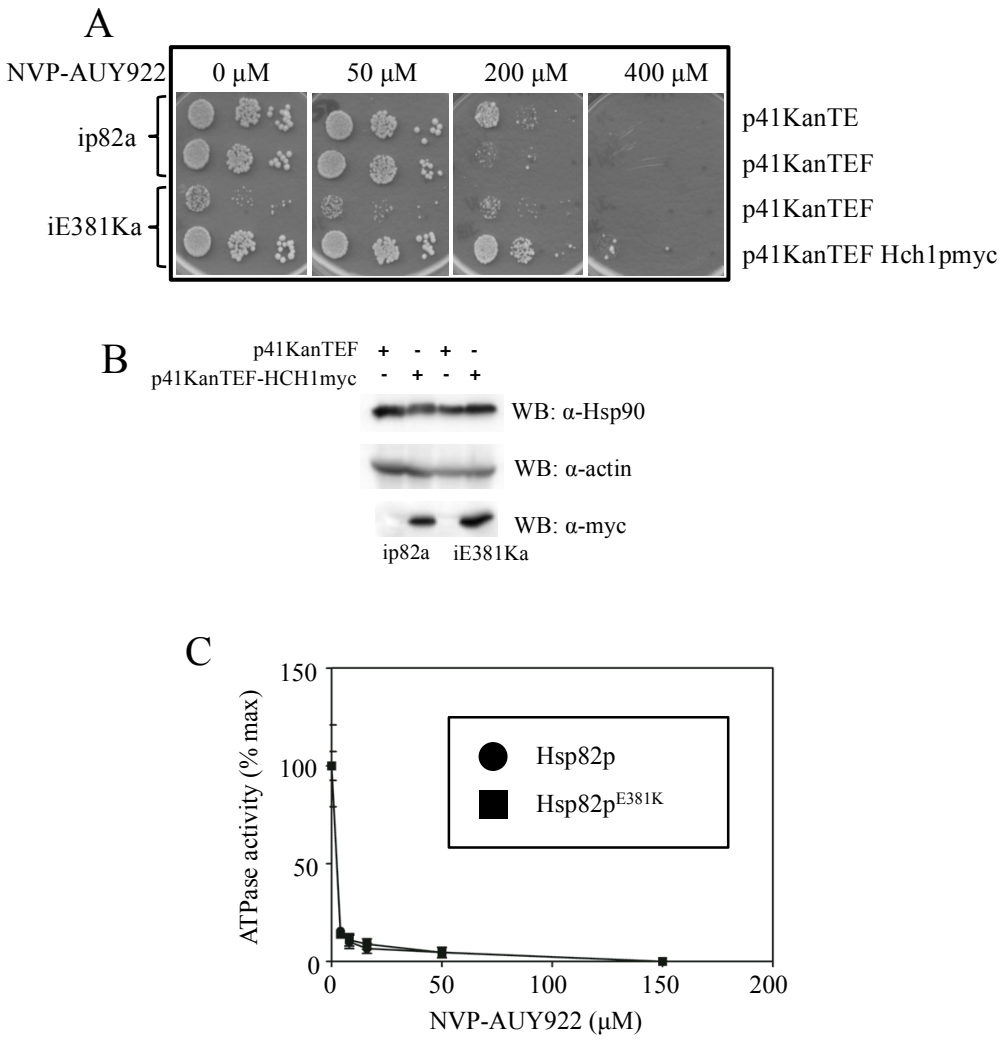


**Figure 3.12 Hsp82p$^{E381K}$ is resistant to Hsp90 inhibitor drugs *in vivo* but not *in vitro*.** A. Viability of yeast strain ip82a and iE381Ka with constitutively overexpressed myc-tagged Hch1p or vector control. Cells were grown overnight at 30 °C in YPD media containing 200 mg/L G418 and followed by a dilution to 1 x $10^8$ cells per ml. 10-fold serial dilutions were prepared and 5 μl aliquots were spotted on YPD agar plates supplemented 200 mg/L G418 and indicated concentrations of NVP-AUY922. Plates were grown for two days at 30 °C. B. Western analysis of yeast shown in A with anti-Hsp90, anti-actin, and anti-myc antibodies. C. Inhibition of 4 μM Hsp82p and 4 μM Hsp82p$^{E381K}$ with indicated concentrations of NVP-AUY922. ATPase rate shown as a percent of the maximum intrinsic rate.

### 3.7 The V391E mutation in Hsp82p blocks Hch1p binding to the middle domains but not phenocopy *HCH1* deletion in vivo

Previous studies show that inserting a glutamic acid at the V391 residue in Hsp82p blocks Aha1p binding to the middle domain of Hsp82p (Section 1.10 and Figure 1.5) (Retzlaff et al., 2010). Hch1p also binds to the middle domain of Hsp82p. The deletion of *HCH1* induces resistance to Hsp90 inhibitor drugs in yeast strains expressing wild-type Hsp82p and Hsp82p$^{A587T}$. I hypothesized that inserting a V391E mutation into Hsp82p would phenocopy *HCH1* deletion in yeast thereby induce resistance to NVP-AUY922 in yeast expressing Hsp82p$^{V391E}$ to near wild-type levels. Consistent with previous reports (Armstrong et al., 2012), *HCH1* deletion induced resistance to NVP-AUY922 in yeast expressing wild-type Hsp82p or Hsp82p$^{A587T}$ (Figure 3.13A). Yeast expressing Hsp82p$^{V391E}$ as their sole source of Hsp82p were hypersensitive to NVP-AUY922 with or without Hch1p (Figure 3.13A). Hsp82p levels expressed in yeast strains lysates were verified by western blot probed with anti-Hsp90 and anti-actin antibodies (Figure 3.13C). Although the expression of Hsp82 is variable among the strains, this does not explain the observed drug sensitivity (Figure 3.13C). Hypersensitivity to NVP-AUY922 conferred in yeast expressing Hsp82p$^{V391E}$ suggests that the V391E mutation does not only block Aha1p/Hch1p binding to the middle domain of Hsp82p but may also block binding of a different co-chaperone. As a result, the V391E mutation may cause a shift the equilibrium of Hsp82p complex formations to favour the formation of a drug sensitive complex *in vivo*.

Sti1p bound to Hsp90C stabilizes the Hsp90 open conformation and inhibits the Hsp90 ATPase activity (Southworth and Agard, 2011; Onuoha et al., 2008). The deletion of *STI1* in yeast expressing wild-type Hsp82p results in hypersensitivity to Hsp90 inhibitor drugs (Piper et al., 2003). The deletion of *HCH1* in yeast expressing wild-type Hsp82p show resistance to NVP-AUY922 (Armstrong et al., 2012). I hypothesized that the V391E mutation, which blocks Hch1p binding to the middle domain of Hsp82p, induces resistance to NVP-AUY922 *in vivo* but my studies show yeast expressing Hsp82p$^{V391E}$ are hypersensitive to NVP-AUY922 (Figure 3.13A). So I hypothesized that V391E mutation blocks the binding of Sti1p to Hsp82p, which could explain the observed hypersensitivity to NVP-AUY922 in yeast expressing Hsp82p$^{V391E}$. To test the possibility that Sti1p cannot inhibit Hsp82p$^{V391E}$, I performed ATPase assays with Hsp82p$^{V391E}$ and Sti1p. Surprisingly, Sti1p was able to inhibit Hsp82p$^{V391E}$ intrinsic ATPase activity as compared to wild-type Hsp82p (Figure 3.14). This result suggests that yeast expressing Hsp82p$^{V391E}$ are hypersensitive to NVP-AUY922 *in vivo* due to Hsp82p$^{V391E}$ blocking the binding of an unknown co-chaperone other than Sti1p (Figure 3.13A).

## 3.8 Hsp82p$^{E381K}$ defect is suppressed by the introduction of a second mutation, A587T *in vivo*

Previous reports have shown that *HCH1* deletion in yeast expressing Hsp82p$^{A587T}$ restores yeast growth to near wild type levels (Armstrong et al., 2012). However, *HCH1* is essential in yeast expressing Hsp82p$^{E381K}$ (Heather Armstrong – unpublished observation). Since Hsp82p$^{A587T}$ and Hsp82p$^{E381K}$ have an opposite relationship with Hch1p at a specific step of the Hsp90 cycle, I hypothesized that the introduction of A587T into Hsp82p$^{E381K}$ would facilitate Hch1p-independent yeast growth. Yeast expressing Hsp82$^{A587T/E381K}$ were viable in *Δhch1* knockout strains suggesting that the A587T mutation is a partial suppressor of Hsp82p$^{E381K}$ defect *in vivo* (Figure 3.13B). Hsp82 levels as well as actin levels were verified by probing lysates by western blot with anti-Hsp90 and anti-actin antibodies (Figure 3.13B). The A587T mutation can overcome the defect of Hsp82p$^{E381K}$ *in vivo* suggesting that A587T adopts a Hsp90 conformation that overcomes the defect of Hsp82p$^{E381K}$ because the A587T and E381K mutations impede the Hsp90 cycle oppositely at the same step.

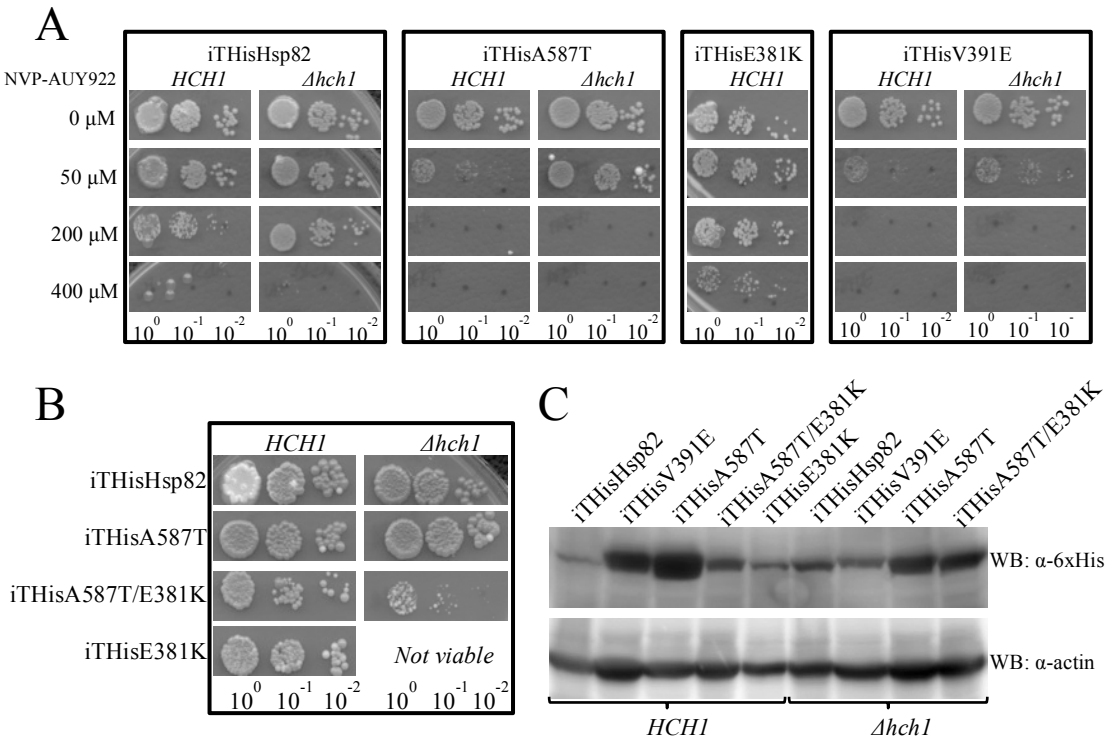


**Figure 3.13 Hsp82p$^{V391E}$ is hypersensitive to NVP-AUY922 and Hsp82p$^{E381K/A587T}$ double mutant can support growth of yeast independent of Hch1p.** A. Viability of yeast strain iTGPDhisHsp82p, iTGPDhisHsp82p$^{E381K}$, iTGPDhisHsp82p$^{A587T}$, and iTGPDhisHsp82p$^{V391E}$ with or without Hch1p and increasing concentrations of NVP-AUY922. B. *HCH1* deletion does not impair yeast strains expressing Hsp82p or Hsp82$^{A587T}$ but is lethal in yeast expressing Hsp82p$^{E381K}$. Insertion of A587T to Hsp82p$^{E381K}$ to construct iTGPDhisHsp82p$^{E381K/A587T}$ yeast strain enables Hch1p independent growth. Cells were grown overnight at 30 °C in YPD media and followed by a dilution to 1 x $10^8$ cells per ml. 10-fold serial dilutions were prepared and 5 μl aliquots were spotted on YPD agar plates or YPD agar plates with indicated concentrations of NVP-AUY922. Plates were grown for two days at 30 °C. C. Western analysis of yeast shown in A and B with anti-Hsp90, and anti-actin antibodies.

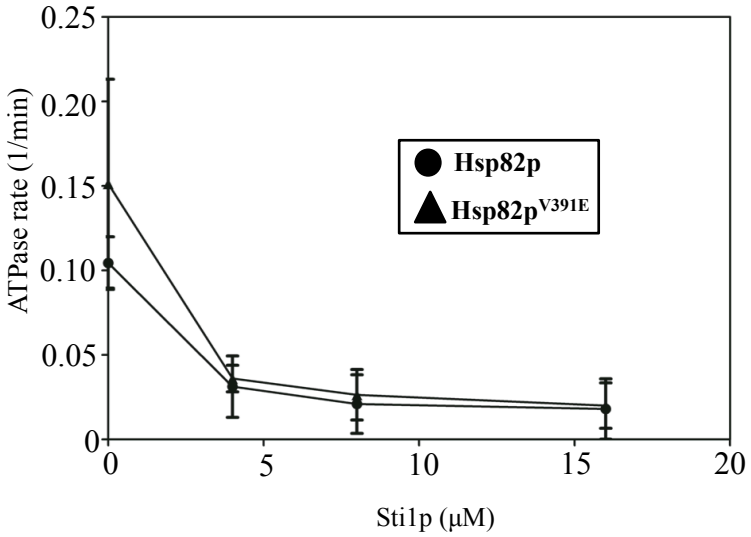


**Figure 3.14 Sti1p can inhibit the Hsp82p$^{V391E}$ ATPase rate.** Reactions contain 4μM Hsp82p, Hsp82p$^{V391E}$ and increasing concentrations of Sti1p as indicated. ATPase rate shown in μM ATP hydrolyzed per minute per μM of enzyme (1/min)

### 3.9 The Hsp82p$^{E381K}$ ATPase activity is resistant to Sti1p inhibition

Previous reports have shown that Hsp82p and Hsp82p$^{E381K}$ have comparable intrinsic ATPase rates (Hawle et al., 2006; Lotz et al., 2003; Meyer et al., 2003). There have been conflicting reports that have shown the Hsp82p$^{E381K}$ ATPase rate is stimulated *in vitro* by Aha1p to a comparable rate as wild-type Hsp82p (Hawle et al., 2006; Meyer et al., 2003). Consistent with the work of Hawle and colleagues, my data shows that Aha1p does not robustly stimulate the Hsp82p$^{E381K}$ ATPase rate (Figure 3.15A). Although the ATPase stimulation of Hsp82p$^{E381K}$ is ~12 fold less than wild-type Hsp82p, the half maximal stimulation ($K_M$), determined by ½ $V_{max}$ rate, for both Hsp82p and Hsp82p$^{E381K}$ is achieved at similar concentrations of Aha1p. This suggests that the impairment of the Hsp82p$^{E381K}$ ATPase activity is due to a mechanical defect and not reduced affinity for Aha1p.

Because Aha1p did not robustly stimulate Hsp82p$^{E381K}$, I wanted to determine if other co-chaperones are able to regulate the ATPase activity of this mutant. The co-chaperone Sti1p is a known inhibitor of Hsp90's ATPase activity as it binds to Hsp90C facilitating the Hsp90 open conformation although recent studies have shown Sti1p can bind to other regions of Hsp90 on Hsp90M and Hsp90N (Southworth and Agard, 2011; Richter et al., 2003). Sba1p also is a well-characterized Hsp90 ATPase inhibitor and binds to Hsp90 in the ATP-bound closed conformation (Richter et al., 2004). Both Sti1p and Sba1p have been shown previously to competitively inhibit Aha1-stimulated Hsp90 ATPase activity, I hypothesized that Sti1p and Sba1p would inhibit the Hsp82p$^{E381K}$

ATPase rate *in vitro*. Sba1p was able to inhibit the Aha1p stimulated Hsp82p$^{E381K}$ ATPase rate (Figure 3.15B). Sti1p was also able to inhibit the Hch1p stimulated Hsp82p$^{E381K}$ ATPase rate (Figure 3.15C). While both of these co-chaperones were able to inhibit the stimulated ATPase rate of Hsp82p$^{E381K}$, Sti1p could not inhibit the intrinsic rate of Hsp82p$^{E381K}$ as compared to wild-type Hsp82p (Figure 3.15C). As the Hsp82p$^{E381K}$ ATPase rate is very low, I verified this result by testing higher concentrations of wild-type Hsp82p, Hsp82p$^{E381K}$ and Sti1p. Even with 10μM Hsp82p and Hsp82p$^{E381K}$, Sti1p only weakly inhibited the intrinsic ATPase activity of Hsp82p$^{E381K}$ (Figure 3.15D). This is surprising as Sti1p binds to the MEEVD peptide at the *C*-terminal domain of Hsp90 and the E381K mutation is located within the middle domain of Hsp90. These assays give us insight into the allosteric mechanism and conformational changes that are responsible for Sti1p-mediated inhibition.

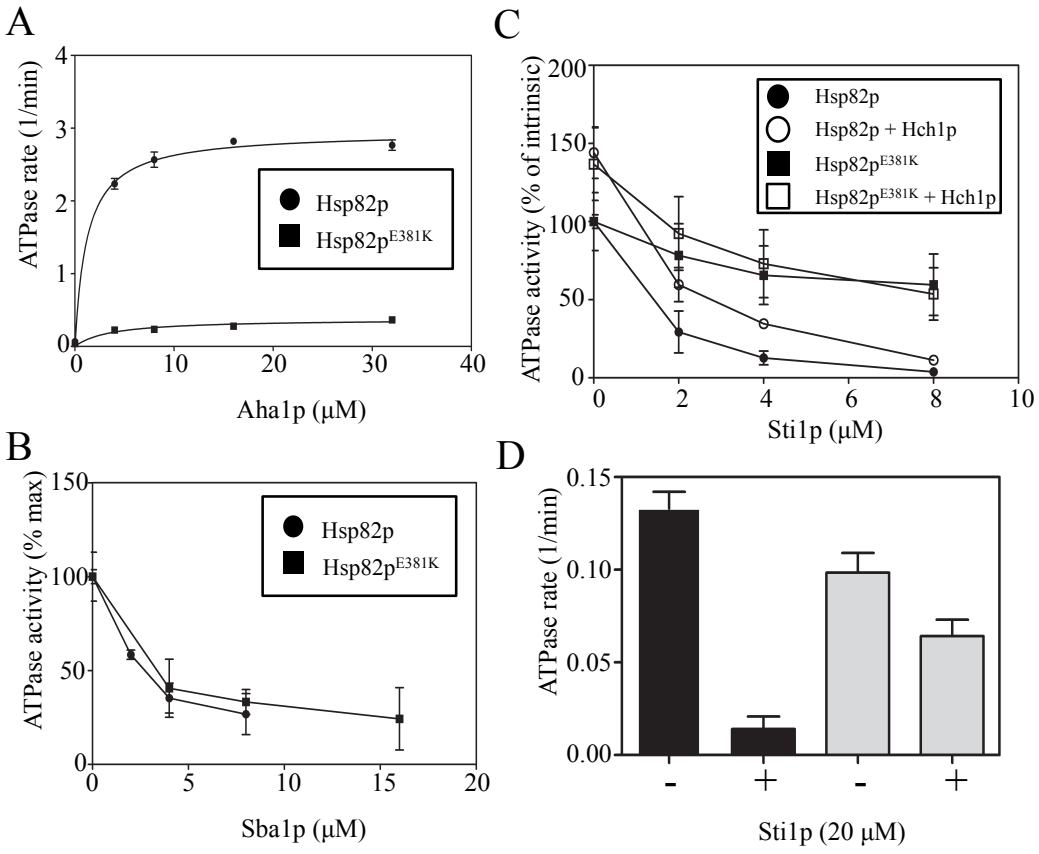
A
ATPase rate (1/min)
Hsp82p
Hsp82p$^{E381K}$
Aha1p (μM)
B
ATPase activity (% max)
Hsp82p
Hsp82p$^{E381K}$
Sba1p (μM)
C
ATPase activity (% of intrinsic)
Hsp82p
Hsp82p + Hch1p
Hsp82p$^{E381K}$
Hsp82p$^{E381K}$ + Hch1p
Sti1p (μM)
D
ATPase rate (1/min)
Sti1p (20 μM)

**Figure 3.15 ATPase activity of Hsp82p$^{E381K}$ is not regulated by all Hsp90 co-chaperones.** A. Aha1p cannot stimulate Hsp82p$^{E381K}$ ATPase rate. Reactions contain 4 μM Hsp82p (circles) or Hsp82p$^{E381K}$ (squares) with indicated concentrations of Aha1p. ATPase rate shown in μM ATP hydrolyzed per minute per μM of enzyme (1/min). B. Inhibition of Aha1p-stimulated ATPase activity of wildtype Hsp82p (2 μM Hsp82p and 4 μM Aha1p, circles) and Hsp82p$^{E381K}$ (4 μM Hsp82p$^{E381K}$ and 8 μM Aha1p, squares) by increasing concentrations of Sba1p. ATPase activity shown as a percent of the maximum stimulated rate. C. Inhibition of the intrinsic or Hch1p-stimulated ATPase activity of wildtype Hsp82p (circles), and Hsp82p$^{E381K}$ (squares) with increasing concentrations of Sti1p. Reactions contain 2 μM Hsp82 or Hsp82p$^{E381K}$ and 4 μM Hch1p with increasing concentrations of Sti1p. ATPase activity shown as a percent of the maximum stimulated rate. D. Inhibition of the intrinsic ATPase activity of wildtype Hsp82p (black), and Hsp82p$^{E381K}$ (grey) by Sti1p. Reactions contained 10 μM Hsp82p or Hsp82p$^{E381K}$ with and without 20 μM Sti1p. ATPase rate shown in μM ATP hydrolyzed per minute per μM of enzyme (1/min).

# Chapter Four

## Discussion

## 4.1 The significance of studying the Hsp90 system

The Hsp90 system regulates the maturation and activation of client proteins, which are important for biological processes such as signal transduction, steroid hormone response and cell cycle regulation (Young et al., 2001; Richter and Buchner, 2001; Panaretou et al., 1998). Many Hsp90 client proteins are oncoproteins, which are involved in the development and progression of cancer (Whitesell and Lindquist, 2005). Recently, the development of Hsp90 inhibitor drugs have shown to be effective therapeutic agents against cancer, as they are showing promising results in clinical drug trials (Neckers and Workman, 2012; Workman, 2004). Unfortunately, some Hsp90 inhibitor drugs exhibit undesirable toxic effects *in vivo* (Supko et al., 1995; Whitesell et al., 1994). Co-chaperones are key components in the Hsp90 system as they regulate client binding and maturation. The co-chaperone, Aha1, is a potent stimulator of the Hsp90 ATPase activity and studies have shown that Aha1 interaction with Hsp90 can stimulate efficient activation of client proteins (Harst et al., 2005). Interestingly, the levels of Aha1 can affect sensitivity to Hsp90 inhibitor drugs in cancer cells (Holmes et al., 2008). Therefore, it is important to understand the role of co-chaperones in regulating the Hsp90 system. My studies show that the Aha1p homologue, Hch1p, regulates the Hsp90 cycle using some motifs that are shared with Aha1p but also unique ones as well. My work suggests that Hch1p regulates the Hsp90 cycle at a step that is different than Aha1p and where Hsp90 is highly vulnerable to inhibition. I propose that Hch1p acts at the beginning of the Hsp90 cycle where nucleotide binding occurs. Distinct characteristics of Hch1p provide us with

further insights into the highly regulated Hsp90 cycle and further understanding of Hsp90 inhibitor drugs for their application in cancer.

## 4.2 Folding of Hch1p and Aha1p$^{1-156}$ is sensitive to sequence swaps

To dissect the specific sequence element of Aha1p$^{1-156}$ mechanism and Hch1p mechanism, I constructed loop swap and domain swap mutants. I used three approaches to determine the unique sequence segment of Aha1p *in vitro* and Hch1p *in vivo*. In the first approach, I swapped a non-conserved loop in Aha1p$^{1-156}$ that is located near the *C*-terminal domain of Hsp90 (Figure 3.3). None of these loop 6 swap mutants were soluble because I predict that the interactions that occur from the newly substituted amino acids likely disrupt important interactions of neighboring amino acids with either the loop across which connects the α helix 2 to the 'd' strand of the β sheet or with the loop that connects α helix 1 to the 'a' strand of the β sheet. The second approach involved swapping larger sections of Aha1p$^{1-156}$ and Hch1p that were bound by conserved regions of amino acids (Figure 3.5). None of these mutants were soluble suggesting that there are sequence specific interactions that occur within Aha1p$^{1-156}$ between α helix 1 and 2 and between the strands of the β sheet and α helix 2 which I predict are necessary to maintain folding of all secondary structures. The last approach involved swapping loops of Aha1p$^{1-156}$ that were located in proximity to the Aha1p-Hsp90M binding interface (Figure 3.7). Although none of my mutants, when expressed *in vivo,* showed signs of rescuing growth of yeast expressing Hsp82p$^{E381K}$, a myc epitope signal was detected from strains over-expressing the

loop swap mutants 1a and 4a in both ip82a and iE381Ka (Figure 3.8). The 1a mutant was constructed as an *in vivo* control to mutant 1b by substituting residues 98-121 of Aha1p$^{1-156}$ sequence into Hch1p. I predicted this Hch1p mutant would not rescue growth of yeast expressing Hsp82p$^{E381K}$. The 1b mutant (Figure 3.7) was constructed for *in vitro* analysis, which I predicted that Hch1p would acquire the ability of Aha1p-like robust stimulation of the Hsp90 ATPase activity. Upon further investigation during purification, I determined that the 1b mutant was insoluble and analysis of this mutant *in vitro* could not be done (Figure 3.8D). The 4a mutant was constructed by inserting Hch1p residues 108-199 into Aha1p$^{1-156}$ (Figure 3.7) and I expected Aha1p$^{1-156}$ mutant to gain the function of Hch1p and suppress the defect of Hsp82p$^{E381K}$ *in vivo*. This mutant did not rescue Hsp82p$^{E381K}$ yeast growth (Figure 3.8A) therefore I concluded that either the substituted amino acids were not the sequence element responsible for Hch1p function to suppress Hsp82p$^{E381K}$ defect *in vivo* or this mutant was simply non-functional and was not degraded. The fact that mutants 3 and 4 are insoluble suggests that the loop between α helix 2 and strand 'd' of the β sheet forms stabilizing interactions with strand 'c' of the beta sheet and the loops that connect strands 'b' and 'c' of the β sheet in a sequence-specific fashion. The amino acid sequences that comprise the structures located near the *C*-terminal domain of Hsp90 are not conserved in Hch1p which suggests that mutants 1 and 2 are insoluble due to disruptive interactions with amino acid sequences in the β sheet. Likewise, the compromised folding of mutants 1 and 2 suggests that the small loop-helix-loop that is between strands of the beta sheet make important

interactions with α helix 2. The next step to determine the differences in the sequence elements of Aha1p and Hch1p would be to construct more complicated substitutions such as multiple discontinuous substitutions. Multiple sections would be selected that are not conserved in Aha1p$^{1-156}$ and Hch1p but also reside proximal to each other, i.e. multiple loops that connect the strands of the β sheet, and are oriented toward the *C*-terminal domain of Hsp90 (Figure 4.1). I predict that substituting multiple discontinuous amino acid sections from Hch1p into Aha1p would preserve the folding of Aha1p while also integrating non-conserved sections of Hch1p to determine the sequences responsible for the functional differences *in vivo* and *in vitro* between these Hch1p and Aha1p, respectively.

In efforts to understand why the hybrid constructs compromised folding of Hch1p and Aha1p$^{1-156}$, our group mapped a homology model of Hch1p (Figure 4.2A). When compared to the crystal structure of Aha1p$^{1-156}$, the model of Hch1p looks similar in structure (Figure 4.2B). But Aha1p$^{1-156}$ and Hch1p share only 36% amino acid sequence identity and the homology model has a poor fit score indicating that the model most likely differs significantly from the structure of Aha1p$^{1-156}$. Specifically, the structure of Hch1p is different from Aha1p$^{1-156}$ in most of the non-conserved regions that occur proximal to the *C*-terminal domain of Hsp90 (Figure 4.2C – highlighted residues in red). Because the structure of Hch1p and Aha1p$^{1-156}$ are more different than originally hypothesized which explains why my hybrid constructs were non-functional.

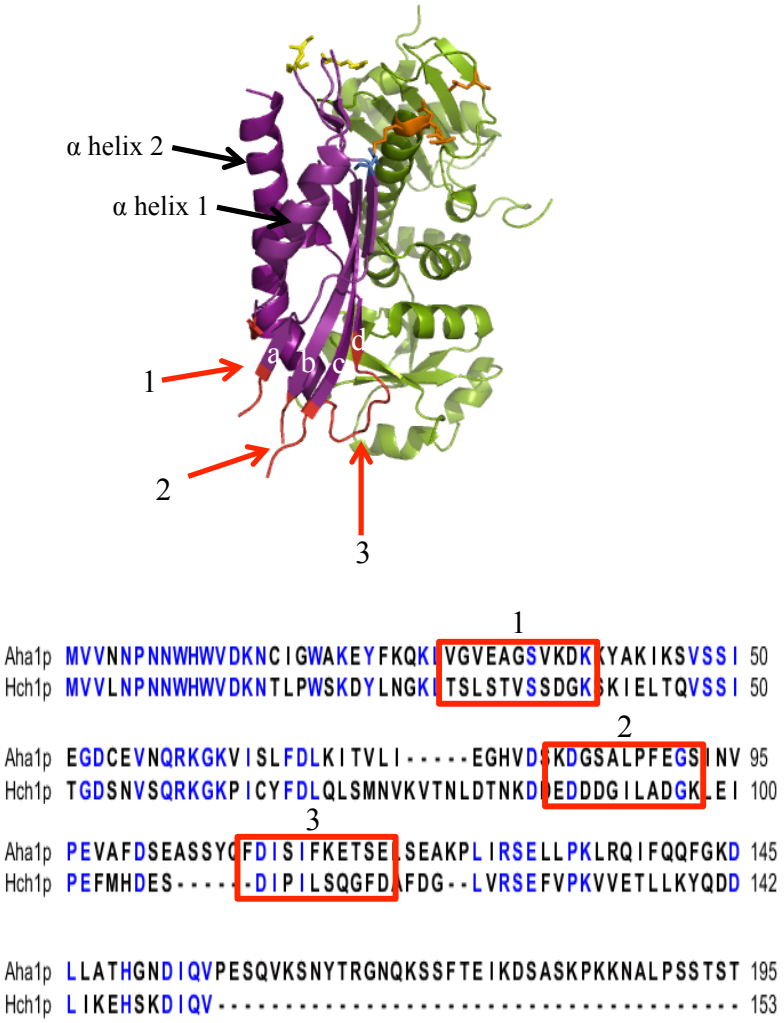


**Figure 4.1 Example of multiple discontinuous amino acid substitutions in Hch1p and Aha1p.** A. Crystal structure of Aha1p$^{1\text{-}156}$ with loops (red) which will be substituted with residues from Hch1p, labeled 1, 2, and 3. B. Alignment of Hch1p and Aha1p$^{1\text{-}156}$ highlighting amino acid sections corresponding to loops highlighted in A.

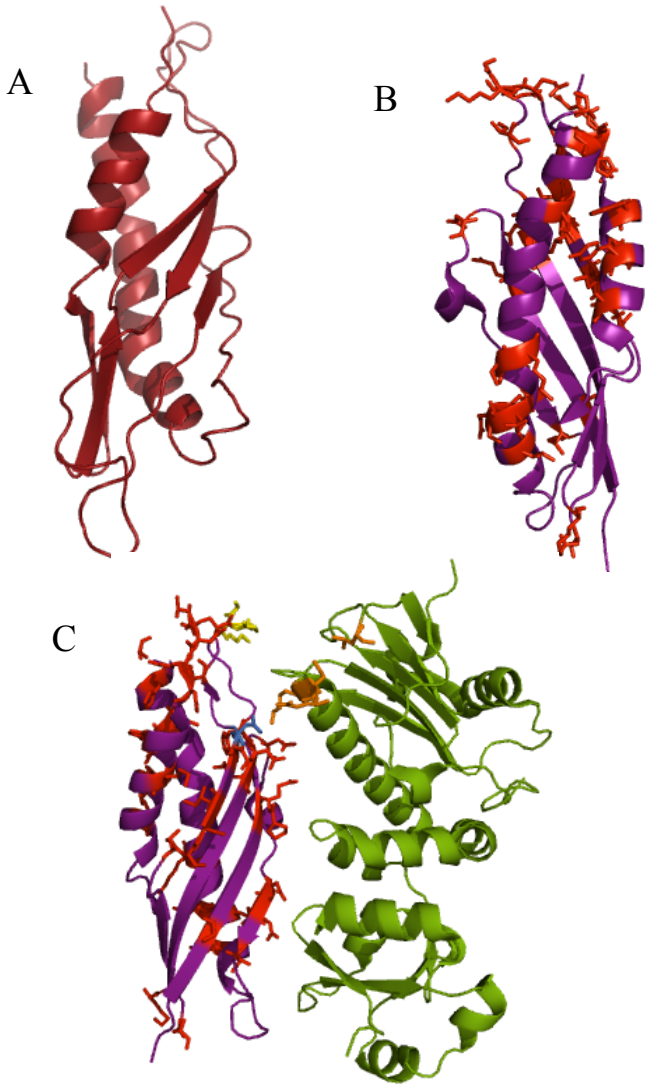


**Figure 4.2 Comparison of Hch1p homology model to crystal structure of Aha1p$^{1-156}$.** A. Homology model of Hch1p. B. Crystal structure of Aha1p$^{1-156}$ with residues conserved with Hch1p highlighted in red. C. Crystal structure of Aha1p$^{1-156}$ bound to the middle domain of Hsp82p with residues conserved with Hch1p highlighted in red.

## 4.3 Hch1p stimulation of the Hsp90 ATPase activity is biologically relevant

The ability of Aha1p to stimulate the Hsp90 ATPase activity involves the RKxK motif to remodel the Hsp90 catalytic loop (residues 370-390) (Figure 3.9). My results confirm previous reports that alanine mutations in the RKxK loop results in the reduction of Aha1p$^{1-156}$ stimulation of the Hsp90 ATPase activity, where K60A results in the largest loss of ATPase stimulation and K62A results in the smallest loss of ATPase stimulation (Meyer et al., 2004). The hierarchy of residues in the RKxK loop involved in Aha1p stimulation of the Hsp90 ATPase activity follow a K60>R59>K62 fashion. This motif is also involved in Hch1p function *in vivo* as my results show that the K60 residue is necessary for Hch1p to rescue growth of yeast expressing Hsp82p$^{E381K}$, R59 is sufficient for Hch1p biological function and K62 is not involved (Figure 3.10). The hierarchy of residue requirement for Hch1p function *in vivo* also follows a K60>R59>K62 fashion which parallels Aha1p function *in vitro*. This suggests that the biological function of Hch1p involves a level of ATPase stimulation to suppress the Hsp82p$^{E381K}$ defect *in vivo*. Previous reports have shown that the level of Hsp90 ATPase stimulation by Hch1p is very weak (Figure 3.1) (Panaretou et al., 2002). Therefore, Hch1p stimulates a low rate of Hsp90 ATPase activity and this low level is sufficient for Hsp90 biological activity *in vivo* at the Hch1p-regulated step. Furthermore, Aha1p can robustly stimulate Hsp90 ATPase activity, which can be characterized as the high rate of Hsp90 ATPase activity. This suggests that Hsp90 biological activity employs a range of levels of ATPase stimulation *in vivo*

in a step-specific fashion. As ATPase stimulation is a necessary part of Hch1p function *in vivo* and the RKxK loop in Hch1p is involved in stimulating the Hsp90 ATPase activity, I predict that introducing K60A, R59A, K62A mutations into Hch1p would stimulate the ATPase activity of Hsp90 in an $Hch1p^{K60A}$>$Hch1p^{R59A}$>$Hch1p^{K62A}$ fashion. This would help us to further characterize Hch1p function to stimulate the Hsp90 ATPase activity.

### 4.4 Differences of Hch1p and Aha1p

My results show that Hch1p and Aha1p use similar motifs, such as RKxK and D53 residues, for their functions *in vivo* and *in vitro*, respectively. Hch1p function *in vitro* stimulates the rate of Hsp90 ATPase activity to the same extent as $Aha1p^{1-156}$. Even though Hch1p and $Aha1p^{1-156}$ levels of stimulated Hsp90 ATPase rate are similar, Hch1p fused to the *C*-terminal domain of Aha1p cannot robustly stimulate the Hsp90 ATPase activity as full length Aha1p (Figure 3.1). Therefore, $Aha1p^{1-156}$ contains a sequence element that is not in Hch1p and this sequence element is responsible for robust stimulation of Hsp90 ATPase activity. How this unknown sequence element stimulates robust rate of Hsp90 ATPase activity can be examined in two ways. The first possibility may be that $Aha1p^{1-156}$ activates $Aha1p^{157-350}$ in a way that allows Aha1p to fully stimulate the Hsp90 ATPase activity. Previous studies have shown that $Aha1p^{1-156}$ and $Aha1p^{157-350}$ are very poor Hsp90 ATPase stimulators on their own (Retzlaff et al., 2010; Panaretou et al., 2002). When $Aha1p^{157-350}$ is titrated into an $Aha1p^{1-156}$ stimulated Hsp90 ATPase reaction, the rate of Hsp90 ATPase activity is higher than when

they are separate but is significantly lower than when the domains of Aha1p are connected. As robust stimulation of Hsp90 ATPase activity requires Aha1p$^{1-156}$ to be connected to Aha1p$^{157-350}$, I predict that Aha1p$^{1-156}$ contains a motif that is not in Hch1p and interacts with an unknown motif in Aha1p$^{157-350}$ in order to stimulate the Hsp90 ATPase activity. This motif in Aha1p$^{1-156}$ is located near the *N*-terminal domain of Hsp90 and near Aha1p$^{157-350}$ (Figure 4.3A, B). I would test this hypothesis by performing NMR analysis where I would titrate Aha1p$^{1-156}$ or Hch1p into $^{15}$N labeled Aha1p$^{157-350}$ reactions and examine whether unique interactions occur between Aha1p$^{1-156}$ to Aha1p$^{157-350}$ and Hch1p to Aha1p$^{157-350}$. I predict that Aha1p$^{1-156}$ titrated into Aha1p$^{157-350}$ would generate peak shifts, which would indicate the Aha1p domains interact together. When Hch1p is titrated into Aha1p$^{157-350}$ reaction, I would not expect any peak shifts indicating that Hch1p does not interact with Aha1p$^{157-350}$. Alternatively, the other possibility of how an unknown motif in Aha1p$^{1-156}$, but not in Hch1p, stimulates the Hsp90 ATPase activity robustly might be that Aha1p$^{1-156}$ has a sequence element that activates the middle domain of Hsp90 whereas Hch1p cannot (Figure 4.3C, D). Since many of the amino acids in Aha1p located near the *C*-terminal domain of Hsp90 are not conserved in Hch1p, I predict that the sequence element in Aha1p that interacts with Hsp90 is located at or within this region of Aha1p$^{1-156}$. I suspect that the Hch1p sequence does not contain the small α helix which folds between β strand 'c' and strand 'd' in the Aha1p$^{1-156}$ crystal structure because many amino acids in Hch1p are missing in this region as compared to Aha1p (Figure 4.3E). Determining the structure of Hch1p bound to Hsp90M by X-ray crystallography

would elucidate the folding of this sequence in Hch1p. I would compare the structure of Hch1p to the known structure of Aha1p$^{1-156}$ and compare the differences of folding that might influence interactions with Hsp90M.

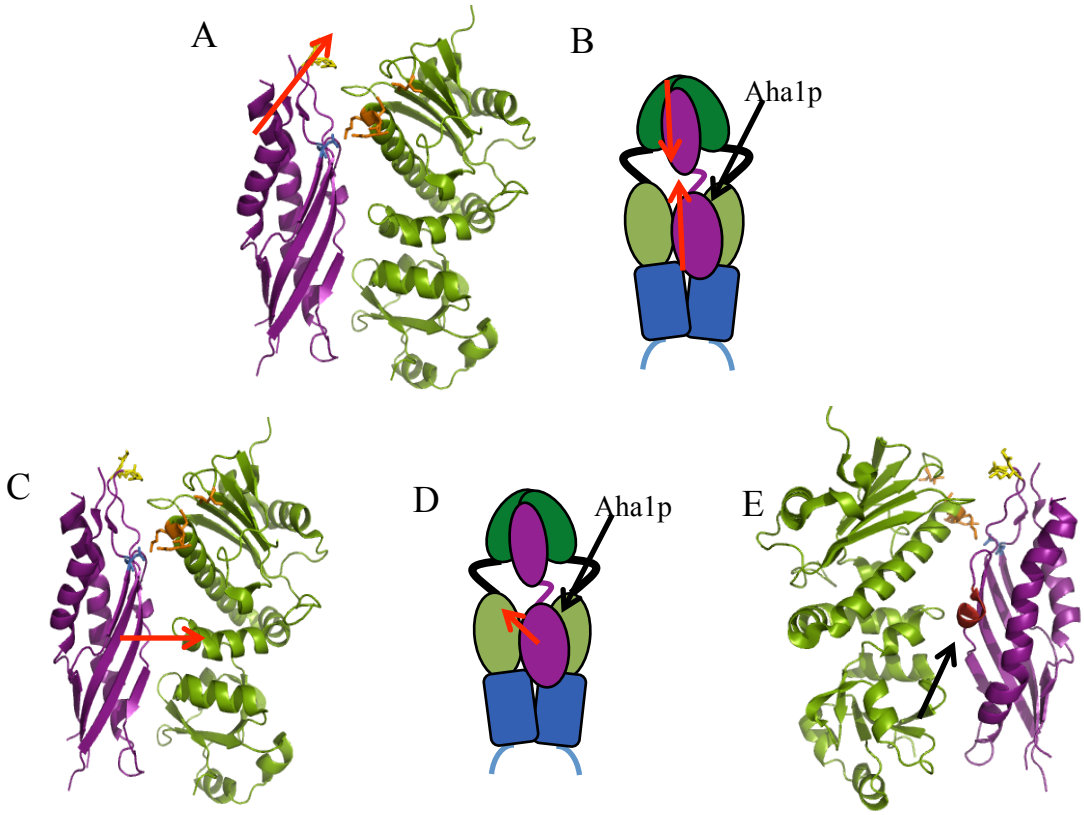


**Figure 4.3 Two possibilities of an unknown sequence motif in Aha1p that is responsible for robustly stimulating the Hsp90 ATPase activity.** A. Unknown sequence motif in Aha1p$^{1\text{-}156}$ that is located near the *N*-terminal domain of Hsp90 and interacts with Aha1p$^{157\text{-}350}$. Red arrow highlights orientation of the unknown sequence motif. B. Activation of the domains of Aha1p and the orientation when bound to Hsp90. C. Unknown sequence motif in Aha1p$^{1\text{-}156}$ that is located and activates the middle domain of Hsp90. D. Unknown sequence motif in C in Aha1p$^{1\text{-}156}$ when bound to Hsp90. E. Small α helix (black arrow) present in Aha1p$^{1\text{-}156}$ which may be the unknown sequence element of Aha1p$^{1\text{-}156}$ not in Hch1p.

## 4.5 Hch1p role in regulating nucleotide exchange of Hsp90 affects Hsp90 drug inhibition

Previous results have shown that Hch1p confers sensitivity to Hsp90 inhibitor drugs in yeast expressing wild-type Hsp82p (Armstrong et al., 2012). Specifically, I was able to determine that Hch1p requires remodeling of the Hsp90 catalytic loop by the RKxK motif to hypersensitize Hsp90 to drug inhibition (Figure 3.11). Studies have shown that ATP binding and release occurs rapidly throughout the Hsp90 cycle (Mickler et al., 2009; Ratzke et al., 2012). Co-chaperones bind to Hsp90 in specific nucleotide bound conformations and influence whether Hsp90 is susceptible to drug inhibition. Sba1p binds to Hsp90 in the ATP-bound closed conformation, which reduces rate of the nucleotide exchange in the Hsp90 *N*-terminal domains and increases Hsp90 affinity for ATP (Ali et al., 2006; McLaughlin et al., 2006). Sba1p over-expression induces drug resistance in yeast to Hsp90 inhibitors (Piper et al., 2003). Conversely, Sti1p binds to Hsp90 in the ADP-bound open conformation, and the rate of nucleotide exchange between ADP and ATP is rapid as affinity for ATP is greatly reduced (Ratzke et al., 2012; Richter et al., 2003). Over-expression of Sti1p also induces drug resistance in yeast to Hsp90 inhibitor drugs (Piper et al., 2003). As both Sti1p and Sba1p induce resistance in yeast to Hsp90 inhibitor drugs even though these two co-chaperones interact with Hsp90 while in very different conformations, it is not clear how this effect is exerted. How co-chaperones regulate ATP binding with respect to Hsp90 conformations that are sensitive to drug inhibition is very complicated. Aha1p binds favorably to Hsp90 in the ATP-

bound, closed conformation, which is an Hsp90 conformation resistant to drug inhibition, and Aha1p does not affect the $K_M$ of ATP to Hsp90 (Panaretou et al., 2002). Hch1p interaction causes Hsp90 to adopt a conformation that is sensitive to drug inhibition *in vivo* but whether the drug sensitivity step is due to Hch1p increasing ATP affinity to Hsp90 is unknown. It would be interesting to measure the effect Hch1p has on the $K_M$ of Hsp82p to ATP by conducting an ATPase assay where an Hch1p stimulated Hsp82p ATPase reaction is measured with increasing amounts of ATP. If the $K_M$ of ATP to Hsp82p by an Hch1p stimulated rate is higher than the known $K_M$ of ATP to Hsp82p by an Aha1p stimulated rate, then Hch1p influences Hsp90 sensitivity to drug inhibition by lowering the affinity of ATP to Hsp90. Moreover, it would be worthwhile to measure the $K_M$ of ATP to Hsp82p and Aha1p$^{1-156}$ stimulated Hsp90 ATPase assay. If the $K_M$ values of ATP in the presence of Hch1p and Aha1p$^{1-156}$ are significantly different, then that would tell us that Hch1p regulates Hsp90 in a conformation that is significantly different than Aha1p$^{1-156}$.

## 4.6 Hch1p regulates a distinct step in the Hsp90 cycle than that regulated by Aha1p

Yeast expressing wild-type Hsp82p are resistant to Hsp90 inhibitors when *HCH1* is deleted and hypersensitive to NVP-AUY922 when Hch1p is over-expressed (Armstrong et al., 2012). Yeast expressing Hsp82p$^{E381K}$ are not viable without Hch1p (Heather Armstrong, unpublished data) but are resistant to NVP-AUY922 (Figure 3.12). The step that is impaired by E381K mutation is rescued

by the A587T mutation as yeast-expressing Hsp82p$^{E381K/A587T}$ can grow independently of Hch1p *in vivo* (Figure 3.13B). Even though both A587T mutation and Hch1p suppress the Hsp82p$^{E381K}$ defect *in vivo*, Hch1p interferes with the conformation adopted by Hsp82p$^{A587T}$ because growth of yeast expressing Hsp82p$^{A587T}$ is rescued when *HCH1* is deleted (Armstrong et al., 2012). Hch1p acts a point in the cycle that repairs Hsp82p$^{E381K}$ and interferes with Hsp82p$^{A587T}$. This step in the cycle is also vulnerable to drug inhibition because Hch1p induces hypersensitivity to Hsp90 inhibitor drugs to wild-type Hsp82p *in vivo*. Another co-chaperone, Sti1p, has been found to suppress the A587T mutation as growth of yeast expressing Hsp82p$^{A587T}$ is rescued when Sti1p is over-expressed (Chang et al., 1997). Interestingly, the step in the Hsp90 cycle that is regulated by Sti1p is also vulnerable to inhibition by Hsp90 inhibitors because the deletion of *STI1* has been shown to confer hypersensitivity to Hsp90 inhibitor drugs in yeast (Piper et al., 2003). The findings listed above are summarized in Figure 4.4. Therefore, the step that Hch1p regulates in the Hsp90 cycle may occur in two different scenarios. The first may be that Hch1p regulates a step in the Hsp90 cycle that occurs after the formation of the Sti1p-Hsp90 complex (Figure 4.5A). The second may be that Hch1p binds at the same time as Sti1p (Figure 4.5B). I could test this by conducting an immunoprecipitation (IP) experiment where I would IP *N*-terminal myc tagged Hch1p to Hsp82p with and without the presence of Sti1p. If Sti1p disrupts Hch1p binding to Hsp82p then Sti1p and Hch1p do not bind to Hsp82p at the same time (Figure 4.5A). If Sti1p binds to the Hch1p-Hsp82p complex and does not disrupt Hch1p binding to Hsp82p, then

Sti1p and Hch1p bind to Hsp82p at the same time (Figure 4.5B). By conducting this experiment, I can determine whether Hch1p regulates Hsp90 at a step at that occurs early in the Hsp90 cycle and at the same time as Sti1p or at a step that is mutually exclusive of Sti1p.

| Yeast Strain | Sti1p | ΔSti1p | Hch1p | ΔHch1p |
|---|---|---|---|---|
| Hsp82p | - | - | - | - |
| Hsp82p$^{E381K}$ | - | - | ↑ | Not Viable[2] |
| Hsp82p$^{A587T}$ | ↑[3] | - | ↓[1] | ↑↑[1] |
| Hsp82p$^{V391E}$ | ND | ND | ND | ND |

**Figure 4.4 Chart summarizing phenotypes of yeast expressing mutant Hsp82p.** The phenotypes of yeast expressing wildtype Hsp82p, and Hsp82p mutants Hsp82p$^{E381K}$, Hsp82p$^{A587T}$, and Hsp82p$^{V391E}$ are listed when co-chaperones Sti1p and Hch1p are either overexpressed or deleted and when yeast strains are treated with Hsp90 inhibitor, NVP-AUY922. [1]- (Armstrong el al., 2012), [2]- (Heather Armstrong, unpublished data), [3]- (Chang et al., 1997).

| | | Drug sensitivity of strains after co-chaperone over-expression or deletion as compared to the parental strain | | | |
|---|---|---|---|---|---|
| Hsp82p variant expressed in yeast | Drug Sensitivity | Sti1p O/E | ΔSti1p | Hch1p O/E | ΔHch1p |
| Hsp82p | - | Resistant | Sensitive[3] | Sensitive[1] | Resistant[1] |
| Hsp82p$^{E381K}$ | Resistant | ND | ND | Resistant | Not Viable[2] |
| Hsp82p$^{A587T}$ | Sensitive | ND | ND | Sensitive[1] | Resistant[1] |
| Hsp82p$^{V391E}$ | Sensitive | ND | ND | ND | Unchanged |

**Figure 4.5 Chart summarizing sensitivity to the Hsp90 inhibitor drug, NVP-AUY922, in yeast expressing wildtype and mutant Hsp82p.** The sensitivity to the Hsp90 inhibitor drug NVP-AUY922 in yeast expressing wildtype Hsp82p, and Hsp82p mutants Hsp82p$^{E381K}$, Hsp82p$^{A587T}$, and Hsp82p$^{V391E}$ are listed and compared to the sensitivity to NVP-AUY922 observed in yeast strains when co-chaperones Sti1p and Hch1p are either over-expressed or deleted. [1]- (Armstrong el al., 2012), [2]- (Heather Armstrong, unpublished data), [3]- (Chang et al., 1997).

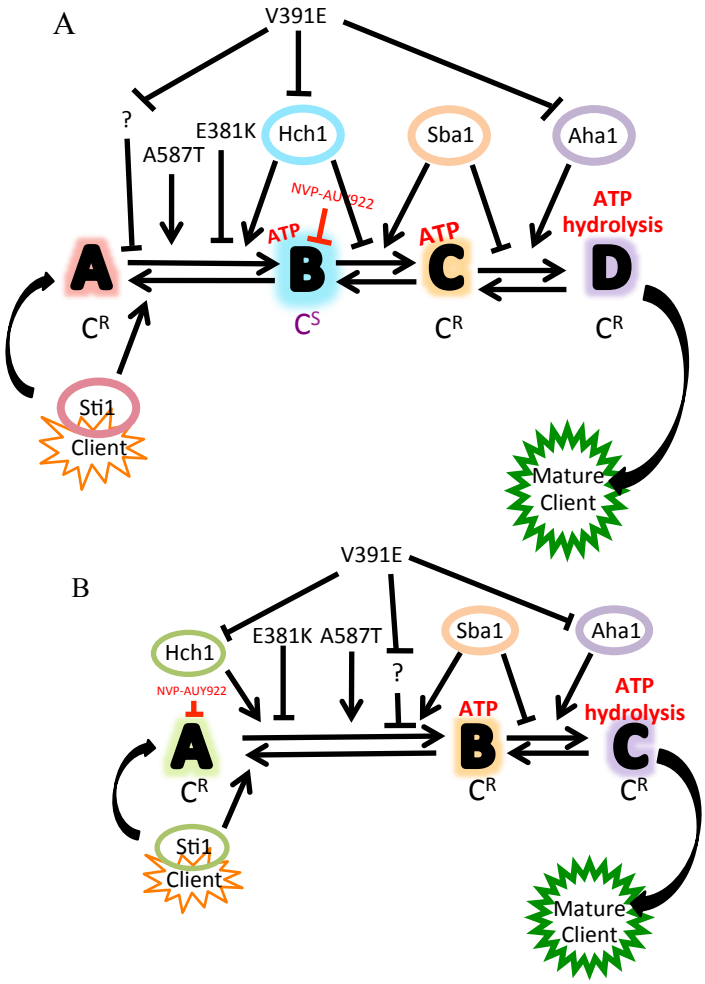


**Figure 4.6 Two possible scenarios of Hch1p regulation of the Hsp90 cycle.** A. Scenario 1: Hch1p regulates a step in the Hsp90 cycle which occurs after the formation of the Sti1p-Hsp90 complex. The Hch1p-Hsp90 complex can bind to ATP or be competitively inhibited by NVP-AUY922. B. Scenario 2: Hch1p regulates a step in the Hsp90 cycle that occurs at the same time as Sti1p. This step is sensitive to drug inhibition when in complex with Hch1p and resistant to drug inhibition without Hch1p.

## 4.7 Future directions and summary

Our group has cloned Ahsa1 and Ahsa2 orthologs from the mouse Hsp90 system, which share high sequence identity to Hch1p and Aha1p. *N*-terminal domain of mAhsa1 and mAhsa2 share high sequence similarity to Hch1p and the *C*-terminal domain of mAhsa1 and mAhsa2 share high sequence similarity to Aha1p$^{157\text{-}350}$ (Figure 4.6). Since Hch1p regulates a step in the Hsp90 cycle that occurs early, I hypothesize this step occurs within the mouse Hsp90 system and is also regulated by mAhsa1 or mAhsa2. Preliminary ATPase experiments show that mAhsa2 can stimulate the Hsp90β ATPase rate more than mAhsa1 (Figure 4.7). Further experiments are needed to confirm this result. Future experiments that can be conducted where mAhsa1 and mAhsa2 are over-expressed in HEK293 cells and the $IC_{50}$ of NVP-AUY922 would be measured. If mAhsa1 or mAhsa2 regulate the Hsp90 cycle similar to Hch1p, then HEK293 cells over-expressing mAhsa1 or mAhsa2 will be more sensitive to Hsp90 inhibitors. Furthermore, the NxxNWHW motif is highly conserved in most fungal Aha1p homologues and all fungal Hch1p homologues (Figure 4.8). It is also found within mAhsa1 and mAhsa2 but interestingly this motif is significantly longer in mAhsa1 and mAhsa2 (Figure 4.6). Even though both Aha1p and Hch1p contain the NxxNWHW motif, it is curious why only Hch1p requires this motif for its function *in vivo*. Since mAhsa1 and mAhsa2 share high sequence similarity to both Hch1p and Aha1p, it would be interesting to examine whether mAhsa1 or mAhsa2 require the NxxNWHW motif to regulate the mouse Hsp90 system. I could test this by over-expressing mAhsa1$^{\Delta 27}$ and mAhsa2$^{\Delta 27}$ mutants in HEK293

cells and measure the $IC_{50}$ of NVP-AUY922 in HEK293 cells. If mAhsa1 or mAhsa2 have specific motif requirements similar to Hch1p, then HEK293 cells over-expressing mAhsa1$^{\Delta 27}$ and mAhsa2$^{\Delta 27}$ will not be hypersensitive. Not only will this help us bridge studies in the yeast Hsp90 system to the mammalian system but also better understand the Hsp90 system in mammalian cells.

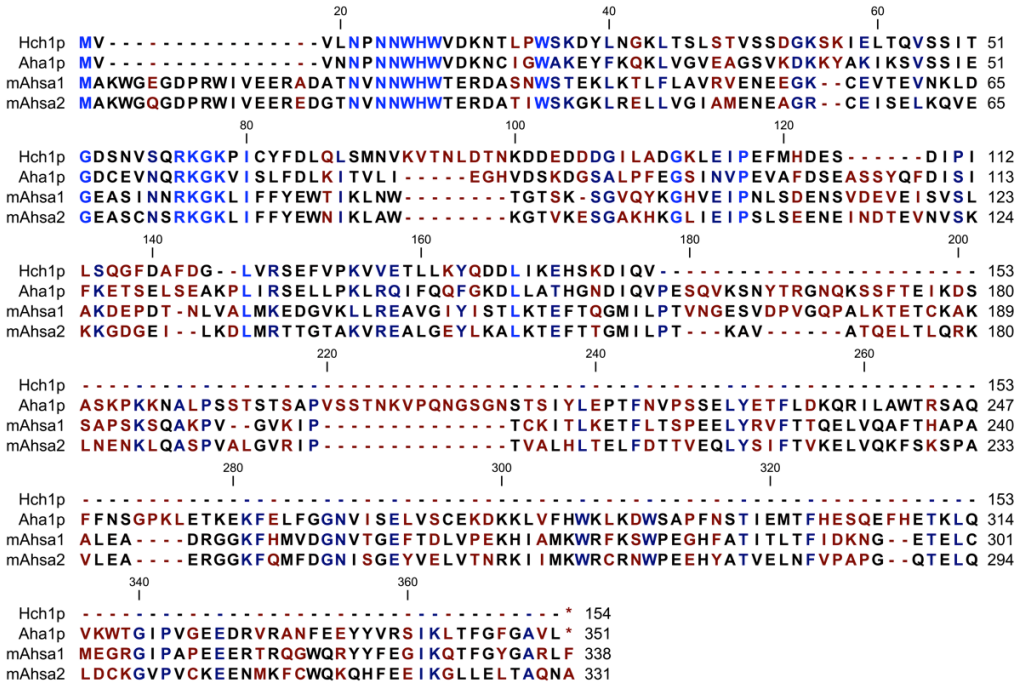


**Figure 4.7 Sequence alignment of mAhsa1, mAhsa2, Aha1p, and Hch1p.** Blue highlighting indicates highly conserved residues and red highlighting indicates semi-conserved residues.

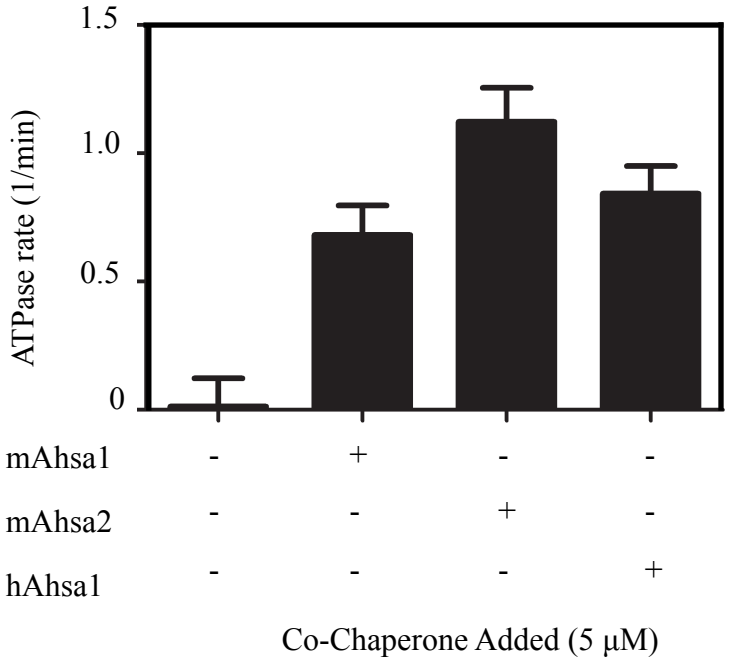


**Figure 4.8 Stimulation of the Hsp90β ATPase activity by mAhsa1, mAhsa2, and hAhsa1.** Reactions contain 5 μM Hsp90β and 5 μM mAhsa1, mAhsa2, or hAhsa1. ATPase rate shown in μM ATP hydrolyzed per minute per μM of enzyme (1/min).

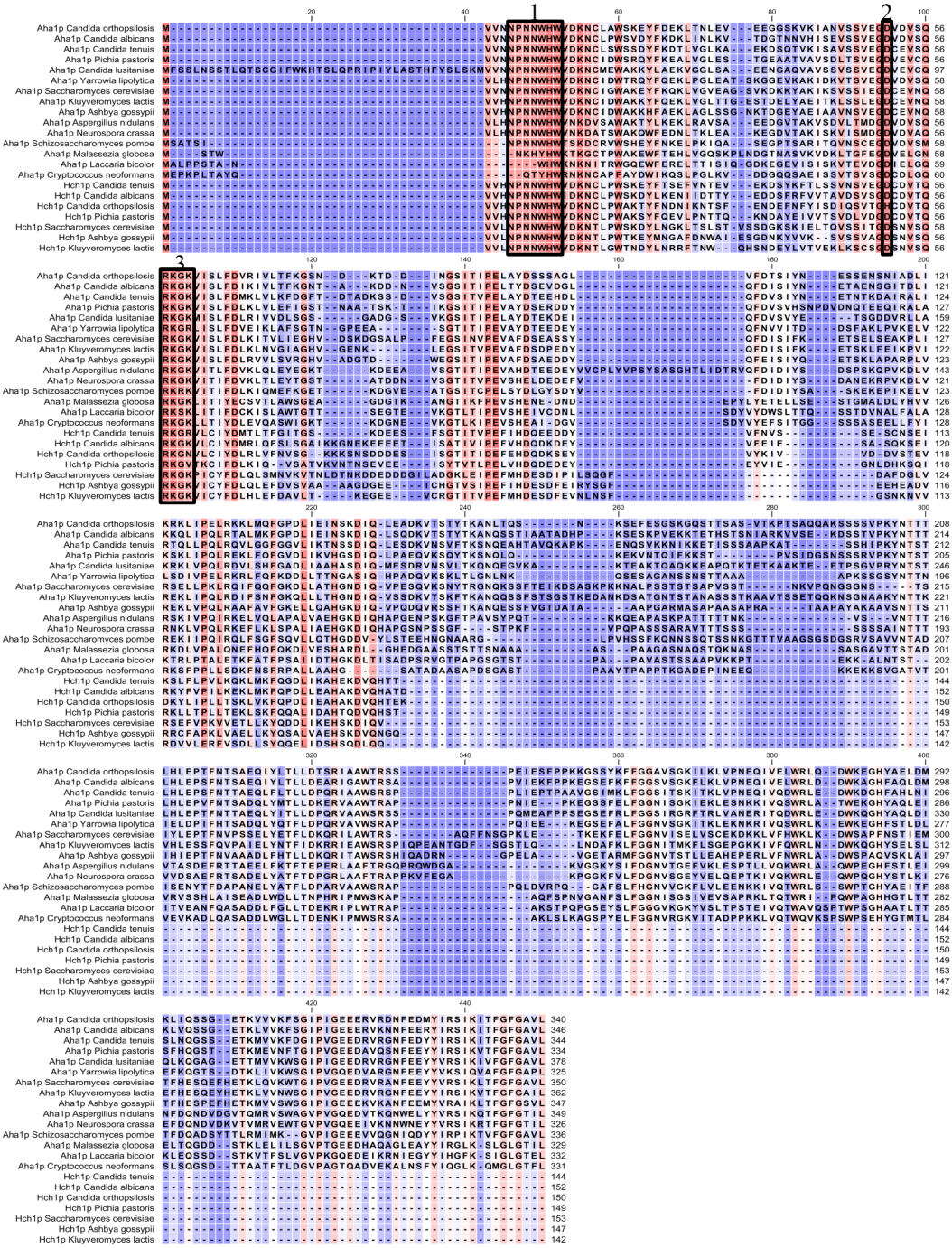


**Figure 4.9 Sequence alignment of fungal Hch1p/Aha1p homologues.** Boxes highlight conserved motifs NxxNWHW (Box 1), D53 (Box 2), and RKxK motif (Box 3).

One mechanism by which Hsp90 inhibitor sensitivity can be altered is by co-chaperone regulation. This mechanism is very complicated because some co-chaperones such as Hch1p and Sti1p have opposite effects on drug sensitivity in yeast. Hch1p over-expression confers hypersensitivity to Hsp90 inhibitors (Armstrong et al., 2012) but Sti1p over-expression induces drug resistance in yeast expressing wild-type Hsp82p (Piper et al., 2003). Recently, post-translational modification of Hsp90 has been shown to be another mechanism of regulation of Hsp90 drug sensitivity (Mollapour et al., 2011). Hsp82p can be phosphorylated at the Thr22 residue and the phosphorylation status of this residue can influence drug inhibition. The Thr22 resides in the *N*-terminal domain of Hsp82p and is part of a hydrophobic patch that forms interactions with the Hsp90 catalytic loop. A phosphomimetic mutant, $Hsp82p^{T22E}$, when expressed in yeast as the sole source of Hsp82p, confers sensitivity to Hsp90 inhibitors in yeast. The non-phosphomimetic Hsp82p mutant, $Hsp82p^{T22A}$, induces resistance to Hsp90 inhibitors in yeast when expressed as their sole source of Hsp82p. How the phosphorylation status of Hsp90 affects co-chaperone regulation of drug sensitivity furthers the complexities of the mechanism of Hsp90 drug inhibition. It would be interesting to test whether the induction of drug sensitivity due to the phosphorylation at the T22 site in Hsp82p regulates the same step in the Hsp90 cycle as Hch1p. I could test this by over-expressing Hch1p in yeast strains expressing either $Hsp82p^{T22E}$ or $Hsp82p^{T22A}$ as their sole source of Hsp90 and examine their sensitivity to Hsp90 inhibitors. If Hch1p induces sensitivity to Hsp90 inhibitors in yeast expressing $Hsp82p^{T22A}$ then drug sensitivity induced by

phosphorylation on Hsp90 occurs at the same step regulated by Hch1p. However, if Hch1p does not induce sensitivity to Hsp90 inhibitors in yeast expressing Hsp82p$^{T22A}$ then regulation of drug sensitivity by phosphorylation on Hsp90 occurs at a different step than Hch1p regulation. These two mechanisms show how complex drug inhibition of Hsp90 is and further studies may take advantage of multiple mechanisms of Hsp90 drug inhibition to elucidate more effective ways of targeting Hsp90 for cancer therapy.

I have identified the conserved motifs, D53 and RKxK, that are required for Hch1p function *in vivo* are also involved in Aha1p function *in vitro*. Moreover, I have also identified the conserved motif, NxxNWHW, which is required for Hch1p function *in vivo* but is not important for Aha1p function *in vitro*. Hch1p requires the use of these conserved motifs to hypersensitize Hsp90 to Hsp90 inhibitor drugs. I have determined that Hch1p acts differently than Aha1p, at a distinct step in the Hsp90 cycle, which occurs early and is also hypersensitive to inhibition. Despite my findings, there remains much to be elucidated about Hch1p role in the Hsp90 cycle and how Hch1p sensitizes Hsp90 to Hsp90 inhibitor drugs. Further studies can use my findings to aid in the understanding of drug sensitive steps of the Hsp90 cycle and to uncover more effective methods to manipulate the Hsp90 cycle for therapies against cancer.

# Chapter Five

## References

Ali, M.M., S.M. Roe, C.K. Vaughan, P. Meyer, B. Panaretou, P.W. Piper, C. Prodromou, and L.H. Pearl. 2006. Crystal structure of an Hsp90–nucleotide–p23/Sba1 closed chaperone complex. *Nature.* 440:1013-1017.

Anfinsen, C.B. 1973. Principles that govern the folding of protein chains. *Science.* 181:223-230.

Armstrong, H., A. Wolmarans, R. Mercier, B. Mai, and P. LaPointe. 2012. The Co-Chaperone Hch1 Regulates Hsp90 Function Differently than Its Homologue Aha1 and Confers Sensitivity to Yeast to the Hsp90 Inhibitor NVP-AUY922. *PloS One.* 7:e49322.

Bartlett, A.I., and S.E. Radford. 2009. An expanding arsenal of experimental methods yields an explosion of insights into protein folding mechanisms. *Nature Structural & Molecular Biology.* 16:582-588.

Basha, E., G.J. Lee, L.A. Breci, A.C. Hausrath, N.R. Buan, K.C. Giese, and E. Vierling. 2004. The identity of proteins associated with a small heat shock protein during heat stress in vivo indicates that these chaperones protect a wide range of cellular functions. *J.Biol.Chem.* 279:7566-7575.

Basso, A.D., D.B. Solit, G. Chiosis, B. Giri, P. Tsichlis, and N. Rosen. 2002. Akt forms an intracellular complex with heat shock protein 90 (Hsp90) and Cdc37 and is destabilized by inhibitors of Hsp90 function. *J.Biol.Chem.* 277:39858-39866.

Bensaude, O., M. Pinto, M. Dubois, N. Van Trung, and M. Morange. 1990. Protein denaturation during heat shock and related stress. *In* Stress Proteins. Springer. 89-99.

Boeke, J.D., F. La Croute, and G.R. Fink. 1984. A positive selection for mutants lacking orotidine-5′-phosphate decarboxylase activity in yeast: 5-fluoro-orotic acid resistance. *Molecular and General Genetics MGG.* 197:345-346.

Bohen, S.P. 1998. Genetic and biochemical analysis of p23 and ansamycin antibiotics in the function of Hsp90-dependent signaling proteins. *Mol.Cell.Biol.* 18:3330-3339.

Bohen, S.P., and K.R. Yamamoto. 1993. Isolation of Hsp90 mutants by screening for decreased steroid receptor function. *Proceedings of the National Academy of Sciences.* 90:11424-11428.

Borkovich, K.A., F.W. Farrelly, D.B. Finkelstein, J. Taulien, and S. Lindquist. 1989. hsp82 is an essential protein that is required in higher concentrations for growth of cells at higher temperatures. *Mol.Cell.Biol.* 9:3919-3930.

Brinker, A., C. Scheufler, F. von der Mülbe, B. Fleckenstein, C. Herrmann, G. Jung, I. Moarefi, and F.U. Hartl. 2002. Ligand Discrimination by TPR Domains RELEVANCE AND SELECTIVITY OF EEVD-RECOGNITION IN Hsp70· Hop· Hsp90 COMPLEXES. *J.Biol.Chem.* 277:19265-19275.

Brough, P.A., W. Aherne, X. Barril, J. Borgognoni, K. Boxall, J.E. Cansfield, K.J. Cheung, I. Collins, N.G. Davies, and M.J. Drysdale. 2007. 4, 5-diarylisoxazole Hsp90

chaperone inhibitors: potential therapeutic agents for the treatment of cancer. *J.Med.Chem.* 51:196-218.

Buchner, J. 1999. Hsp90 & Co.–a holding for folding. *Trends Biochem.Sci.* 24:136-141.

Cannon, W.B. 1929. Organization for physiological homeostasis. *Physiol.Rev.* 9:399-431.

Carrigan, P.E., G.M. Nelson, P.J. Roberts, J. Stoffer, D.L. Riggs, and D.F. Smith. 2004. Multiple domains of the co-chaperone Hop are important for Hsp70 binding. *J.Biol.Chem.* 279:16185-16193.

Chadli, A., I. Bouhouche, W. Sullivan, B. Stensgard, N. McMahon, M.G. Catelli, and D.O. Toft. 2000. Dimerization and N-terminal domain proximity underlie the function of the molecular chaperone heat shock protein 90. *Proceedings of the National Academy of Sciences.* 97:12524-12529.

Chandler, D. 2005. Interfaces and the driving force of hydrophobic assembly. *Nature.* 437:640-647.

Chang, H., D.F. Nathan, and S. Lindquist. 1997. In vivo analysis of the Hsp90 cochaperone Sti1 (p60). *Mol.Cell.Biol.* 17:318-325.

Chen, B., M. Retzlaff, T. Roos, and J. Frydman. 2011. Cellular strategies of protein quality control. *Cold Spring Harbor Perspectives in Biology.* 3.

Chen, S., and D.F. Smith. 1998. Hop as an adaptor in the heat shock protein 70 (Hsp70) and hsp90 chaperone machinery. *J.Biol.Chem.* 273:35194-35200.

Citri, A., D. Harari, G. Shohat, P. Ramakrishnan, J. Gan, S. Lavi, M. Eisenstein, A. Kimchi, D. Wallach, and S. Pietrokovski. 2006. Hsp90 recognizes a common surface on client kinases. *J.Biol.Chem.* 281:14361-14369.

Cliff, M.J., R. Harris, D. Barford, J.E. Ladbury, and M.A. Williams. 2006. Conformational diversity in the TPR domain-mediated interaction of protein phosphatase 5 with Hsp90. *Structure (London, England: 1993).* 14:415.

Csermely, P., T. Schnaider, Z. Prohászka, and G. Nardai. 1998. The 90-kDa molecular chaperone family: structure, function, and clinical applications. A comprehensive review. *Pharmacol.Ther.* 79:129-168.

Dill, K.A. 1990. Dominant forces in protein folding. *Biochemistry (N.Y.).* 29:7133-7155.

Dill, K.A., and H.S. Chan. 1997. From Levinthal to pathways to funnels. *Nat.Struct.Biol.* 4:10-19.

Echeverría, P.C., A. Bernthaler, P. Dupuis, B. Mayer, and D. Picard. 2011. An interaction network predicted from public data as a discovery tool: application to the Hsp90 molecular chaperone machine. *PloS One.* 6:e26044.

Eckl, J.M., D.A. Rutz, V. Haslbeck, B.K. Zierer, J. Reinstein, and K. Richter. 2013. Cdc37 (Cell Division Cycle 37) Restricts Hsp90 (Heat Shock Protein 90) Motility by Interaction with N-terminal and Middle Domain Binding Sites. *J.Biol.Chem.* 288:16032-16042.

Ellis, R.J. 2007. Protein Misassembly. *In* Molecular Aspects of the Stress Response: Chaperones, Membranes and Networks. Springer. 1-13.

Fabio Falsone, S., S. Leptihn, A. Osterauer, M. Haslbeck, and J. Buchner. 2004. Oncogenic mutations reduce the stability of SRC kinase. *J.Mol.Biol.* 344:281-291.

Feder, M.E., and G.E. Hofmann. 1999. Heat-shock proteins, molecular chaperones, and the stress response: evolutionary and ecological physiology. *Annu.Rev.Physiol.* 61:243-282.

Felitsky, D.J., M.A. Lietzow, H.J. Dyson, and P.E. Wright. 2008. Modeling transient collapsed states of an unfolded protein to provide insights into early folding events. *Proceedings of the National Academy of Sciences.* 105:6278-6283.

Felts, S.J., B.A. Owen, P. Nguyen, J. Trepel, D.B. Donner, and D.O. Toft. 2000. The hsp90-related protein TRAP1 is a mitochondrial protein with distinct functional properties. *J.Biol.Chem.* 275:3305-3312.

Flynn, G.C., J. Pohl, M.T. Flocco, and J.E. Rothman. 1991. Peptide-binding specificity of the molecular chaperone BiP.

Frydman, J. 2001. Folding of newly translated proteins in vivo: the role of molecular chaperones. *Annu.Rev.Biochem.* 70:603-647.

Gorre, M.E., K. Ellwood-Yen, G. Chiosis, N. Rosen, and C.L. Sawyers. 2002. BCR-ABL point mutants isolated from patients with imatinib mesylate–resistant chronic myeloid leukemia remain sensitive to inhibitors of the BCR-ABL chaperone heat shock protein 90. *Blood.* 100:3041-3044.

Grenert, J.P., W.P. Sullivan, P. Fadden, T.A. Haystead, J. Clark, E. Mimnaugh, H. Krutzsch, H. Ochel, T.W. Schulte, and E. Sausville. 1997. The amino-terminal domain of heat shock protein 90 (hsp90) that binds geldanamycin is an ATP/ADP switch domain that regulates hsp90 conformation. *J.Biol.Chem.* 272:23843-23850.

Harst, A., H. Lin, and W.M. Obermann. 2005. Aha1 competes with Hop, p50 and p23 for binding to the molecular chaperone Hsp90 and contributes to kinase and hormone receptor activation. *Biochem.J.* 387:789.

Hartl, F.U., A. Bracher, and M. Hayer-Hartl. 2011. Molecular chaperones in protein folding and proteostasis. *Nature.* 475:324-332.

Hartson, S.D., E.A. Ottinger, W. Huang, G. Barany, P. Burn, and R.L. Matts. 1998. Modular folding and evidence for phosphorylation-induced stabilization of an hsp90-dependent kinase. *J.Biol.Chem.* 273:8475-8482.

Haslbeck, M., S. Walke, T. Stromer, M. Ehrnsperger, H.E. White, S. Chen, H.R. Saibil, and J. Buchner. 1999. Hsp26: a temperature-regulated chaperone. *EMBO J.* 18:6744-6751.

Hawle, P., M. Siepmann, A. Harst, M. Siderius, H.P. Reusch, and W.M. Obermann. 2006. The middle domain of Hsp90 acts as a discriminator between different types of client proteins. *Mol.Cell.Biol.* 26:8385-8395.

Hessling, M., K. Richter, and J. Buchner. 2009. Dissection of the ATP-induced conformational cycle of the molecular chaperone Hsp90. *Nature Structural & Molecular Biology.* 16:287-293.

Heyrovská, N., J. Frydman, J. Höhfeld, and F.U. Hartl. 1998. Directionality of polypeptide transfer in the mitochondrial pathway of chaperone-mediated protein folding. *Biol.Chem.* 379:301-310.

Holmes, J.L., S.Y. Sharp, S. Hobbs, and P. Workman. 2008. Silencing of HSP90 cochaperone AHA1 expression decreases client protein activation and increases cellular sensitivity to the HSP90 inhibitor 17-allylamino-17-demethoxygeldanamycin. *Cancer Res.* 68:1188-1197.

Invernizzi, G., E. Papaleo, R. Sabate, and S. Ventura. 2012. Protein aggregation: mechanisms and functional consequences. *Int.J.Biochem.Cell Biol.* 44:1541-1554.

Ito, H., Y. Fukuda, K. Murata, and A. Kimura. 1983. Transformation of intact yeast cells treated with alkali cations. *J.Bacteriol.* 153:163-168.

Jhaveri, K., T. Taldone, S. Modi, and G. Chiosis. 2012. Advances in the clinical development of heat shock protein 90 (Hsp90) inhibitors in cancers. *Biochimica Et Biophysica Acta (BBA)-Molecular Cell Research.* 1823:742-755.

Johnson, B.D., R.J. Schumacher, E.D. Ross, and D.O. Toft. 1998. Hop modulates Hsp70/Hsp90 interactions in protein folding. *J.Biol.Chem.* 273:3679-3686.

Johnson, J.L., A. Halas, and G. Flom. 2007. Nucleotide-dependent interaction of Saccharomyces cerevisiae Hsp90 with the cochaperone proteins Sti1, Cpr6, and Sba1. *Mol.Cell.Biol.* 27:768-776.

Kabakov, A., and V. Gabai. 1993. Protein aggregation as primary and characteristic cell reaction to various stresses. *Experientia.* 49:706-710.

Kampinga, H.H., and E.A. Craig. 2010. The HSP70 chaperone machinery: J proteins as drivers of functional specificity. *Nature Reviews Molecular Cell Biology.* 11:579-592.

Kauzmann, W. 1959. OF PROTEIN DENATURATION1. *Adv.Protein Chem.* 14:1.

Kelland, L.R., S.Y. Sharp, P.M. Rogers, T.G. Myers, and P. Workman. 1999. DT-Diaphorase expression and tumor cell sensitivity to 17-allylamino, 17-

demethoxygeldanamycin, an inhibitor of heat shock protein 90. *J.Natl.Cancer Inst.* 91:1940-1949.

Koulov, A.V., P. LaPointe, B. Lu, A. Razvi, J. Coppinger, M. Dong, J. Matteson, R. Laister, C. Arrowsmith, and J.R. Yates. 2010. Biological and structural basis for Aha1 regulation of Hsp90 ATPase activity in maintaining proteostasis in the human disease cystic fibrosis. *Mol.Biol.Cell.* 21:871-884.

Kourtis, N., and N. Tavernarakis. 2011. Cellular stress response pathways and ageing: intricate molecular relationships. *EMBO J.* 30:2520-2531.

Krukenberg, K.A., T.O. Street, L.A. Lavery, and D.A. Agard. 2011. Conformational dynamics of the molecular chaperone Hsp90. *Q.Rev.Biophys.* 44:229-255.

Laemmli, U.K. 1970. Cleavage of structural proteins during the assembly of the head of bacteriophage T4. *Nature.* 227:680-685.

Landry, S.J., and L.M. Gerasch. 1991. Recognition of nascent polypeptides for targeting and folding. *Trends Biochem.Sci.* 16:159-163.

Langer, T., C. Lu, H. Echols, J. Flanagan, M.K. Hayer, and F.U. Hartl. 1992. Successive action of DnaK, DnaJ and GroEL along the pathway of chaperone-mediated protein folding. *Nature.* 356:683-689.

Laufen, T., M.P. Mayer, C. Beisel, D. Klostermeier, A. Mogk, J. Reinstein, and B. Bukau. 1999. Mechanism of regulation of hsp70 chaperones by DnaJ cochaperones. *Proceedings of the National Academy of Sciences.* 96:5452-5457.

Lee, G.J., A.M. Roseman, H.R. Saibil, and E. Vierling. 1997. A small heat shock protein stably binds heat-denatured model substrates and can maintain a substrate in a folding-competent state. *EMBO J.* 16:659-671.

Lee, G.J., and E. Vierling. 2000. A small heat shock protein cooperates with heat shock protein 70 systems to reactivate a heat-denatured protein. *Plant Physiol.* 122:189-198.

Lee, P., A. Shabbir, C. Cardozo, and A.J. Caplan. 2004. Sti1 and Cdc37 can stabilize Hsp90 in chaperone complexes with a protein kinase. *Mol.Biol.Cell.* 15:1785-1792.

Lepock, J.R., H.E. Frey, A.M. Rodahl, and J. Kruuv. 1988. Thermal analysis of CHL V79 cells using differential scanning calorimetry: implications for hyperthermic cell killing and the heat shock response. *J.Cell.Physiol.* 137:14-24.

Levinthal, C. 1968. Are there pathways for protein folding. *J.Chim.Phys.* 65:44-45.

Li, J., K. Richter, and J. Buchner. 2010. Mixed Hsp90–cochaperone complexes are important for the progression of the reaction cycle. *Nature Structural & Molecular Biology.* 18:61-66.

Li, J., J. Soroka, and J. Buchner. 2012. The Hsp90 chaperone machinery: Conformational dynamics and regulation by co-chaperones. *Biochimica Et Biophysica Acta (BBA)-Molecular Cell Research.* 1823:624-635.

Lindquist, S., and E. Craig. 1988. The heat-shock proteins. *Annu.Rev.Genet.* 22:631-677.

Lindquist, S. 1986. The heat-shock response. *Annu.Rev.Biochem.* 55:1151-1191.

Lotz, G.P., H. Lin, A. Harst, and W.M. Obermann. 2003. Aha1 binds to the middle domain of Hsp90, contributes to client protein activation, and stimulates the ATPase activity of the molecular chaperone. *J.Biol.Chem.* 278:17228-17235.

Manning-Krieg, U., P. Scherer, and G. Schatz. 1991. Sequential action of mitochondrial chaperones in protein import into the matrix. *EMBO J.* 10:3273.

McCarty, J.S., A. Buchberger, J. Reinstein, and B. Bukau. 1995. The role of ATP in the functional cycle of the DnaK chaperone system. *J.Mol.Biol.* 249:126-137.

McLaughlin, S.H., H.W. Smith, and S.E. Jackson. 2002. Stimulation of the weak ATPase activity of human hsp90 by a client protein. *J.Mol.Biol.* 315:787-798.

McLaughlin, S.H., F. Sobott, Z. Yao, W. Zhang, P.R. Nielsen, J.G. Grossmann, E.D. Laue, C.V. Robinson, and S.E. Jackson. 2006. The co-chaperone p23 arrests the Hsp90 ATPase cycle to trap client proteins. *J.Mol.Biol.* 356:746-758.

McLaughlin, S.H., L. Ventouras, B. Lobbezoo, and S.E. Jackson. 2004. Independent ATPase activity of Hsp90 subunits creates a flexible assembly platform. *J.Mol.Biol.* 344:813-826.

Meyer, P., C. Prodromou, B. Hu, C. Vaughan, S.M. Roe, B. Panaretou, P.W. Piper, and L.H. Pearl. 2003. Structural and Functional Analysis of the Middle Segment of Hsp90-Implications for ATP Hydrolysis and Client Protein and Cochaperone Interactions. *Mol.Cell.* 11:647-658.

Meyer, P., C. Prodromou, C. Liao, B. Hu, S.M. Roe, C.K. Vaughan, I. Vlasic, B. Panaretou, P.W. Piper, and L.H. Pearl. 2004. Structural basis for recruitment of the ATPase activator Aha1 to the Hsp90 chaperone machinery. *EMBO J.* 23:511-519.

Mickler, M., M. Hessling, C. Ratzke, J. Buchner, and T. Hugel. 2009. The large conformational changes of Hsp90 are only weakly coupled to ATP hydrolysis. *Nature Structural & Molecular Biology.* 16:281-286.

Minami, Y., Y. Kimura, H. Kawasaki, K. Suzuki, and I. Yahara. 1994. The carboxy-terminal region of mammalian HSP90 is required for its dimerization and function in vivo. *Mol.Cell.Biol.* 14:1459-1464.

Mollapour, M., S. Tsutsumi, Y.S. Kim, J. Trepel, and L. Neckers. 2011. Casein kinase 2 phosphorylation of Hsp90 threonine 22 modulates chaperone function and drug sensitivity. *Oncotarget.* 2:407.

Morishima, Y., K.C. Kanelakis, A.M. Silverstein, K.D. Dittmar, L. Estrada, and W.B. Pratt. 2000. The Hsp organizer protein hop enhances the rate of but is not essential for glucocorticoid receptor folding by the multiprotein Hsp90-based chaperone system. *J.Biol.Chem.* 275:6894-6900.

Mumberg, D., R. Müller, and M. Funk. 1995. Yeast vectors for the controlled expression of heterologous proteins in different genetic backgrounds. *Gene.* 156:119-122.

Münster, P.N., D.C. Marchion, A.D. Basso, and N. Rosen. 2002. Degradation of HER2 by ansamycins induces growth arrest and apoptosis in cells with HER2 overexpression via a HER3, phosphatidylinositol 3′-kinase-AKT-dependent pathway. *Cancer Res.* 62:3132-3137.

Nathan, D.F., and S. Lindquist. 1995. Mutational analysis of Hsp90 function: interactions with a steroid receptor and a protein kinase. *Mol.Cell.Biol.* 15:3917-3925.

Nathan, D.F., M.H. Vos, and S. Lindquist. 1999. Identification of SSF1, CNS1, and HCH1 as multicopy suppressors of a Saccharomyces cerevisiae Hsp90 loss-of-function mutation. *Proceedings of the National Academy of Sciences.* 96:1409-1414.

Nathan, D.F., M.H. Vos, and S. Lindquist. 1997. In vivo functions of the Saccharomyces cerevisiae Hsp90 chaperone. *Proceedings of the National Academy of Sciences.* 94:12949-12956.

Neckers, L. 2002. Hsp90 inhibitors as novel cancer chemotherapeutic agents. *Trends Mol.Med.* 8:S55-S61.

Neckers, L., and P. Workman. 2012. Hsp90 molecular chaperone inhibitors: are we there yet? *Clinical Cancer Research.* 18:64-76.

Nelson, G.M., V. Prapapanich, P.E. Carrigan, P.J. Roberts, D.L. Riggs, and D.F. Smith. 2004. The heat shock protein 70 cochaperone hip enhances functional maturation of glucocorticoid receptor. *Molecular Endocrinology.* 18:1620-1630.

Nelson, R.J., M. Heschl, and E.A. Craig. 1992. Isolation and characterization of extragenic suppressors of mutations in the SSA hsp70 genes of Saccharomyces cerevisiae. *Genetics.* 131:277-285.

Nemoto, T., Y. Ohara‐Nemoto, M. Ota, T. Takagi, and K. Yokoyama. 1995. Mechanism of Dimer Formation of the 90‐kDa Heat‐Shock Protein. *European Journal of Biochemistry.* 233:1-8.

Nover, L., K. Scharf, and D. Neumann. 1983. Formation of cytoplasmic heat shock granules in tomato cell cultures and leaves. *Mol.Cell.Biol.* 3:1648-1655.

Obermann, W.M., H. Sondermann, A.A. Russo, N.P. Pavletich, and F.U. Hartl. 1998. In vivo function of Hsp90 is dependent on ATP binding and ATP hydrolysis. *J.Cell Biol.* 143:901-910.

Onuoha, S., E. Coulstock, J. Grossmann, and S. Jackson. 2008. Structural studies on the co-chaperone Hop and its complexes with Hsp90. *J.Mol.Biol.* 379:732-744.

Panaretou, B., C. Prodromou, S.M. Roe, R. O'Brien, J.E. Ladbury, P.W. Piper, and L.H. Pearl. 1998. ATP binding and hydrolysis are essential to the function of the Hsp90 molecular chaperone in vivo. *EMBO J.* 17:4829-4836.

Panaretou, B., G. Siligardi, P. Meyer, A. Maloney, J.K. Sullivan, S. Singh, S.H. Millson, P.A. Clarke, S. Naaby-Hansen, and R. Stein. 2002. Activation of the ATPase activity of hsp90 by the stress-regulated cochaperone aha1. *Mol.Cell.* 10:1307.

Parsell, D.A., A.S. Kowal, M.A. Singer, and S. Lindquist. 1994. Protein disaggregation mediated by heat-shock protein Hspl04. *Nature.* 372:475-478.

Pastore, A., and P. Temussi. 2012. Protein aggregation and misfolding: good or evil? *Journal of Physics: Condensed Matter.* 24:244101.

Pearl, L.H., and C. Prodromou. 2006. Structure and mechanism of the Hsp90 molecular chaperone machinery. *Annu.Rev.Biochem.* 75:271-294.

Pearl, L.H., and C. Prodromou. 2000. Structure and< i> in vivo function of Hsp90. *Curr.Opin.Struct.Biol.* 10:46-51.

Pearl, L., C. Prodromou, and P. Workman. 2008. The Hsp90 molecular chaperone: an open and shut case for treatment. *Biochem.J.* 410:439-453.

Picard, D., B. Khursheed, M.J. Garabedian, M.G. Fortin, S. Lindquist, and K.R. Yamamoto. 1990. Reduced levels of hsp90 compromise steroid receptor action in vivo.

Piper, P.W., S.H. Millson, M. Mollapour, B. Panaretou, G. Siligardi, L.H. Pearl, and C. Prodromou. 2003. Sensitivity to Hsp90‐targeting drugs can arise with mutation to the Hsp90 chaperone, cochaperones and plasma membrane ATP binding cassette transporters of yeast. *European Journal of Biochemistry.* 270:4689-4695.

Pratt, W.B., and D.O. Toft. 2003. Regulation of signaling protein function and trafficking by the hsp90/hsp70-based chaperone machinery. *Exp.Biol.Med.* 228:111-133.

Prince, T., and R.L. Matts. 2004. Definition of protein kinase sequence motifs that trigger high affinity binding of Hsp90 and Cdc37. *J.Biol.Chem.* 279:39975-39981.

Proctor, C.J., and I.A. Lorimer. 2011. Modelling the role of the Hsp70/Hsp90 system in the maintenance of protein homeostasis. *PLoS One.* 6:e22038.

Prodromou, C. 2012. The ‘active life’of Hsp90 complexes. *Biochimica Et Biophysica Acta (BBA)-Molecular Cell Research.* 1823:614-623.

Prodromou, C., B. Panaretou, S. Chohan, G. Siligardi, R. O'Brien, J.E. Ladbury, S.M. Roe, P.W. Piper, and L.H. Pearl. 2000. The ATPase cycle of Hsp90 drives a

molecular'clamp'via transient dimerization of the N-terminal domains. *EMBO J.* 19:4383-4392.

Prodromou, C., S.M. Roe, R. O'Brien, J.E. Ladbury, P.W. Piper, and L.H. Pearl. 1997a. Identification and structural characterization of the ATP/ADP-binding site in the Hsp90 molecular chaperone. *Cell.* 90:65-75.

Prodromou, C., S.M. Roe, P.W. Piper, and L.H. Pearl. 1997b. A molecular clamp in the crystal structure of the N-terminal domain of the yeast Hsp90 chaperone. *Nature Structural & Molecular Biology.* 4:477-482.

Prodromou, C., G. Siligardi, R. O'Brien, D.N. Woolfson, L. Regan, B. Panaretou, J.E. Ladbury, P.W. Piper, and L.H. Pearl. 1999. Regulation of Hsp90 ATPase activity by tetratricopeptide repeat (TPR)-domain co-chaperones. *EMBO J.* 18:754-762.

Prodromou, C., and L.H. Pearl. 2003. Structure and functional relationships of Hsp90. *Current Cancer Drug Targets.* 3:301-323.

Pullen, L., and D.N. Bolon. 2011. Enforced N-domain proximity stimulates HSP90 ATPase activity and is compatible with function in vivo. *J.Biol.Chem.* 286:11091-11098.

Ran, F., M. Bali, and C.A. Michels. 2008. Hsp90/Hsp70 chaperone machine regulation of the Saccharomyces MAL-activator as determined in vivo using noninducible and constitutive mutant alleles. *Genetics.* 179:331-343.

Ratzke, C., F. Berkemeier, and T. Hugel. 2012. Heat shock protein 90's mechanochemical cycle is dominated by thermal fluctuations. *Proceedings of the National Academy of Sciences.* 109:161-166.

Retzlaff, M., F. Hagn, L. Mitschke, M. Hessling, F. Gugel, H. Kessler, K. Richter, and J. Buchner. 2010. Asymmetric activation of the hsp90 dimer by its cochaperone aha1. *Mol.Cell.* 37:344-354.

Richter, K., and J. Buchner. 2001. Hsp90: chaperoning signal transduction. *J.Cell.Physiol.* 188:281-290.

Richter, K., P. Muschler, O. Hainzl, and J. Buchner. 2001. Coordinated ATP hydrolysis by the Hsp90 dimer. *J.Biol.Chem.* 276:33689-33696.

Richter, K., P. Muschler, O. Hainzl, J. Reinstein, and J. Buchner. 2003. Sti1 Is a Non-competitive Inhibitor of the Hsp90 ATPase BINDING PREVENTS THE N-TERMINAL DIMERIZATION REACTION DURING THE ATPASE CYCLE. *J.Biol.Chem.* 278:10328-10333.

Richter, K., J. Reinstein, and J. Buchner. 2002. N-terminal residues regulate the catalytic efficiency of the Hsp90 ATPase cycle. *J.Biol.Chem.* 277:44905-44910.

Richter, K., J. Soroka, L. Skalniak, A. Leskovar, M. Hessling, J. Reinstein, and J. Buchner. 2008. Conserved conformational changes in the ATPase cycle of human Hsp90. *J.Biol.Chem.* 283:17757-17765.

Richter, K., S. Walter, and J. Buchner. 2004. The co-chaperone Sba1 connects the ATPase reaction of Hsp90 to the progression of the chaperone cycle. *J.Mol.Biol.* 342:1403-1413.

Roe, S.M., C. Prodromou, R. O'Brien, J.E. Ladbury, P.W. Piper, and L.H. Pearl. 1999. Structural basis for inhibition of the Hsp90 molecular chaperone by the antitumor antibiotics radicicol and geldanamycin. *J.Med.Chem.* 42:260-266.

Romero, M.F. 2004. In the beginning, there was the cell: cellular homeostasis. *Adv.Physiol.Educ.* 28:135-138.

Ross, P.D., and S. Subramanian. 1981. Thermodynamics of protein association reactions: forces contributing to stability. *Biochemistry (N.Y.).* 20:3096-3102.

Sato, S., N. Fujita, and T. Tsuruo. 2000. Modulation of Akt kinase activity by binding to Hsp90. *Proceedings of the National Academy of Sciences.* 97:10832-10837.

Scheibel, T., T. Weikl, and J. Buchner. 1998. Two chaperone sites in Hsp90 differing in substrate specificity and ATP dependence. *Proceedings of the National Academy of Sciences.* 95:1495-1499.

Scheufler, C., A. Brinker, G. Bourenkov, S. Pegoraro, L. Moroder, H. Bartunik, F.U. Hartl, and I. Moarefi. 2000. Structure of TPR domain-peptide complexes: critical elements in the assembly of the Hsp70-Hsp90 multichaperone machine. *Cell.* 101:199-210.

Schirmer, E.C., J.R. Glover, M.A. Singer, and S. Lindquist. 1996. HSP100/Clp proteins: a common mechanism explains diverse functions. *Trends Biochem.Sci.* 21:289-296.

Schuh, S., W. Yonemoto, J. Brugge, V.J. Bauer, R.M. Riehl, W.P. Sullivan, and D.O. Toft. 1985. A 90,000-dalton binding protein common to both steroid receptors and the Rous sarcoma virus transforming protein, pp60v-src. *J.Biol.Chem.* 260:14292-14296.

Schulte, T.W., M.V. Blagosklonny, L. Romanova, J.F. Mushinski, B.P. Monia, J.F. Johnston, P. Nguyen, J. Trepel, and L.M. Neckers. 1996. Destabilization of Raf-1 by geldanamycin leads to disruption of the Raf-1-MEK-mitogen-activated protein kinase signalling pathway. *Mol.Cell.Biol.* 16:5839-5845.

Scroggins, B.T., T. Prince, J. Shao, S. Uma, W. Huang, Y. Guo, B. Yun, K. Hedman, R.L. Matts, and S.D. Hartson. 2003. High affinity binding of Hsp90 is triggered by multiple discrete segments of its kinase clients. *Biochemistry (N.Y.).* 42:12550-12561.

Shapiro, A.L., and E. Viñuela. 1967. Molecular weight estimation of polypeptide chains by electrophoresis in SDS-polyacrylamide gels. *Biochem.Biophys.Res.Commun.* 28:815-820.

Shiu, R., J. Pouyssegur, and I. Pastan. 1977. Glucose depletion accounts for the induction of two transformation-sensitive membrane proteinsin Rous sarcoma virus-transformed chick embryo fibroblasts. *Proceedings of the National Academy of Sciences.* 74:3840-3844.

Siligardi, G., B. Hu, B. Panaretou, P.W. Piper, L.H. Pearl, and C. Prodromou. 2004. Co-chaperone regulation of conformational switching in the Hsp90 ATPase cycle. *J.Biol.Chem.* 279:51989-51998.

Siligardi, G., B. Panaretou, P. Meyer, S. Singh, D.N. Woolfson, P.W. Piper, L.H. Pearl, and C. Prodromou. 2002. Regulation of Hsp90 ATPase activity by the co-chaperone Cdc37p/p50 cdc37. *J.Biol.Chem.* 277:20151-20159.

Smith, D.F., W.P. Sullivan, T.N. Marion, K. Zaitsu, B. Madden, D. McCormick, and D. Toft. 1993. Identification of a 60-kilodalton stress-related protein, p60, which interacts with hsp90 and hsp70. *Mol.Cell.Biol.* 13:869-876.

Sőti, C., and P. Csermely. 1998. Characterization of the nucleotide binding properties of the 90 kDa heat shock protein (Hsp90). *J.Biosci.* 23:347-352.

Southworth, D.R., and D.A. Agard. 2011. Client-loading conformation of the Hsp90 molecular chaperone revealed in the cryo-EM structure of the human Hsp90: Hop complex. *Mol.Cell.* 42:771-781.

Stancato, L., Y. Chow, K. Hutchison, G. Perdew, R. Jove, and W. Pratt. 1993. Raf exists in a native heterocomplex with hsp90 and p50 that can be reconstituted in a cell-free system. *J.Biol.Chem.* 268:21711-21716.

Stebbins, C.E., A.A. Russo, C. Schneider, N. Rosen, F.U. Hartl, and N.P. Pavletich. 1997. Crystal structure of an Hsp90-geldanamycin complex: targeting of a protein chaperone by an antitumor agent. *Cell.* 89:239-250.

Stepanova, L., X. Leng, S.B. Parker, and J.W. Harper. 1996. Mammalian p50Cdc37 is a protein kinase-targeting subunit of Hsp90 that binds and stabilizes Cdk4. *Genes Dev.* 10:1491-1502.

Subjeck, J., J. Sciandra, and R. Johnson. 1982. Heat shock proteins and thermotolerance; a comparison of induction kinetics. *Br.J.Radiol.* 55:579-584.

Supko, J.G., R.L. Hickman, M.R. Grever, and L. Malspeis. 1995. Preclinical pharmacologic evaluation of geldanamycin as an antitumor agent. *Cancer Chemother.Pharmacol.* 36:305-315.

Szabo, A., T. Langer, H. Schröder, J. Flanagan, B. Bukau, and F.U. Hartl. 1994. The ATP hydrolysis-dependent reaction cycle of the Escherichia coli Hsp70 system DnaK, DnaJ, and GrpE. *Proceedings of the National Academy of Sciences.* 91:10345-10349.

Taipale, M., D.F. Jarosz, and S. Lindquist. 2010. HSP90 at the hub of protein homeostasis: emerging mechanistic insights. *Nature Reviews Molecular Cell Biology.* 11:515-528.

Taipale, M., I. Krykbaeva, M. Koeva, C. Kayatekin, K.D. Westover, G.I. Karras, and S. Lindquist. 2012. Quantitative analysis of hsp90-client interactions reveals principles of substrate recognition. *Cell.* 150:987-1001.

Tanford, C. 1978. The hydrophobic effect and the organization of living matter. *Science.* 200:1012-1018.

Tanford, C. 1962. Contribution of hydrophobic interactions to the stability of the globular conformation of proteins. *J.Am.Chem.Soc.* 84:4240-4247.

Taxis, C., and M. Knop. 2006. System of centromeric, episomal, and integrative vectors based on drug resistance markers for Saccharomyces cerevisiae. *BioTechniques.* 40:73.

Tillotson, B., K. Slocum, J. Coco, N. Whitebread, B. Thomas, K.A. West, J. MacDougall, J. Ge, J.A. Ali, and V.J. Palombella. 2010. Hsp90 (heat shock protein 90) inhibitor occupancy is a direct determinant of client protein degradation and tumor growth arrest in vivo. *J.Biol.Chem.* 285:39835-39843.

Trepel, J., M. Mollapour, G. Giaccone, and L. Neckers. 2010. Targeting the dynamic HSP90 complex in cancer. *Nature Reviews Cancer.* 10:537-549.

Tsutsumi, S., M. Mollapour, C. Prodromou, C. Lee, B. Panaretou, S. Yoshida, M.P. Mayer, and L.M. Neckers. 2012. Charged linker sequence modulates eukaryotic heat shock protein 90 (Hsp90) chaperone activity. *Proceedings of the National Academy of Sciences.* 109:2937-2942.

Varela, F.G., H.R. Maturana, and R. Uribe. 1974. Autopoiesis: The organization of living systems, its characterization and a model. *BioSystems.* 5:187-196.

Vendruscolo, M., T.P. Knowles, and C.M. Dobson. 2011. Protein solubility and protein homeostasis: a generic view of protein misfolding disorders. *Cold Spring Harbor Perspectives in Biology.* 3.

Verghese, J., J. Abrams, Y. Wang, and K.A. Morano. 2012. Biology of the heat shock response and protein chaperones: budding yeast (Saccharomyces cerevisiae) as a model system. *Microbiology and Molecular Biology Reviews.* 76:115-158.

Wandinger, S.K., K. Richter, and J. Buchner. 2008. The Hsp90 chaperone machinery. *J.Biol.Chem.* 283:18473-18477.

Wang, X., J. Venable, P. LaPointe, D.M. Hutt, A.V. Koulov, J. Coppinger, C. Gurkan, W. Kellner, J. Matteson, and H. Plutner. 2006. Hsp90 cochaperone Aha1 downregulation rescues misfolding of CFTR in cystic fibrosis. *Cell.* 127:803-815.

Wegele, H., P. Muschler, M. Bunck, J. Reinstein, and J. Buchner. 2003. Dissection of the contribution of individual domains to the ATPase mechanism of Hsp90. *J.Biol.Chem.* 278:39303-39310.

Wegele, H., S.K. Wandinger, A.B. Schmid, J. Reinstein, and J. Buchner. 2006. Substrate transfer from the chaperone Hsp70 to Hsp90. *J.Mol.Biol.* 356:802-811.

Weikl, T., P. Muschler, K. Richter, T. Veit, J. Reinstein, and J. Buchner. 2000. C-terminal regions of Hsp90 are important for trapping the nucleotide during the ATPase cycle. *J.Mol.Biol.* 303:583.

Werner-Washburne, M., J. Becker, J. Kosic-Smithers, and E. Craig. 1989. Yeast Hsp70 RNA levels vary in response to the physiological status of the cell. *J.Bacteriol.* 171:2680-2688.

Westhoff, B., J.P. Chapple, J. van der Spuy, J. Höhfeld, and M.E. Cheetham. 2005. HSJ1 is a neuronal shuttling factor for the sorting of chaperone clients to the proteasome. *Current Biology.* 15:1058-1064.

Whitesell, L., and S.L. Lindquist. 2005. HSP90 and the chaperoning of cancer. *Nature Reviews Cancer.* 5:761-772.

Whitesell, L., E.G. Mimnaugh, B. De Costa, C.E. Myers, and L.M. Neckers. 1994. Inhibition of heat shock protein HSP90-pp60v-src heteroprotein complex formation by benzoquinone ansamycins: essential role for stress proteins in oncogenic transformation. *Proceedings of the National Academy of Sciences.* 91:8324-8328.

Workman, P. 2004. Combinatorial attack on multistep oncogenesis by inhibiting the Hsp90 molecular chaperone. *Cancer Lett.* 206:149-157.

Xu, W., and L. Neckers. 2007. Targeting the molecular chaperone heat shock protein 90 provides a multifaceted effect on diverse cell signaling pathways of cancer cells. *Clinical Cancer Research.* 13:1625-1629.

Xu, W., X. Yuan, Z. Xiang, E. Mimnaugh, M. Marcu, and L. Neckers. 2005. Surface charge and hydrophobicity determine ErbB2 binding to the Hsp90 chaperone complex. *Nature Structural & Molecular Biology.* 12:120-126.

Xu, Y., and S. Lindquist. 1993. Heat-shock protein hsp90 governs the activity of pp60v-src kinase. *Proceedings of the National Academy of Sciences.* 90:7074-7078.

Xu, Y., M.A. Singer, and S. Lindquist. 1999. Maturation of the tyrosine kinase c-src as a kinase and as a substrate depends on the molecular chaperone Hsp90. *Proceedings of the National Academy of Sciences.* 96:109-114.

Young, J.C., I. Moarefi, and F.U. Hartl. 2001. Hsp90: a specialized but essential protein-folding tool. *J.Cell Biol.* 154:267.

Young, J.C., W.M. Obermann, and F.U. Hartl. 1998. Specific binding of tetratricopeptide repeat proteins to the C-terminal 12-kDa domain of hsp90. *J.Biol.Chem.* 273:18007-18010.

Zhao, R., M. Davey, Y. Hsu, P. Kaplanek, A. Tong, A.B. Parsons, N. Krogan, G. Cagney, D. Mai, and J. Greenblatt. 2005. Navigating the chaperone network: an integrative map of physical and genetic interactions mediated by the hsp90 chaperone. *Cell.* 120:715-727.